MARIANA APARECIDA BRUNINI ROSALES

O Estresse Nitrosativo na Patogênese da Retinopatia Diabética. Implicações na Barreira Hemato-Retiniana Externa e Possíveis Alvos Terapêuticos.

Nitrosative Stress in the Pathogenesis of Diabetic Retinopathy. Implications in the Outer Blood Retinal Barrier and Possible Therapeutics Targets.

CAMPINAS

2014

UNIVERSIDADE ESTADUAL DE CAMPINAS

FACULDADE DE CIÊNCIAS MÉDICAS

MARIANA APARECIDA BRUNINI ROSALES

O Estresse Nitrosativo na Patogênese da Retinopatia Diabética. Implicações na Barreira Hemato-Retiniana Externa e Possíveis Alvos Terapêuticos.

Orientadora: Profª. Drª. Jacqueline Mendonça Lópes de Faria
Coorientador: Prof. Dr. Jose Butori Lopes de Faria

Nitrosative Stress in the Pathogenesis of Diabetic Retinopathy. Implications in the Outer Blood Retinal Barrier and Possible Therapeutics Targets.

Tese de Doutorado apresentada ao Programa de Pós-Graduação em Clínica Médica da Faculdade de Ciências Médicas da Universidade Estadual de Campinas, para obtenção do título de Doutora em Clínica Médica na área Clínica Médica.

Doctorate Thesis presented to the Clinical Science Postgraduation Programme of the Faculty of Medical Sciences of the University of Campinas to obtain the Ph.D. grade in Clinical Science.

ESTE EXEMPLAR CORRESPONDE À VERSÃO FINAL DA TESE DEFENDIDA PELA ALUNA MARIANA APARECIDA BRUNINI ROSALES ORIENTADA PELA PROFª. DRª. JACQUELINE MENDONÇA LÓPES DE FARIA

Assinatura do Orientador

_____

CAMPINAS
2014

Ficha catalográfica
Universidade Estadual de Campinas
Biblioteca da Faculdade de Ciências Médicas
Maristella Soares dos Santos - CRB 8/8402

R71e

Rosales, Mariana Aparecida Brunini, 1983-
O estresse nitrosativo na patogênese da retinopatia diabética : implicações na barreira hemato-retiniana externa e possíveis alvos terapêuticos / Mariana Aparecida Brunini Rosales. – Campinas, SP : [s.n.], 2014.

Orientador: Jacqueline Mendonça Lopes de Faria.
Coorientador: José Butori Lopes de Faria.
Tese (doutorado) – Universidade Estadual de Campinas, Faculdade de Ciências Médicas.

1. Retinopatia diabética. 2. Epitélio pigmentado da retina. 3. Óxido nítrico sintase. I. Faria, Jacqueline Mendonça Lopes de. II. Faria, Jose Butori Lopes de,1955-. III. Universidade Estadual de Campinas. Faculdade de Ciências Médicas. IV. Título.

Informações para Biblioteca Digital

Título em outro idioma: Nitrosative stress in the pathogenesis of diabetic retinopathy : implications in the outer blood retinal barrier and possible therapeutics targets
Palavras-chave em inglês:
Diabetic retinopathy
Retinal pigment epithelium
Nitric oxide synthase
Área de concentração: Clínica Médica
Titulação: Doutora em Clínica Médica
Banca examinadora:
Jacqueline Mendonça Lopes de Faria [Orientador]
Erich Vinicius de Paula
Roger Frigerio Castilho
Eduardo Melani Rocha
Adriana Karla Cardoso Amorim Reis
Data de defesa: 28-02-2014
Programa de Pós-Graduação: Clínica Médica

BANCA EXAMINADORA DA DEFESA DE DOUTORADO

MARIANA APARECIDA BRUNINI ROSALES

ORIENTADORA: PROF. DR. JACQUELINE MENDONÇA LÓPES DE FARIA
COORIENTADOR: PROF. DR. JOSE BUTORI LOPES DE FARIA

MEMBROS:

1. **PROF. DR. JACQUELINE MENDONÇA LÓPES DE FARIA** 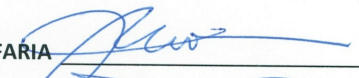
2. **PROF. DR. ERICH VINICIUS DE PAULA** 
3. **PROF. DR. ROGER FRIGERIO CASTILHO** 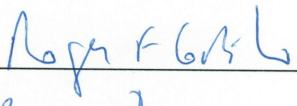
4. **PROF. DR. EDUARDO MELANI ROCHA** 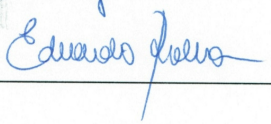
5. **PROF. DR. ADRIANA KARLA CARDOSO AMORIM REIS** 

Programa de Pós-Graduação em Clínica Médica da Faculdade de Ciências Médicas da Universidade Estadual de Campinas.

Data: 28 de fevereiro de 2014

DEDICATÓRIA

À minha família:

Aos meus pais, Silvia e Mário, que embora com personalidades diferentes, constituem a minha base de valores, princípios e essência. Neles eu encontro a energia para percorrer este caminho nada fácil, sendo minha mãe o meu alicerce, suporte e exemplo de dedicação incondicional e ao meu pai, o meu eterno herói e fonte de garra, o qual me incentiva a sonhar, acreditar e conquistar... Ao meu irmão Victor, o qual eu amo muito...

A dedicação e preocupação comigo de meu avô Raul Brunini Sobrinho, médico veterinário pesquisador aposentado, desde criança até os dias de hoje... Foi ele quem me mostrou os primeiros "vidrinhos" de laboratório... Espero também contribuir para a pesquisa do mesmo modo que ele contribuiu... Fiquei com medo do senhor não estar aqui logo quando iniciei a escrita desta tese... No entanto, o exemplo atualmente de superação do senhor me faz ser mais forte e enfrentar qualquer barreira...

Ao meu companheiro:

Ao meu companheiro, melhor amigo, recém doutor e futuro esposo Franco, pela partilha da vida acadêmica, experimentos, desabafos, amor, paciência e ajuda em todos os momentos... Sempre me ensinando desde o dia em que eu o conheci, como os cuidados com as celulinhas... E principalmente, por compartilhar os mesmos valores, princípios, ideais e sonhos científicos... Assim como Marie Curie e Pierre Curie, acredito na força dos casais na ciência...

A Deus por iluminar a minha mente o meu caminho.

AGRADECIMENTOS

À minha orientadora, profa. Dra. Jacqueline Mendonça Lopes de Faria, pela orientação, paciência, confiança no meu trabalho e pela sua principal característica, agilidade na correção de meus relatórios, resumos, manuscritos e minha tese. Agradeço pelos trabalhos em que fui co-autora e pelas oportunidades concedidas através de minhas participações em congressos nacionais e internacionais. Acredito que parte de minha formação acadêmica seja resultado de sua orientação, afinal estou há quase oito anos neste laboratório e já passei por quase todas as funções, estagiária, TT-3, mestrado e no momento encerrando mais um ciclo, o doutorado.

Ao professor Dr. José Butori Lopes de Faria, um professor e pesquisador completo, o qual eu admiro muito pela sua honestidade. Agradeço pela sua contribuição com perguntas inteligentes que fazem com que eu busque as soluções. Às vezes é muito difícil aceitar as suas críticas, mas acredito que elas são importantes para o nosso amadurecimento. Por outro lado, o seu sorriso de aprovação durante as apresentações orais, é a confiança que me ajuda para tentar fazer o melhor.

Neste período, também tive a oportunidade de contar com a convivência e colaboração de muitos colegas e amigos de laboratório. Dentre eles, Kamila, Aline, Sandra, Juliana, Patrícia, Elisa, Alex, Diego, Natasha, Jefferson, Chiara, Virginia, Josie, Sidnei, Vitor, Daniel, Pati, Rute, Nilza, Ana, Cris, Erika, Flávia entre outros. Agradeço também por ter tido a oportunidade de orientar, pois eu observei que ensinar o próximo é também aprender. Foi muito gratificante quando os meus desenhos facilitavam a compreensão e despertavam o entusiasmo dos meus "pupilos".

Em especial à minha amiga e companheira de laboratório Kamila, pelo carinho, dedicação, participação e companheirismo em praticamente tudo o que faço desde o primeiro dia em que entrei neste laboratório. Embora com perfis diferentes, nossas idéias se completam experimentalmente, eticamente e intelectualmente. A nossa relação é essencial no que desenvolvemos, assim como a "pipeta e a ponteira".

Aos laboratórios do Instituto de Química e principalmente ao prof. Marcelo Ganzarolli pela síntese do colírio de GSNO e orientação; ao Laboratório de Bioenergética do prof. Dr. Anibal Eugênio Vercesi pelo uso de materiais, equipamentos e informações técnicas; ao laboratório INNOVARE, sob orientação do prof. Rodrigo Catharino pelas análises em UHPLC; e pelo uso do microscópio confocal do Hemocentro, que atualmente está no LaCTAD sob supervisão da técnica Janine, a qual sempre me ajudou muito.

A toda a minha família, avós, "boadrasta" e amiga Bete, tios, primos, padrinhos, sogros e amigos pelo carinho, amor, respeito, apoio e reconhecimento de meu trabalho.

A todos aquele que não foram citados, mas que contribuíram de alguma forma para a realização deste trabalho.

A CAPES e FAPESP, pelo apoio financeiro.

EPÍGRAFE

Sete gênios que foram subestimados e rejeitados antes de alcançar o sucesso:

1- Albert Einsten

2- Louis Pasteur

3- Thomas Edison

4- Charles Darwin

5- Ludwig van Beethoven

6- Alexander Graham Bell

7- Henry Ford

Eles já foram chamados de “burros”, “medíocres”, “loucos”, “sonhadores”... Foram rebaixados, apontados como incapacitados. Mas hoje fazem parte da História e suas descobertas e invenções ditam e regram o nosso mundo.

“O insucesso é apenas uma oportunidade para recomeçar de novo com mais inteligência (H. Ford).”

“Muitas das falhas da vida acontecem quando as pessoas não percebem o quão perto estão quando desistem (*T. Edison).”*

“Nos campos da observação, o acaso favorece apenas as mentes preparadas (L. Pasteur).”

“A imaginação é mais importante que o conhecimento (A. Einsten).”

“Persistir e não dar ouvidos a tudo que falam pode ser o caminho para vitória...”

SUMÁRIO

LISTA DE ABREVIATURAS

8-OH-dG - 8-hidroxi-2'-desoxiguanosina

ADH III - álcool desidrogenase III

AGEs - *advanced glycated end-products* (produtos finais da glicosilação avançada)

AIF - *apoptosis induced factor* (fator indutor de apoptose)

ARPE-19 - *human retinal pigment epithelial cells line* (linhagem celular humana do epitélio pigmentar da retina)

ASGR1 - *asialoglycoprotein receptor 1*(receptor de asialoglicoproteína)

ATP - adenosina trifosfato

BHR - barreira hemato-retiniana

Ca^{2+} - cálcio

CAV-1 - caveolina-1

CCB - camada dos cones e bastonetes

CCG - camada das células ganglionares

CE - células endoteliais

cGMP - guanosina monofosfato cíclica

Cl^- - cloro

CNE - camada da nuclear externa;

CNI - camada da nuclear interma;

$CO_3^{\bullet-}$ - íon carbonato

CPE - camada da plexiforme externa;

CPI - camada da plexiforme interna;

C-SH ou **R-SH** - grupo sulfidril da cisteína na cadeia protéica com grupos tiol

CTs - controles

DM - diabetes mellitus

DNA - ácido desoxirribonucleico

Dnm - dinamina

DOR - *delta opioid receptor* (receptor δ-opióide)

eNOS - *endothelial nitric-oxide synthase* (óxido nítrico sintetase endotelial)

EP - epicatequina

EPR - epitélio pigmentado da retina

ERG - eletrorretinografia

ERK - *extracellular signal-regulated kinases* (proteína cinase extracelular reguladora)

ERN - espécies reativas do nitrogênio

ERO - espécies reativas do oxigênio

ESAM - *endothelial cell-selective adhesion molecule* (molécula de adesão seletiva da célula endotelial)

ET-1 - endotelina 1

FAD-FMN - domínio redutase contendo flavina

FLOT - flotilina

FN - fibronectina

GC - guanilato ciclase solúvel

GLUT 3 - transportador de glicose 3

GLUT1 - transportador de glicose 1

GSH - glutationa reduzida

GSNHOH - glutationa S-hidroxisulfonamida

GSNO - S-nitrosoglutationa

GSNO-R - GSNO redutase

GSSG - glutationa oxidada

GTP - guanosina trifosfato

HA - hipertensão arterial

HCO^-_3 - bicarbonato

HNE - hidroxinonenal

iNOS - *inducible nitric oxide synthase* (óxido nítrico sintetase induzida)

JAMs - *junctional adhesion molecules* (moléculas de junções de adesão)

JI - junções intercelulares

K^+ - potássio

L-Arg - L-arginina

L-Cit - L-citrulina

LPS - lipopolissacarídeo

MAPK - *mitogen-activated protein kinases* (proteína quinase ativada por mitógeno)

MB - membrana de Bruch

MEC - matriz extracelular

mRNA - ácido ribonucléico mensageiro

MV - microvilosidades

Na^+ - sódio

NAD+ - nicotinamida adenina

NADPH - nicotinamida adenina dinucleotídeo fosfato

NF-kB - fator nuclear kappa B

NH_3 - amônia

NMDA - receptor N-metil-D-aspártico

nNOS - *neuronal nitric oxide synthase* (óxido nítrico sintetase neuronal)

$NO^{\bullet}$ - óxido nítrico

$NO_2^{\bullet}$ - dióxido de nitrogênio

NOS - óxido nítrico sintetase

NSF - *N-ethylmaleimide sensitive fusion proteins* (fator sensível a N-etilmaleimida)

$O_2^{\bullet-}$ - superóxido

$OH^{\bullet}$ - radical hidroxila

$ONOO^-$ - peroxinitrito

PAR - poli ADP-ribose

PARP - poli ADP-ribose polimerase

PKC - proteína quinase C

PV - proteínas de membrana associada a vesículas

PUMA - *p53 upregulated modulator of apoptosis* (modulador de apoptose super regulado p53)

RAGE - *advanced glycated end-products receptor* (receptor de AGE)

RD - retinopatia diabética

RNA - ácido ribonucléico

SEF - segmento externo dos fotorreceptores

SF - segmento dos fotorreceptores

SHR - *spontaneously hipertensive rats* (animais espontaneamente hipertensos)

SIF - segmento interno dos fotorreceptores

SNAP - *synaptosomal-associated protein* (proteína associada ao sinaptossoma)

SNARE - *soluble NSF attachment receptor* (receptor de fator sensível a N-etilmaleimida solúvel)

SNO - S-nitrosotióis

STZ - estreptozotocina

TER - *transepithelial electrical resistance* (resistência elétrica transepitelial)

TGF-ß - *transforming growth factor beta* (fator de crescimento transformado beta)

TNF-α - *tumor necrosis factor alpha* (fator de necrose tumoral alfa)

VAMP - *vesicle associated membrane proteins* (proteína de membrana associada a vesículas)

VEGF - *vascular endothelial growth factor* **(**fator de crescimento endotelial vascular)

WTAP - *Wilms tumor 1 associated protein* (proteína de tumor de Wilms)

ZO-1 - zônulas de oclusão

RESUMO

A patogênese da retinopatia diabética (RD) está associada ao estresse nitrosativo. Alterações na barreira hemato-retiniana (BHR) externa, formada pelas células do epitélio pigmentado da retina (EPR), estão associadas às fases precoces da RD e podem acarretar no desequilíbrio da manutenção dos fotorreceptores e consequentemente promoverem mudanças nas células neuronais da retina. O estresse nitrosativo como consequência do aumento da produção de óxido nítrico ($NO^{\bullet}$) produzido pela super expressão da óxido nítrico sintetase induzida (iNOS) esteve presente em todas as camadas da retina, inclusive no EPR em condições de RD experimental *in vivo* precoce ou na linhagem celular humana do EPR (ARPE-19) expostas à alta concentração de glicose. O tratamento com agentes químicos como a S-nitrosoglutationa (GSNO), ou naturais (cacau enriquecido com polifenol) atuaram em diferentes vias de inibição da iNOS, prevenindo o estresse nitrosativo. Para o estudo *in vivo* com o colírio de GSNO (artigo I) foram utilizados animais espontaneamente hipertensos (SHR) com 4 semanas de idade. O diabetes (DM) foi induzido por STZ. Após a confirmação do DM (48 horas), os animais foram divididos em 6 grupos: controles (CTs) veículo; GSNO 900nm e GSNO 10µm ou DMs veículo; GSNO 900nm e GSNO 10µm. O efeito do tratamento com colírio de GSNO foi dependente da presença ou ausência da condição do DM. Nos animais CT, o GSNO atuou como um agente nitrosativo e nos animais DM preveniu o aumento da expressão da iNOS, preservando a retina funcional. Os estudos *in vitro*, demonstraram que o efeito do GSNO foi deletério ou protetor dependente da concentração de glicose. Nas células ARPE-19 expostas a condições normais de glicose, o tratamento promoveu um aumento na produção de $NO^{\bullet}$ sem aumentar a expressão de iNOS e nas células sob alta glicose induziu uma modificação pós-translacional de proteína, a S-glutationilação da iNOS prevenindo o estresse nitrosativo. No estudo do cacau (artigo II), foi avaliado *in vitro* (ARPE-19 exposta a alta concentração de glicose)

o seu efeito protetor dependente da concentração de polifenóis. Para isso foram testadas duas formulações de cacau que diferiram somente na concentração de polifenol: 0,5% para o cacau com baixo teor de polifenol e 60,5% para o cacau com alto teor de polifenol. A epicatequina (EC), encontrada na concentração de 12% no cacau com alto teor de polifenol foi tão eficaz quanto o próprio e esteve envolvida no controle da expressão da iNOS através da estimulação do receptor δ-opióide (DOR) diminuindo os níveis de TNF-α. A modulação da iNOS, preveniu a S-nitrosilação da caveolina-1 (CAV-1) e diminuição da expressão das junções intercelulares claudina-1 e ocludina através da prevenção da interação CAV-1/junções. Em ambos os estudos, o alvo terapêutico foi a iNOS em duas diferentes modalidades: modificação pós-translacional de proteína e modulação do TNF-α via DOR no EPR em modelos experimentais de RD. Os tratamentos apresentados neste trabalho demonstraram a iNOS como alvo terapêutico e mostraram-se eficaz em conter danos funcionais e morfológicos promovidas pela situação de mimetismo do DM no EPR demonstrando o importante papel da iNOS no desenvolvimento da RD.

The pathogenesis of diabetic retinopathy (DR) is associated with nitrosative stress. Changes in outer blood-retinal barrier (BRB), formed by retinal pigment epithelium cells (RPE) are associated in the early stages of DR and can cause imbalance in the maintenance of photoreceptors and thereby cause changes on retinal neuronal cells. The nitrosative stress as a result of increased production of nitric oxide (NO) produced by overexpression of nitric oxide synthase (iNOS) was present in all layers of the retina and mainly in RPE cells in early *in vivo* experimental DR or in human RPE cell line (ARPE-19) exposed to high glucose condition. Therapy with chemical agents such as S-Nitrosoglutathione (GSNO) or natural compounds (enriched cocoa polyphenol) acted in different pathways of iNOS inhibition, preventing nitrosative stress. For the *in vivo* study with GSNO eye drops (article I), it were used spontaneously hypertensive rats (SHR) rats with 4 week old. Diabetes (DM) was induced by streptozotocin (STZ). After DM confirmation (48 hours), the animals were divided into 6 groups: controls (CTs) vehicle; GSNO 900nm and GSNO 10μm or DMs vehicle; GSNO 900nm e GSNO 10μm. The effects of treatments were dependent on glucose concentration. In CT animals, GSNO acted as a nitrosative agent and in DM rats prevented iNOS overexpression, preserving the retina function. *In vitro* study showed that GSNO protective or deleterious effects were dependent on the glucose concentration. In ARPE-19 cells exposed to normal glucose, the treatment promoted an increase of $NO^{\bullet}$ production without increase iNOS expression and in cells under high glucose (HG) condition induced post-translational protein modification, S-glutationylation of iNOS, preventing nitrosative stress. In the study with cocoa (article II), it was evaluated its protective effect dependent on concentration of polyphenols in ARPE-19 cells under HG condition. For this study, the composition of cocoa was the same in both preparations with the only difference in the amounts of polyphenol, 0.5% for low

polyphenol cocoa (LPC) and 60.5% for high polyphenol cocoa (HPC). Epicatechin (EC), found in 12% of HPC was similarly protective compare to HPC and it was involved in controlling iNOS expression by stimulation of the delta opioid receptor decreasing TNF- α levels. The modulation of iNOS prevented S-nitrosylation of caveolin-1 (CAV-1) and decreased expression of claudin-1 and occluding tight junctions by preventing CAV-1/junctions interactions. The treatments presented here showed iNOS as a therapeutic target containing functional and morphological changes promoted by DM milieu in RPE showing the important role of iNOS in the development of DR.

1- INTRODUÇÃO

1.1– A Retina

A retina é a camada mais interna do globo ocular, possui cerca de 0,5 mm de espessura e é responsável pela visão. Possui células sensíveis à estimulação luminosa e responsáveis por enviar as imagens ao cérebro. Durante a embriogênese, o desenvolvimento e a diferenciação da retina, exige a concomitante formação de elementos neuronais e gliais, juntamente com uma densa rede vascular. Em adultos, esses três compartimentos interagem entre si para manter a estrutura e função da retina normal (Provis, 2001; Saint-Geniez e D'Amore, 2004).

A retina neural é composta por 10 camadas: membrana limitante interna, camada de fibras nervosas, camada de células ganglionares, plexiforme interna (células amácrinas), nuclear interna (células bipolares), plexiforme externa (células horozontais), os fotorreceptores (nuclear externa, segmento interno e o externo) e epitélio pigmentado da retina. A camada dos fotorreceptores é composta de células chamadas cones e bastonetes. Essas células estão próximas à superfície externa da retina e a luz, para atingi-la, deve atravessar toda a cavidade vítrea e a retina interna. Após a fotorrecepção, o sinal é conduzido para as células bipolares, que transmitem os sinais para a camada de células ganglionares, cujos axônios que chegam ao cérebro se agrupam na superfície interna da retina para formar o nervo óptico. As células horizontais também recebem informações dos fotorreceptores e influenciam as células bipolares enquanto as células amácrinas influenciam a excitabilidade das células ganglionares. O nervo óptico também contém os vasos sanguíneos que irrigam as camadas internas da retina. Ele situa-se no centro da retina e possui cerca de 2 x 1,5 mm de diâmetro. A camada mais externa da retina é o epitélio pigmentado da retina (EPR), o qual está em íntimo contato com os segmentos externos dos fotorreceptores. A retina também possui colunas de

sustentação, compostas pelas células gliais (ou fibras de Müller), que sustentam o metabolismo dos neurônios da retina (Cormack, 1996; Heegand, 1997).

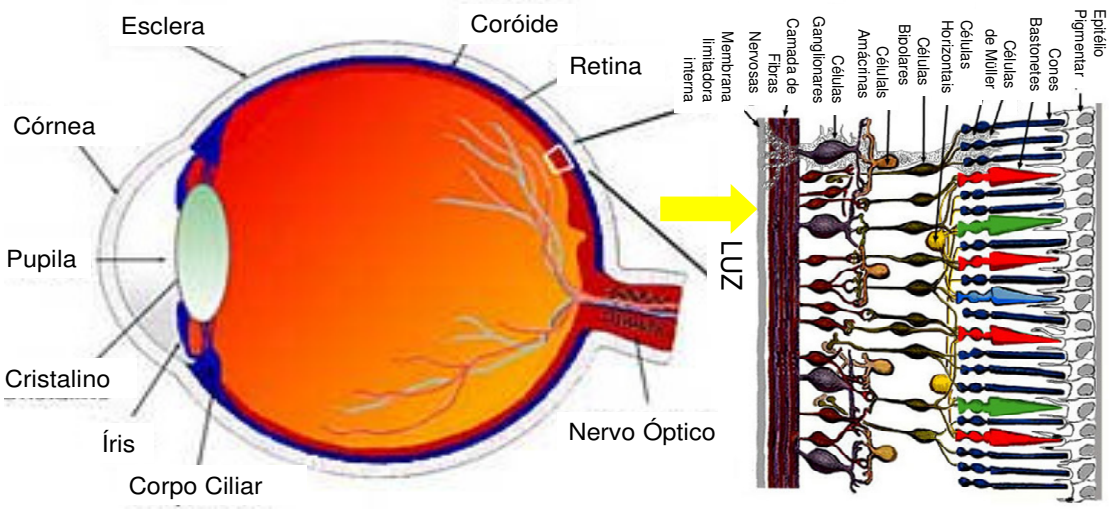

Figura 1. Diagrama do circuito básico da retina. Os três canais das células neurais: os fotorreceptores, as células bipolares e as células ganglionares – determinando a mais direta rota para a transmissão visual da informação para o cérebro. Células horizontais e células amácrinas mediadas lateralmente nas camadas plexiformes externas e internas, respectivamente.

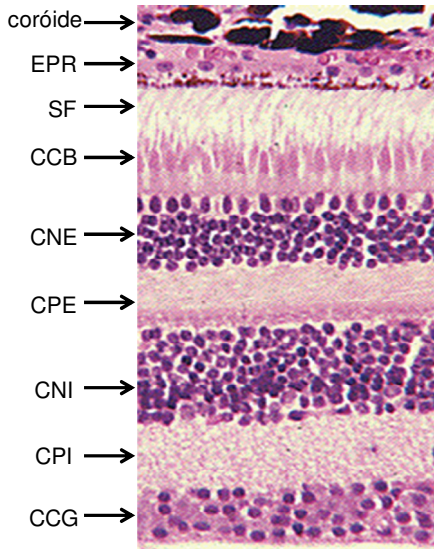

Figura 2. Figura representativa de um corte histológico de retina. A membrana apical do epitélio pigmentado da retina (EPR) conecta-se com os segmentos dos fotorreceptores e a membrana basolateral com a membrana de Bruch, que separa o EPR

do endotélio fenestrado da coriocapilar. **SF:** segmento dos fotorreceptores; **CCB:** camada dos cones e bastonetes; **CNE:** camada da nuclear externa; **CPE:** camada da plexiforme externa; **CNI:** camada da nuclear interma; **CPI:** camada da plexiforme interna; **CCG:** camada das células ganglionares (adaptado de Simó, Villarroel *et al*., 2010).

O suprimento sangüíneo da retina interna advém de dois sistemas circulatórios distintos: sistema retiniano e sistema uveal. O sistema retiniano origina a partir da artéria central da retina, e o sistema uveal origina a partir das artérias ciliares posteriores, ambos ramos da artéria oftálmica (ramo direito da carótida interna). O suporte para a retina externa é dado por difusão através dos vasos da coróide que estão adjacentes ao EPR.

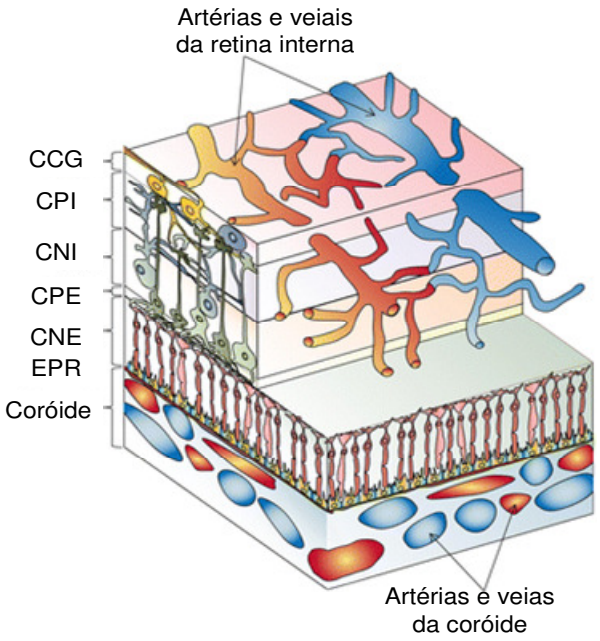

Figura 3. A retina neuro-vascular. O suprimento sanguíneo das camadas da retina interna provenientes do ramo direito da carótida interna e da camada dos fotorreceptores por difusão de nutrientes dos vasos da coroide através do epitélio pigmentado da retina (EPR). **CCG:** camada das células ganglionares; **CPI:** camada da plexiforme interna; **CNI:** camada da nuclear interma; **CPE:** camada da plexiforme externa; **CNE:** camada da nuclear externa.

Juntos, o endotélio dos vasos da retina (barreira interna) e o EPR (barreira externa) formam a barreira hemato-retiniana (BHR), uma forte barreira contra

macromoléculas, fazendo da retina neural um tecido imunologicamente privilegiado e propiciando mecanismo para controlar fluxo de fluidos e metabólitos. A principal característica desta barreira é a presença de junções intercelulares, responsáveis pela alta permeabilidade seletiva.

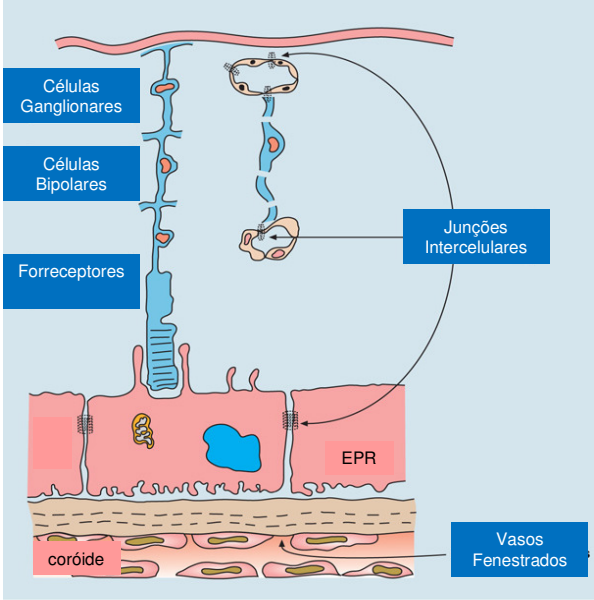

Figura 4. A barreira-hemato retiniana interna composta pelo endotélio responsável pelo fornecimento de nutrientes para a retina interna (células ganglionares e bipolares) e a barreira hemato-retiniana externa formada pelo epitélio pigmentado da retina (EPR) que regula o transporte de duas vias de fluidos: nutrientes e resíduos entre os fotorreceptores e o rápido escoamento do alto volume de sangue da corrente sanguínea proveniente da coróide. A presença de junções intercelulares em ambas as barreiras conferem a característica de alta permeabilidade seletiva (adaptado de Forrester e Xu, 2012).

1.1.2. A Barreira Hemato-Retiniana Interna

Os capilares são revestidos por uma membrana basal que ancora suas células endoteliais à matriz intersticial adjacente. O endotélio dos capilares é rodeado, em intervalos irregulares, por células chamadas pericito. Há controvérsias se os pericitos exercem papel regulador no fluxo sangüíneo dos capilares, pós-capilares e vênulas, mas a presença de actina, miosina e tropomiosina sugere capacidade contrátil (Schroder, Brad *et al*., 1990).

Os vasos da retina de humanos e animais são caracterizados por células endoteliais contínuas, não fenestradas, com junções intercelulares impermeáveis, que se apresentam para formar a BHR. A interação entre as células endoteliais forma a barreira que permite ao tecido, criarem condições para um tecido com integridade funcional. Há duas vias de permeabilidade vascular, o transporte paracelular o qual envolve as proteínas de junções e o transporte transcelular mediado por vesículas endocíticas. A junção intercelular representa um pequeno poro (9 a 11nm) que é responsável pelas trocas transcapilares de água e outras moléculas hidrofílicas menores que 15Å. Há três tipos de junções intercelulares que fazem essa mediação no endotélio: as junções ou zonas de oclusão (*tight junctions*), as zonas de adesão e as junções *gap* (Schroder, Brad *et al*., 1990; Cormack, 1996).

As proteínas de junção envolvidas no transporte paracelular, ou seja, situadas no espaço intercelular da célula endotelial da retina são as *tight junctions* (ocludina, claudina, proteínas de junções de adesão (JAMs), proteínas de adesão seletiva da célula endotelial (ESAM) e NECTIN) e as de zônulas de oclusão (ZO-1). As caderinas (VE-caderina e N-caderina) e a ß-catenina, também presentes na retina, são proteínas de junção de adesão dependente do cálcio que permitem a ligação entre as células vizinhas.

O transporte de vesículas transcelular, envolve as seguintes proteínas: caveolina-1 (CAV-1), dinamina (Dnm), flotilina (FLOT), proteínas de membrana associada a vesículas (PV) e proteínas do complexo SNARE: Pacsina, NSF, SNAP, VAMP (Klaassen, Hughes *et al*., 2009).

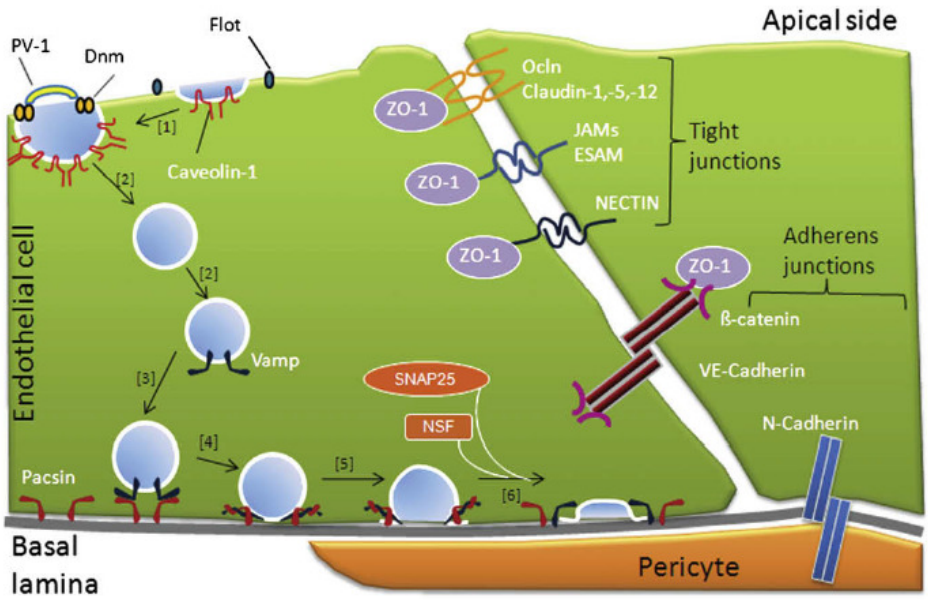

Figura 5. Esquema de localização de proteínas envolvidas no transporte intracelular e paracelular na barreira hemato-retiniana interna (Klaassen, Hughes *et al*., 2009).

1.1.3. A Barreira Hemato-Retiniana Externa

O EPR é uma monocamada de células pigmentadas situada na interface entre a retina neural e a coróide. A membrana apical do EPR conecta-se com os segmentos dos fotorreceptores e a membrana basolateral com a membrana de Bruch, que separa o EPR do endotélio fenestrado da coriocapilar. A polaridade apical-basolateral do EPR é determinado pela estrutura, organização de organelas e distribuição das proteínas de membrana. Na porção apical, o EPR estende microvilosidades longas, e na porção basolateral, a membrana possui dobraduras profundas. A maioria das mitocôndrias estão localizadas próximas ao lado basolateral (Marmorstein, 2001).

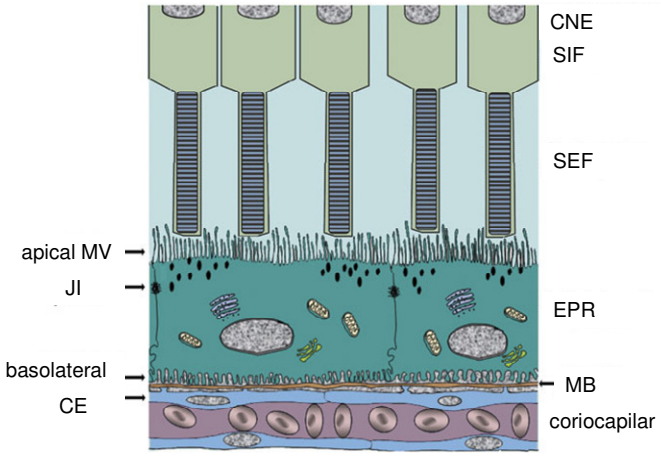

Figura 6. Desenho representativo do epitélio pigmentado da retina (EPR). Na porção apical, o EPR estende microvilosidades (MV) longas que se conectam com os segmentos dos fotorreceptores, e na porção basolateral possui dobraduras profundas que se conectam com a membrana de Bruch (MB), que separa o EPR do endotélio fenestrado da coriocapilar. **CNE:** camada da nuclear externa; **SIF:** segmento interno dos fotorreceptores; **SEF:** segmento externo dos fotorreceptores; **JI:** junções intercelulares; **CE:** células endoteliais (Adaptado de Sonoda, Spee *et* al., 2009).

Além da função de barreira, o EPR participa nos seguintes processos: 1) transporte principal de fluxo de nutrientes entre a retina neural e a coriocapilar, onde transporta íons, água e produtos metabólicos do espaço sub-retiniano para a coróide (Dornonville de la Cour, 1993; Hamann, 2002; Marmor. 1999) e na outra direção, o EPR transporta glicose, retinol e ácidos graxos do sangue para as células fotorreceptoras (Ban e Rizzolo, 2000; Baehr, Wu *et al*.,, 2003; Bazan, Gordon *et al*.,1992); 2) na absorção de luz e proteção contra oxidação fotoquímica (Bok, 1993); 3) na reisomerização da forma de all-trans-retinal para 11-cis-retinal, que é um elemento-chave do ciclo visual (Steinberg, Linsenmeier *et al*., 1983); 4) na fagocitose dos discos de membranas que são transmitidos pelos segmentos externos dos fotorreceptores (Finnemann, 2003); 5) na liberação de fatores tróficos para a retina neural, promovendo a diferenciação e sobrevivência dos fotorreceptores e a integridade estrutural da retina

(Adamis, Shima *et al*., 1993); 6) no estado "imune privilegiado" do olho (Ishida, Panjwani, *et al*., 2003; Streilein, Ma, *et al*., 2002).

A importância das junções intercelulares no transporte paracelular e das vesículas endocíticas no transporte transcelular no EPR é semelhante ao endotélio. No entanto, o transporte entre a retina neural e a coriocapilar, e vice e versa, é bastante complexo.

A retina neural produz uma grande quantidade de água derivada principalmente como conseqüência do grande fluxo metabólico dos neurônios e células fotorreceptoras. Portanto, é necessária a remoção constante de água da retina (Hamann, 2002; Marmor MF. Eye, 1990). A água na retina interna é transportada pelas células de Muller (Nagelhus, Horio *et al*., 1999) e a água no espaço sub-retiniano é eliminado pelo EPR. Além disso, o transporte de água é necessário para a interação estrutural da retina com os seus tecidos de suporte no estabelecimento de uma força adesiva entre o EPR e a retina (Kita e Marmor, 1992). A enzima Na^+-K^+-ATPase, localizada na membrana apical, fornece a energia o transporte transepitelial (Marmorstein, 2001; Gundersen, Orlowski *et al*., 1991) e estabelece um gradiente para o sódio do espaço extracelular para o espaço intracelular. Na parte apical, este gradiente facilita a absorção de HCO^-_3 via co-transporte de Na^+- HCO^-_3 e absorção de K^+ and Cl^- via the Na^+-K^+-$2Cl^-$ co-transporte (Adorante e Miller, 1990). O transporte de água ocorre principalmente via transcelular conduzido pelo transporte de Cl^- e K^+(Frambach, Valentine *et al*, 1989). Em uma recente publicação foi detectada a expressão da proteína funcional aquaporina-1 no EPR que também facilita o transporte transepitelial de água (Stamer, Bok *et al*., 2003).O principal produto removido pelo EPR produzido pelos fotorreceptores é o ácido lático (Adler e Southwick, 1992).

Na outra direção, o EPR transporta glicose e outros nutrientes do sangue para os foterreceptores. Para o transporte da glicose, o EPR contém quantidades elevadas de transportadores de glicose em ambas as membranas, apical e basolateral. Ambos GLUT1 e GLUT 3 são altamente expressos no EPR (Ban e Rizzolo, 2000; Bergersen, Jóhannsson *et al* ., 1999; Senanayake , Calabro *et al*., 2006). Outra função importante do EPR é o transporte de retinol para garantir o fornecimento para os fotorreceptores. Esta interação é responsável pelo processo de ciclo visual onde all-trans-retinol (vitamina A) fornecido aos fotorreceptores é removido pelo EPR, convertido em 11-cis-retinal e liberado novamente para os fotorreceptores onde se liga a opsina e inicia a cascata de fototransdução (Baehr, Wu *et al.*, 2003). O transporte de ácido docosahexaenóico para os fotorreceptores também é importante para a função visual (Bazan, Gordon *et al*., 1992). As membranas dos neurônios e fotorreceptores assim como as membranas dos discos dos fotorreceptores são seletivamente construídas a partir de fosfolipídios altamente enriquecidos com ácido docosahexaenóico (Anderson, O'Brien *et al.*, 1992). Este composto não pode ser sintetizado pelos tecidos neuronais. Sendo assim, o tecido neuronal é dependente do transporte de ácido docosahexaenóico pelo EPR.

As junções intercelulares formam a barreira entre o espaço subretiniano e a coriocapilar (Ban e Rizzolo, 2000; Kniesel e Wolburg, 1993) e são responsáveis pelo estabelecimento da polaridade (Rizzolo e Heiges,1991). As principais ocludentes ou *tight* do EPR da retina adulta são ZO-1, ocludina e claudinas 1, 2, 5, 12 (Rahner, Fukuhara *et al*., 2004). Desempenham um papel muito importante na modulação do fluxo paracelular, atuando como uma barreira semipermeável que regula a passagem de íons, solutos e água. A ocludina é uma proteína que apresenta quatro passagens pela membrana, dois loops extracelulares e os domínios C- e N-terminal intracelulares,

foram as primeiras proteínas integrais de membrana a serem identificadas nas *tight junctions* (Feldman *et al*., 2005). As claudinas compreendem uma família de proteínas com cerca de 24 membros em humanos. Possuem quatro passagens pela membrana, dois loops extracelulares e os domínios C- e N-terminal intracelulares, no entanto sem nenhuma similaridade com a ocludina. As proteínas ZOs (ZO-1, -2 e -3) fazem parte da família de proteínas guanilato quinase associadas à membrana (MAGUK), possuem domínios PDZ que permitem a interação com as proteínas integrais de membrana da junção *tight*, como JAM, ocludina e claudina, e atuam na ligação destas proteínas ao citoesqueleto (González-Mariscal *et al*., 2008).O transporte paracelular possui uma resistência 10 vezes maior do que a resistência transcelular e por isso podemos classificar o EPR como um epitélio "estreito" (Miller e Steinberg, 1977; Miller e Steinberg RH, 1977). O término da formação embriogênica das junções intercelulares coincide com início do transporte epitelial, onde EPR começa a expressar os transportadores como o transportador de glicose, o que é essencial para o transporte de glicose transepitelial (Ban e Rizzolo, 2000). A forte adesão intercelular é uma característica tissular mantida pelo complexo juncional. O complexo juncional constituído por estruturas de membrana especializadas que regulam a adesão célula-célula como as junções ocludentes, aderentes e desmossomos são essenciais para morfologia e função epitelial. Elas se conectam ao citoesqueleto (junções aderentes e *tight* se conectam a microfilamentos, e desmossomos a filamentos intermediários), estabilizando a adesão célula-célula (Braga, 2002).

Com estas funções complexas, o EPR é essencial para a função visual e, portanto, anormalidades dessas funções podem comprometer a sua função alterando a retina neural e os fotorreceptores.

1.1.4. Caveolina-1 e seu Papel Crucial na Manutenção Funcional da Barreira Hemato-Retiniana Externa

Como descrito acima, uma das proteínas envolvidas no transporte de vesículas transcelular, é a caveolina (CAV). A CAV é o principal componente estrutural das cavéolas e é composta por uma sequência helicoidal lipofílica incorporado no folheto interno da membrana plasmática com domínios citoplasmáticos ambos N - e C - terminais. O domínio N-terminal liga-se a moléculas de sinalização que são necessárias para a multimerização da CAV. A cavéola possui papel fundamental em processos de endocitose independente da clatrina, transcitose, sinalização de cálcio e de outros eventos de sinalização celular. A compreensão do tráfico de CAV e a formação da cavéola tem sido crucial para a investigação de seu papel em diversos tipos celulares (Parton e Simons, 2007).

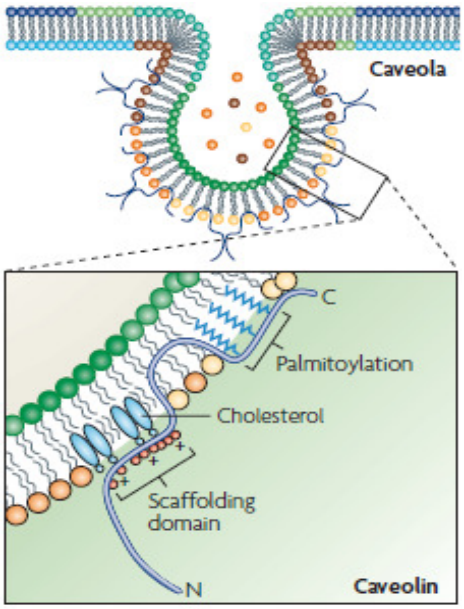

Figura 7. Desenho representativo de uma cavéola que se apresenta invaginado na membrana plasmática e seu principal componente estrututal, caveolina (CAV), envolvida no tráfego transcelular e sinalização celular. A CAV apresenta domínios citoplasmáticos N- e C-terminais. O domínio N-terminal liga-se a moléculas de sinalização que são necessárias para a multimerização da CAV-1 (Parton e Simons, 2007).

As junções intercelurares são relativamente ricas em colesterol (Feltkamp e Van der Waerden, 1983). A CAV - 1 foi identificada como um dos componentes dos microdomínios de membrana das junções intercelulares ao longo de uma década por Nursrat e colaboradores (Nusrat, Parkos *et al*., 2000). Muitos estudos demonstraram evidências do envolvimento da CAV- 1 na regulação da permeabilidade endotelial (Schubert, Frank *et al*, 2001; Bauer, Yu *et al*., 2005) e na endocitose da junção intercelular ocludina em células epiteliais do intestino (Marchiando, Shen *et al*., 2010). Modificações pós-translacionais da CAV-1 no domínio N-terminal estão envolvidas no seu tráfego exacerbado, como a ubiquitinação (Kirchner, Bug *et al*., 2013) e fosforilação (Takeuchi, Morizane *et al*., 2013).

A CAV-1 é expressa em diversos tipos celulares da retina: fotorreceptores (Kachi, Yamazaki *et al*., 2001), EPR (Mora, Bonilha *et al*.,2006), células gliais de Müller (Roesch, Jadhav *et al*., 2008) e células vasculares (Feng, Venem *et al*., 1999).Um estudo recente com camundongos *knock-out* para CAV-1 demonstrou a sua importância fundamental na manutenção funcional do EPR, que não foi dependente dos fotorreceptores, mas sim a um distúrbio no microambiente do espaço sub-retiniano como diminuição na absorção de íons, aumento da adesão do EPR na superfície da retina e aumento no espaço entre células. Neste trabalho foi demonstrado que o EPR co-localiza com a Na^+-K^+-ATPase e que a ausência de CAV-1 diminuiu a afinidade de K^+ sugerindo uma diminuição na atividade Na^+-K^+-ATPase. A desregulação de Na^+-K^+-ATPase foi associado aos distúrbios no pH, fluídos e homeostase do íons pelo EPR no espaço sub-retiniano (Li, McClellan *et al*., 2012).

Sendo assim, a proteína CAV-1 possui papel fundamental na regulação de junções celulares, homeostase no espaço sub-retiniano e consequentemente na função BHR externa no EPR. No entanto, mais estudos serão necessários para a compreensão

da regulação molecular e os mecanismos envolvidos no tráfego e sinalização celular da CAV-1 em condições fisiológicas normais e patológicas.

1.1.5. O Exame Funcional da Retina

A eletrorretinografia (ERG) é um método eletrofisiológico não invasivo que registra os potenciais elétricos da resposta retiniana produzido entre a córnea e a retina frente a estímulos luminosos permitindo uma informação objetiva da função da retina. Esta técnica permite acessar a função dos diferentes tipos de células neuronais da retina e também do EPR em humano e modelos animais. A onda "a" é a primeira deflexão negativa onde se origina e representa a atividade dos fotorreceptores. A onda "b" é uma deflexão positiva gerada pelas células de Muller, que representa a atividade elétrica das células bipolares. A onda “c” (onda positiva de aparecimento bem mais tardio) está relacionada com a polarização do EPR e só pode ser observada quando é feito um ERG de flashes longos. Enquanto as ondas “a” e “b” aparecem na escala de milissegundos, a onda “c” aparece na escala de segundos. O aparecimento da onda “c” no EPR depende do fluxo de potássio das outras camadas da retina, mas o fluxo extracelular de potássio depende da fototransdução. Portanto, a onda “c” pode nos dar um panorama da fototransdução como um todo, da integridade do EPR e de sua interação com o restante da retina. A investigação da onda “c” não é rotineira, geralmente só é pesquisada quando já se sabe que há algo errado com o ERG de flash-padrão e, conseqüentemente, com a retina.

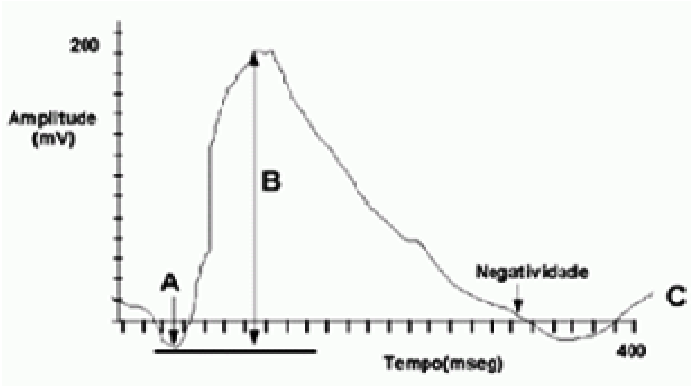

Figura 8. Exame funcional da retina. Exemplo de um eletroretinograma obtido por eletroretinografia (ERG). Amplitude da onda "A" (atividade dos fotorreceptores), amplitude da onda "B" (atividade elétrica das células bipolares) e amplitude da onda "C" (polarização do EPR).

1.2. A Retinopatia Diabética

A retinopatia diabética (RD) é uma das complicações do diabetes (DM). Atualmente è compreendida como uma doença neuronal degenerativa progressiva acompanhada por extensas alterações vasculares. Pode estar presente no DM tipo 1 e tipo 2 da doença (Arden, 2004; Zheng, Gong *et al.*, 2007). Estas complicações estão diretamente associadas ao tempo de duração do DM (Klein, Klein *et al.*,1989) e ao controle glicêmico (DCCT, 1993).

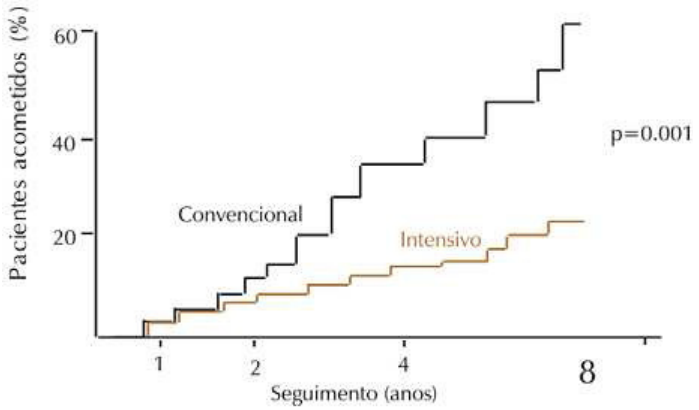

Figura 9. Efeito do controle glicêmico intensivo na progressão da RD em pacientes DM tipo 1 (DCCT, 1993).

Alguns fatores de risco são descritos associados ao desenvolvimento e progressão da RD, dentre eles destacam-se principalmente a hipertensão arterial (HA) como fator de risco independente mais importante associado à RD em pacientes com DM tipo 1 e 2 (Klein, Klein *et al*., 1998; UKPDS, 1998). Foi observado que pacientes com DM tipo 1 e HA apresentam 3 vezes mais chance de desenvolver a forma mais grave da RD, a RD proliferativa (Roy, 2000). Estudos do nosso grupo demonstraram que em modelos de RD experimental com ratos espontaneamente hipertensos (SHR) e diabéticos induzidos por estreptozotocina (STZ), a concomitância da RD e HA exacerbam parâmetros inflamatórios e oxidativos (Silva, Pinto *et al*., 2007; Silva, Pinto *et al*., 2007; Pinto, Silva *et al*., 2007; Lopes de Faria, Silva *et al*., 2011; Duarte, Silva *et al*., 2013). Outros fatores também estão associados como a dislipedemia, nefropatia diabética, tabagismo, gravidez e a genética (Mitchell e Foran, 2008).

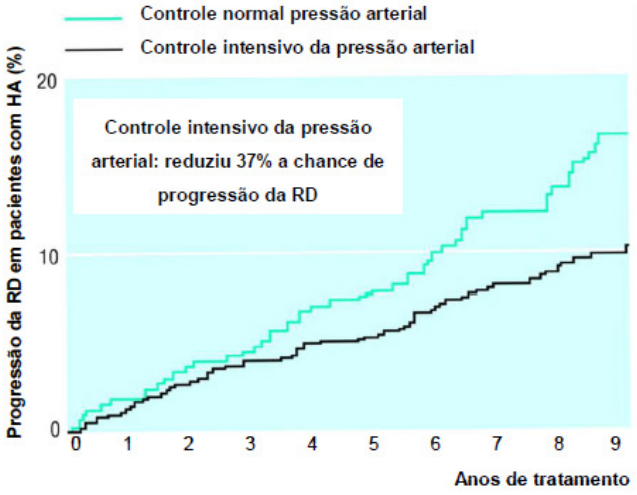

Figura 10. Tratamento intensivo da pressão arterial reduz a chance da progressão da RD em pacientes hipertensos e DM tipo 2 (UKPDS, 1998).

As possíveis causas das alterações anatômicas da retina são agrupadas em três categorias: bioquímicas, hemodinâmicas, endócrinas (Fong, Aiello *et al*., 2004). As categorias interagem entre si e apresentam sequência temporal, sendo a bioquímica a

anormalidade mais consistentemente ligada ao início destas alterações (Alder, Su *et al*., 1997).

1.2.1. Epidemiologia, Relevância e Prevalência da Retinopatia Diabética

A RD é uma das complicações mais temidas entre os pacientes com DM comprometendo a qualidade de vida. No ano de 2000, o número de indivíduos com DM no mundo foi aproximadamente 171 milhões e destes, mais de 5 milhões tornaram-se cegos devido a RD. Estima-se que até 2030 estes valores aumentem (Bragge, Gruen *et al*., 2011; Zhang , Saaddine *et al*., 2010). A RD é a principal causa de cegueira adquirida em adultos em idade produtiva nos países desenvolvidos (Wild, Roglic *et al*., 2004; Sharma, Oliver-Fernandez *et al.,* 2005). Aproximadamente 25 à 44% das pessoas com DM desenvolvem alguma forma de RD em algum momento da doença (Mitchell e Foran, 2008). Em pacientes com DM de início precoce (o que corresponde aos pacientes com DM tipo 1), a prevalência da RD aumenta com o tempo de duração do DM, sendo que após 15-20 anos praticamente todos os indivíduos apresentarão alguma forma de RD. Por outro lado, a forma proliferativa acomete apenas um subgrupo de aproximadamente 17%, que além da hiperglicemia algum outro fator seja importante para o seu desenvolvimento. No grupo de pacientes com DM de início tardio (o que corresponde aos pacientes com DM tipo 2), a RD também apresenta correlação com a duração da doença. A doença com duração de dois anos tem uma prevalência de 23% de RD, porém, atinge 80% após 15 anos de duração. A prevalência já alta no início da doença deve-se à dificuldade de detectar o seu início, uma vez que os pacientes se mantêm assintomáticos por vários anos antes do diagnóstico. Cerca de 4% dos pacientes com DM tipo 2 já apresentam RD proliferativa na ocasião do diagnóstico (Klein, Klein *et al*., 1989).

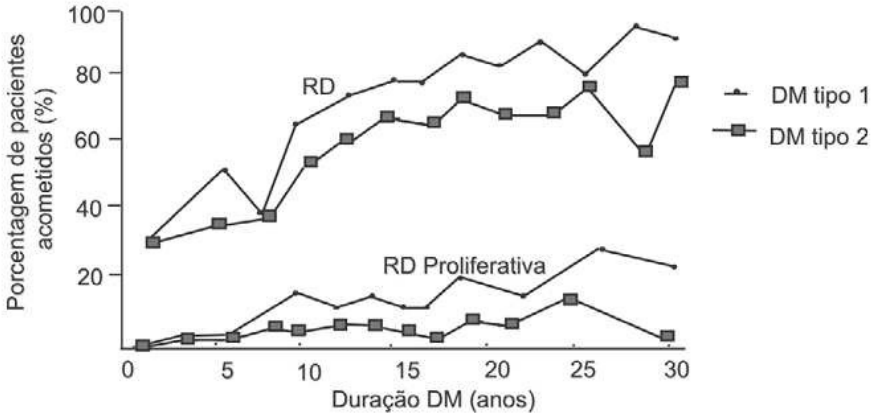

Figura 11. Prevalência de RD e RD proliferativa em pacientes com DM tipo 1 e 2 (Klein, Klein *et al*., 1989).

1.2.2. A Barreira Hemato-Retiniana Externa e a Retinopatia Diabética

A maioria das investigações sobre a patogênese da RD se detém no comprometimento da retina neural e na BHR interna formada pelas células endoteliais BRB (Frank, 2004; Jackson e Barber, 2010). No entanto, estudos têm demonstrado o importante papel da BHR externa (formada pelo EPR) no início e progressão da RD (Pautler e Ennis, 1980; Simó, Villarroel *et al*., 2010; Xu e Le, 2011). É bem documentado que alterações funcionais do EPR podem estar envolvidas em uma série de condições que comprometem a visão, como a degeneração macular relacionada à idade (Eagle, 1984), vitreoretinopatia diabética (Dorey, Wu *et al*., 1989) e RD (Vinores SA, Gadegbeku *et* al.,1989; Hewitt e Adler *et al*.,1994; Simó, Villarroel *et al*., 2010; Xu e Le, 2011).

Disfunções na função visual do EPR, avaliadas por ERG através da quantificação da diminuição da amplitude da "onda c", foram observadas em ratos com apenas 2 semanas de duração do DM induzido por STZ (Pautler e Ennis, 1980).

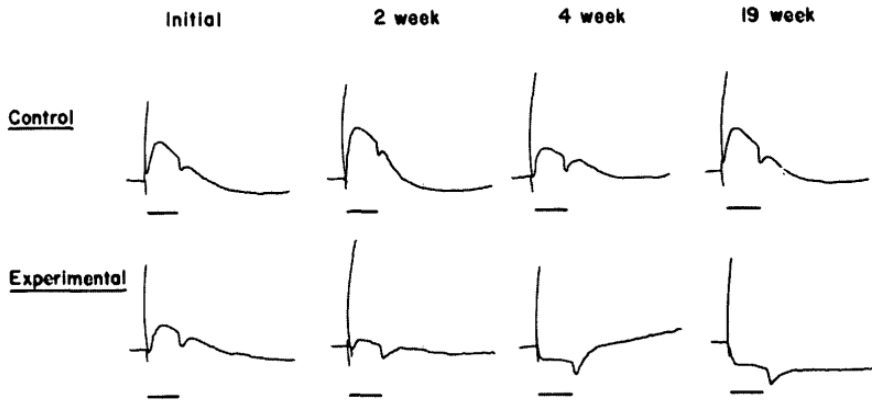

Figura 12. Eletroretinograma representativo da "onda c" obtido por exame de eletrorretinografia em ratos pigmentados (Long-Evans) observados 2, 4, e 19 semanas após a indução de DM por STZ (Pautler e Ennis, 1980).

Estudos prévios demonstraram que a alta concentração de glicose promove alterações nas funções de transporte do EPR entre coriocapilar e a retina neural ou espaço sub-retiniano para a coróide (Simó, Villarroel *et al*., 2010). Estudos anteriores demonstraram que a alta glicose promove diminuição na expressão do transportador de glucose, GLUT-1 (Kim, Lim *et al*., 2007); alterações no transporte de retinol via diminuição da proteína de ligação do retinol intersticial e do ácido ascórbico limitando o sistema antioxidante do EPR (Salceda e Contreras-Cubas, 2007; Minamizono, Tomi *et al*., 2006). Em células do EPR bovina cultivadas sob alta concentração de glicose, foi observado uma perda na função da Na^+/ K^+ ATPase, diminuindo, assim, a permeabilidade (Crider, Yorio *et* al., 1997); sendo assim, a hiperglicemia pode prejudicar o transporte de água a partir do espaço sub-retiniano aos coriocapilares e, conseqüentemente, contribuir para o desenvolvimento do edema macular diabético (Simó, Villarroel *et al*., 2010).

A expressão das junções intercelulares, presentes no EPR, responsáveis pelo controle seletivo de solutos e fluídos que atravessam a retina, também é prejudicada em condição de RD experimental *in vitro* e *in vivo* (Villarroel, Garcia-Ramirez *et al*., 2.009; Silva , Rosales *et al*., 2013; Xu e Le, 2011). No entanto, os efeitos da alta concentração de glicose ou hiperglicemia na integridade das junções intercelulares e a consequência no transporte e outras funções da BHR externa não estão completamente esclarecidos e apresentam resultados contraditórios. Foi descrito que altas concentrações glicose resultam em uma redução da permeabilidade celular acompanhado pelo aumento da resistência elétrica transepitelial (TER) em linha celular humana do EPR (ARPE-19) que foram independentes do aumento da expressão do RNA mensageiro da claudina-1 (Villarroel, Garcia-Ramirez *et al*., 2.009). No entanto, células ARPE-19 expostas sob estresse do retículo endoplasmático induzido por tunicamicina ou thapsigargin apresentou um aumento significativo na expressão das proteínas ZO-1, ocludina e claudina -1 associado com o aumento do TER (Yoshikawa, Ogata, *et al*., 2011). Por outro lado, com um ensaio de imagens microscópicas foi possível observar o aumento de macromoléculas que extravasaram a BHR externa em roedores DM induzidos por STZ (Xu e Le, 2011). Resultados recentes do nosso grupo demonstram que a linhagem celular ARPE-19 exposta a condições de alta glicose durante 24 horas apresenta uma diminuição na expressão da proteína de junção intercelular claudina-1 acompanhada do aumento de espécies reativas do oxigênio (ERO) (Silva, Rosales *et al*., 2013).

A. B.

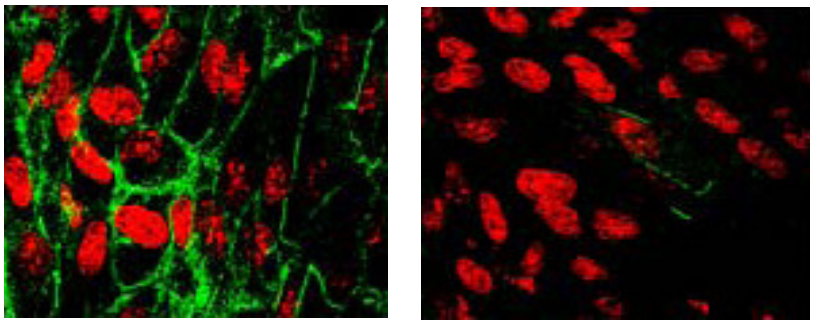

Figura 13. Fotomicrografia representativa de imunofluorescência da proteína de junção intercelular claudina-1(verde) em linhagem celular ARPE-19 exposta a concentração de glicose normal (5mM)(A) e elevada (30mM) (B) durante 24 horas. O núcleo apresenta-se em vermelho corado com iodeto de propídeo (Silva , Rosales *et al*., 2013).

A linhagem celular humana ARPE-19 apresenta as características do EPR quanto à função das junções intercelulares, habilidade de fagocitose dos segmentos externos dos fotorreceptores, polaridade, entre outras (Dunn, Aotaki-Keen *et al*., 1996; Finnemann, Bonilha *et al*., 1997; Dunn, Marmorstein *et al*., 1998). A ARPE-19 tem sido muito utilizada em estudos para avaliação da função, organização e mecanismos para compreensão da BHR externa da retina, mas poucos dados estão disponíveis a respeito da ARPE-19 em alta concentração de glicose. A maioria dos efeitos da alta concentração de glicose foi observada nesta linhagem após semanas de exposição, tais como aumento na expressão de nitrotirosina, poli ADP-ribose polimerases (PARP) (Ihnat, Thorpe *et* al., 2007); acúmulo de matriz extracelular (MEC) fibronectina (FN) e colágeno-IV (Trudeau, , Roy *et* al., 2011). No entanto, há estudos recentes que demonstram efeitos precoces da exposição à alta concentração de glicose durante 48 horas como, por exemplo, apoptose (Song, Roufogalis *et* al., 2012); diminuição da superóxido dismutase e glutationa reduzida (GSH) (Xie , Fujii *et al*., 2012); super regulação do NF-κB e TNF-α (fator de necrose tumoral alfa)/VEGF (Chen XL, Zhang *et* al., 2013).

Atualmente, foram demonstrados alguns estudos com o proteoma desta linhagem celular na presença de alta concentração de glicose onde foram observadas alterações como aumento na expressão de catepsina B, glutationa peroxidase, *heat shock protein 27* e diminuição na atividade da cobre/zinco superóxido dismutase citosólica comparados ao controle (Yokoyama, Yamane *et al*., 2006); secreção de proteínas associada ao citoesqueleto adesão/junção (tais como a proteína de ligação da galectina-3), transporte (proteína associada a resistência de múltiplos fármacos) (Chen, Chou *et al*., 2012) e mudanças na expressão de proteínas presentes no DM tipo 2 como lâmina nuclear B2, *PUMA, WTAP, ASGR1*, e proibitina 2 (Chen, Chen *et al*., 2012).

Estes achados demonstraram que a hiperglicemia ou alta concentração de glicose induzem alterações no EPR e podem estar envolvidos na patogênese da RD. No entanto, os mecanismos envolvidos nas alterações promovidas pela alta concentração de glicose não estão completamente elucidados e necessitam ser investigados, uma vez que a integridade do EPR é necessária para a homeostase dos fotorreceptores e retina neural.

1.2.3. A Bioquímica da Patogênese da Retinopatia Diabética

A patogênese da RD é complexa e multifatorial e implica em compreender como a hiperglicemia prolongada causa lesões nas células vasculares e neurais da retina. Várias vias bioquímicas têm sido propostas para explicar as lesões na retina secundárias à hiperglicemia. Esses mecanismos, que também ocorrem na nefropatia e neuropatia diabéticas, são: glicação não-enzimática de proteínas intra e extracelulares, ativação da via do poliol, aumento da atividade da proteína quinase C (PKC), lesão tecidual por aumento na produção dos radicais livres e ativação de processos inflamatórios. Esses

mecanismos atuam no processo de lesão tecidual por meio dos seus efeitos no metabolismo celular, sinalização e fatores de crescimento. Igualmente importante é compreender a origem de alterações específicas da retina, como, por exemplo, disfunções na BHR (Lopes de Faria, Silva KC *et al*., 2014).

A lesão tecidual pode ser consequência de ambas, hiperglicemia intra e extracelular. A primeira é importante particularmente em células nas quais a entrada da glicose se faz independentemente da insulina, como é o caso do nervo, o glomérulo, cristalino e retina. O aumento da glicose extracelular resulta na glicação não enzimática de proteínas, processo universal de ligação da glicose a proteínas que é dependente do nível de glicose. A ligação glicose-proteína dá origem aos produtos iniciais e avançados (*advanced glycated end-products*, AGEs) da glicação não-enzimática. Um exemplo do primeiro, que é reversível, é a glicação da hemoglobina utilizada na prática clínica como indicador da glicemia. Os AGEs interage com o receptor de AGE (RAGE) na membrana plasmática e promove a produção de espécies reativas do oxigênio (ERO). O aumento intracelular de glicose conduz um aumento da atividade mitocondrial, NADPH oxidase, PKC e promove um aumento do fluxo da via do poliol e como consequência a geração de ERO. O excesso de ERO poderá interferir em diversas vias de sinalização, ativar fatores de transcrição, aumentar fatores inflamatórios e acarretar no acúmulo de MEC. Células e consequentemente órgãos do rim, olhos e sistema nervoso sofrem mudanças fenotípicas como resultado do ERO gerado pela hiperglicemia. O aumento de ERO, também induzir ao aumento de espécies reativas do nitrogênio (ERN) que também podem ativar fatores de transcrição ou agir diretamente em proteínas, lipídeos e DNA alterando as suas funções (Calcutt, Cooper *et al*., 2009).

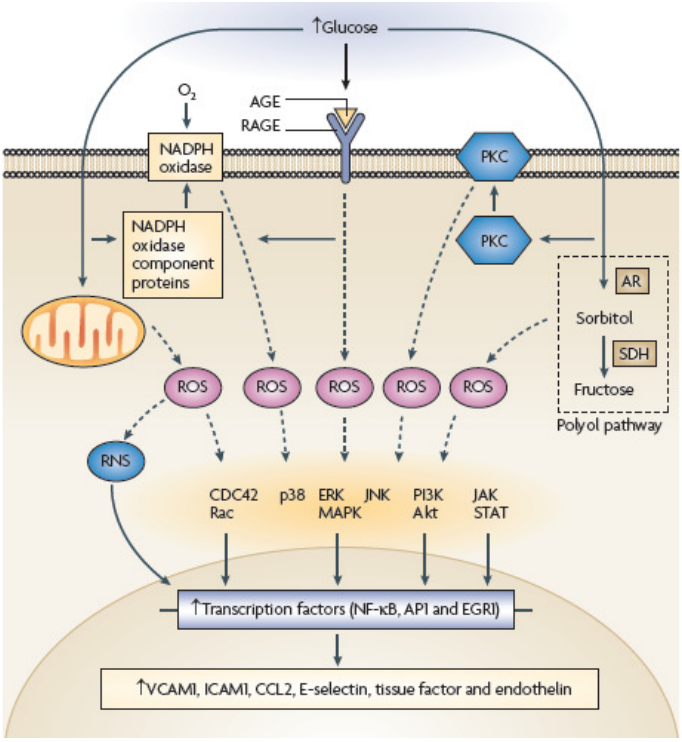

Figura 14. A hiperglicemia extracelular produz a glicação não enzimática nas proteínas e subsequente formação de AGE que interage com o receptor RAGE na membrana plasmática e promove a produção de espécies reativas do oxigênio (*reactive oxygen species*-ROS). O aumento intracelular de glicose pode atuar na via mitocondrial, aumento da atividade da NADPH, aumento da via do poliol e atividade da PKC. O aumento de ROS e RNS prejudicará em algumas vias de sinalização e nos fatores de transcrição. Como consequência ocorrerá acúmulo de moléculas de adesão, alterações de fatores vasoativos que resultará na alteração do fluxo sanguíneo e acarretará produção de proteínas de MEC (Calcutt, Cooper *et al*., 2009).

Como citado, o aumento de ERN está envolvido nas complicações patogênicas do DM. No entanto, o estresse nitrosativo per se, como resultado dos níveis elevados de óxido nítrico (NO) produzidos pela enzima óxido nítrico sintetase induzida (iNOS), está implicado na patogênese da RD (Tilton, Chang *et al*., 1993; Goldstein, Ostwald *et* al., 1996; Schmetterer, Findl *et* al.,1997; Zheng, Du *et al*., 2007).

1.3. A Biossíntese do Óxido Nítrico

Para compreendermos o papel do NO na patogênese da RD, devemos entender a sua biossíntese e fisiologia. O final do século XX é marcado por uma revolução na Biologia, ocasionada pelo radical livre que até então era mais conhecido pelos químicos como pequeno, gasoso e poluente NO. A descoberta de sua função em processos fisiológicos rendeu o prêmio Nobel para os pioneiros cientistas Furchgott, Ignarro e Murad em 1998. No entanto, Moncada também contribuiu para caracterizar as diferentes atividades fisiológicas do NO, mas não compartilhou o prêmio, pois o comitê nunca indica mais que três. Atualmente, sabe-se que o NO é uma molécula instável de sinalização celular endógena envolvida na regulação de funções fisiológicas e também de processos fisiopatológicos dependente de sua concentração, contexto celular e de sua biossíntese (Augusto, 2006). Dentre suas funções, podemos citar vasodilatação, relaxamento muscular, proliferação celular, apoptose, liberação de neurotransmissores, neurotoxicidade, citotoxicidade, diferenciação, entre outras (Griffith e Stuehr, 1995; Knowles e Moncada, 1994; Moncada e Bolanos, 2006; Schmidt e Walter, 1994).

A síntese de NO se realiza por ação de uma enzima, a óxido nítrico sintetase (NOS) a partir de uma oxidação sequencial, onde o aminoácido L-arginina é convertido em L-citrulina e ocorre liberação de produção de NO, necessitando da presença de dois cofatores, o oxigênio e a nicotinamida adenina dinucleotídeo fosfato (NADPH).

Existem três isoformas de NOS, a forma induzida (iNOS) e as constitutivas endotelial (eNOS) e neuronal (nNOS) (Rodeberg, Chaet *et al*., 1995). As isoformas constitutivas são reguladas por íons de cálcio ligados à proteína calmodulina (proteína de baixo peso molecular, que funciona como cofator) e produzem baixas concentrações (estimados na faixa de nM) de NO em um período curto. A nNOS está presente em células neuronais e musculares ligadas a proteínas de membrana e a eNOS, solúvel,

pode ser encontrada em células endoteliais, epiteliais, cardiomiócitos, certos neurônios e está localizada no complexo de Golgi e cavéolo. A forma induzida, que não depende do complexo cálcio-calmodulina produz uma grande concentração de NO (ordem de μM), 1.000 vezes maior comparado ao gerado pelas formas constitutivas (Patel, Levonen *et* al.,2000) por um longo período em resposta à estímulos inflamatórios lipopolissacarídeo (LPS), citocinas e está presente nos macrófagos, hepatócitos, astrócitos e outros. Pode ser solúvel e localizada no citosol (Augusto 2006).

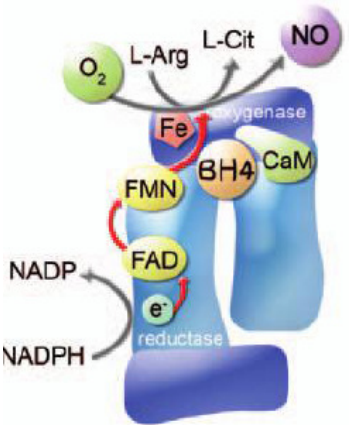

Figura 15. Esquema representativo da forma dímera da enzima óxido nítrico sintase (NOS). Biossíntese do NO: na presença de Ca^{2+}/calmodulina, a enzima NOS produz NO através da conversão da L-arginina (L-Arg) em L-citrulina (L-Cit) pela transferência de elétrons da NADPH via domínio redutase contendo flavina para o oxigênio ligado ao grupo heme do domínio oxigenase, o qual contem sítios para tetrahidrobiopterina (BH4) e L-Arg.

O NO derivado da eNOS promove vasodilatação, inibição da agregação plaquetária, inibição da aderência de leucócitos e da proliferação de células musculares lisas vasculares (Wong e Marsden, 1996). O processo de vasodilatação se dá pelo aumento do fluxo de cálcio para o interior da célula. O cálcio e a calmodulina irão ligar-se a eNOS. Esta ligação irá ativá-la e ocorrerá a catálise da transformação da L-arginina em L-citrulina e NO. Será produzida uma pequena quantidade de NO, porém suficiente para difundir-se para a musculatura lisa. Neste caso, o NO não precisa de

transportadores específicos e nem de canais específicos. Ao difundir-se para a musculatura lisa o NO irá ligar-se ao ferro do grupo prostético heme da enzima guanilato ciclase solúvel (GC), e dessa forma a reação da guanosina trifosfato (GTP) em guanosina monofosfato cíclica (cGMP) irá acontecer. A cGMP é responsável pelo relaxamento da musculatura lisa e consequente aumento do diâmetro dos vasos sangüíneos, levando ao aumento do fluxo sanguíneo e redução da pressão arterial (Moncada e Higgs,1993).

A produção neuronal de NO obtida através da nNOS é conduzida quando um neurônio ativado, libera um mensageiro químico que difunde para o neurônio vizinho e interage com receptores específicos, que ativam a célula, transmitindo, assim, o impulso nervoso. Como por exemplo, o mensageiro químico glutamato que é liberado de vesículas no neurônio pré-sináptico e liga-se ao receptor N-metil-D-aspártico (NMDA) do neurônio adjacente. Esta ligação abre um canal no receptor, admitindo Ca^{2+} para o interior da célula, onde se liga a calmodulina que age como uma subunidade para muitas enzimas de $Ca^{2+.}$ O complexo Ca^{2+}/calmodulina liga-se a forma da NOS encontrada nas células nervosas, nNOS. Esta ligação ativa a enzima, que catalisa a oxidação de L-arginina para L-citrulina e NO. O NO formado ativa então outra enzima, guanilato ciclase, pela ligação do ferro do grupo prostético heme da enzima. O NO difunde-se para o neurônio pré-sináptico ativando a guanilato ciclase naquela célula. Dessa forma, o NO pode desempenhar um papel importante nos circuitos neurais envolvidos na memória. O NO aumenta a liberação de glutamato no neurônio présináptico, estabilizando a transmissão sináptica (Moncada e Higgs, 1993).

A isoforma iNOS não requer Ca^{2+} para ativação e é sintetizada como uma nova proteína em resposta a uma mistura de citocinas. A enzima é induzida pelo LPS bacteriano e/ou citocinas sintetizadas em resposta ao LPS, notavelmente interferon-

gama, cujo efeito antiviral é explicado por essa ação. Em resposta ao interferon-gama e ao TNF-α, que atua de modo sinérgico com o interferon-alfa, seqüências do DNA do macrófago relativas à síntese da iNOS, são transcritas no núcleo para formar o RNA mensageiro, depois de processado, este mRNA é liberado para o citosol, onde será traduzido em proteína pelos ribossomos. Na presença de cofatores apropriados, a cadeia de proteína nascente enovela-se a formação da iNOS ativa. A nova enzima produzida começa imediatamente a converter L-arginina em NO e L-citrulina. O NO difunde-se livremente através das membranas celulares, o que explica adequadamente suas ações parácrinas locais sobre o músculo liso vascular ou sobre os monócitos e plaquetas que aderem ao endotélio (Rang, Dale *et al*., 2001).

1.3.1. O Estresse Nitrosativo e a Lesão Tecidual

O estresse nitrosativo é causado pelo aumento da produção excessiva de NO promovido pela isoforma iNOS. Assim que esta enzima é expressa, ela sintetiza $NO^{\bullet}$ continuamente, ao que parece até o esgotamento do aminoácido arginina. Nesta o $NO^{\bullet}$ atinge concentrações locais de ordem de μM que podem gerar ERN mais oxidantes como o radical hidroxila ($OH^{\bullet}$), íon carbonato ($CO_3^{\bullet-}$), dióxido de nitrogênio ($NO_2^{\bullet}$), peroxinitrito ($ONOO^-$). Estas espécies reativas estão também envolvidas em várias doenças crônicas não-transmissíveis como doenças cardiovasculares, diabetes, hipertensão, síndrome metabólica, artrite reumatóide e doenças neurodegenerativas (doença de Alzheimer, doença de Parkinson). A lesão tecidual ocorre, uma vez que as ERN em excesso podem reagir em proteínas, lipídeos e DNA. Destacam-se alguns exemplos de lesões teciduais promovidas por reações com as ERN: nitração da tirosina, onde o ânion $ONOO^-$ ou o radical $NO_2^{\bullet}$ reage com o resíduo do aminoácido tirosina e

formam o produto final nitrotirosina; reação do radical $OH^{\bullet}$ com a base desoxiguanosina do DNA resultando no- 8-hidroxi-desoxiguanosina (8-OH-dG) ou de sua reação com os ácidos graxos polinsaturados dos lipídeos resultado na formação de hidroxinonenal (HNE). As ERN estão associadas também a inativação enzimática, ativação excessiva de genes pró-inflamatórios como fator TNF-α, interleucinas, fator nuclear kappa beta (NF-kB), fator de crescimento transformado beta (TGF-β) (Augusto 2006; Ferrari, França, *et* al., 2009).

Doenças	Biomarcadores de dano
Câncer	MDA, razão GSH/GSSG, NO_2-Tyr, 8-OH-dG
Doença cardiovascular	HNE, razão GSH/GSSG, acroleína, NO_2-Tyr, F_2-isoprostano
Artrite reumatóide	razão GSH/GSSG, F_2-isoprostano
Doença de Alzheimer	MDA, HNE, razão GSH/GSSG, acroleína, NO_2-Tyr, F_2-isoprostano, AGE
Doença de Parkinson	HNE, razão GSH/GSSG, proteínas carboniladas, nível de ferro
Isquemia reperfusão	razão GSH/GSSG, F_2-isoprostano
Aterosclerose	MDA, HNE, acroleína, NO_2-Tyr, F_2-isoprostano, NO_2-Tyr
Diabetes mellitus	MDA, razão GSH/GSSG, proteínas S-glutationadas, NO_2-Tyr, F_2-isoprostano, AGE.

Figura 16. Espécies Reativas do Nitrogênio (ERN) – Biomarcadores de doenças em sangue humano (Valko, Leibfritz *et al*., 2007).

Outra forma direta de ação biólogica do instável NO endógeno é através da S-nitrosilação, isto é, a transferência do íon nitrosonium (NO^+) ao grupo sulfidril da cisteína na cadeia protéica com grupos tiol (C-SH ou R-SH), para formar S-nitrosotióis (SNO) que são mais estáveis. Os tióis com baixo peso molecular, tais como cisteína, glutationa (GSH) e penicilamina são moléculas candidatas para o transporto de NO no sistema biológico. A S-nitrosilação de proteínas tem sido amplamente estudada como

um protótipo de modificações pós-translacionais, redox-dependente e independente da cGMP (Stamler, Lamas *et al*., 2001), responsável por diversas ações do grupo NO em vários processos biológicos (Hess, Matsumoto *et al*., 2001).

Os SNO endógenos têm gerado considerável interesse devido à sua capacidade de agir como doadores de NO, atuar em sistemas bioregulatórios e controlar inflamação. Discute-se se existem mecanismos transportadores análogos em mamíferos, como proteínas contendo cisteína e/ou grupo sulfidril–SH, permitindo a atuação do NO fora do seu local de síntese. Foram demonstradas aproximadamente mais de 100 proteínas S-nitrosiladas *in vitro*, em cultura de células e *in vivo*. E muitas destas proteínas, a S-nitrosilação esteve associada com às alterações funcionais, tais como vasodilatação, inflamação, e neurodegeneração (Stamler, Simon *et al*., 1992). Recentemente a S-nitrosilação e denitrosilação tem sido reconhecida como um componente regulatório de tradução de sinal comparado com a fosforilação e defosforilação (Mannick e Schonhoff, 2002; Liu, Yan *et al*., 2004).

1.3.2. O Estresse Nitrosativo na Patogênese da Retinopatia Diabética

Todas as isoformas da NOS são expressas na retina (Park, Pardhasaradhi *et al*., 1994). No cenário diabético, o aumento da produção de NO como resultado da indução de iNOS está associado a resposta inflamatória, bem como o aumento do estresse oxidativo, nas retinas de modelos experimentais (Du, Sarthy *et al*., 2004).

O aumento de ERN provenientes da super regulação da iNOS pode promover lesões teciduais como citado acima, ocasionados por exemplo por danos no DNA, e consequentemente, ativação de enzimas reparadoras de DNA, como as Poli ADP-ribose polimerases (PARPs). A PARP-1 é responsável pela organização espacial e temporal do reparo do DNA. Em resposta à fragmentação do DNA, ela transfere unidades de ADP

ribose do NAD^+ para as proteínas nucleares. Esta transferência é considerada uma modificação pós-translacional que recebe o nome de poli (ADPribosil)ação. A intensa poli ADP-ribosilação resulta em níveis elevados de apoptose, pois aumenta o consumo de NAD^+ celular que acarreta na depleção de NAD+ e ATP. A PARP-1 irá induzir a morte celular independente da caspase, a qual envolve a liberação da proteína indutora de apoptose (AIF), flavoproteína, da mitocôndria (Yu, Wang *et al*., 2002). Como as caspases não estão envolvidas neste processo, a PARP-1 se mantém intacta para ser ativada pelo DNA fragmentado, o que resulta na síntese excessiva de PAR, NAD^+, esgotamento de ATP e, finalmente, morte celular. Sua ativação contribui para a formação de pericitos fantasmas e capilares acelulares, (Zheng, Szabo *et al*., 2004), aumento da adesão de leucócitos nas células endoteliais (Sugawara, Hikichi *et al*., 2004), formação de VEGF (Obrosova, Minchenko *et al*., 2004) e angiogênese (Tentori, Lacal *et al*., 2007). Na RD, dentre as características iniciais, observa-se o aumento da produção de fatores vasoativos, como a endotelina 1 (ET-1) e o aumento da síntese de proteínas de MEC como a FN (Xu, Chiu *et al*., 2008).

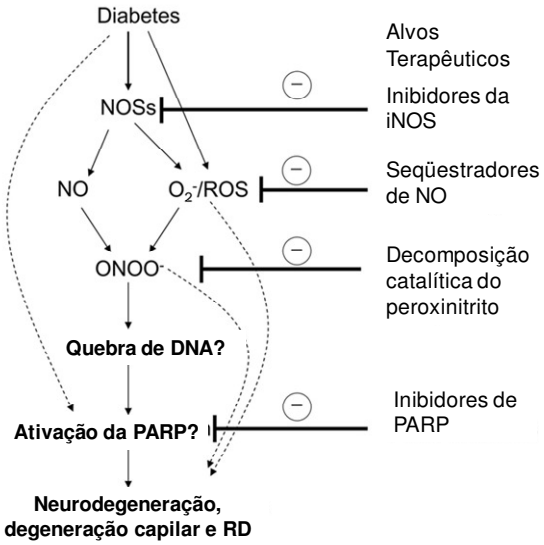

Figure 17. Papel postulado da contribuição do estresse oxidativo e nitrosativo no desenvolvimento da RD (Zheng e Kern, 2009) e abordagens terapêuticas.

Estudos têm demonstrado que o NO é responsável pela neurotoxicidade, pelo menos em parte, da retina após a injúria causada pela isquemia e reperfusão (Neufeld, Kawai *et al*., 2002). Em um estudo realizado com camundongos DM induzidos por STZ e *knock out* para $iNOS^{-/-}$, foi demonstrado a prevenção do aumento de metabólitos de NO, nitração de proteínas e ativação da PARP seguido posteriormente da preservação dos compartimentos vasculares (Zheng, Du *et al*., 2007). Em estudos publicados pelo nosso grupo, demonstramos o aumento da expressão da iNOS acompanhada do aumento na concentração dos metabólitos do NO e formação de nitrotirosina na retina de ratos espontaneamente hipertensos com apenas 20 dias de duração de DM (Rosales, Silva *et al*., 2010). Foi demonstrado em retinas de pacientes com DM e com retinopatia não proliferativa, maior imuno-reatividade da iNOS localizada na camada nuclear interna, provavelmente em células gliais de Müller, em comparação com indivíduos sem DM e sem doença ocular (Abu El-Asrar, Desmet *et al*., 2001). Além disso, metabólitos finais estáveis do NO (nitritos e nitratos) foram significativamente elevados no vítreo de pacientes com RD proliferativa em comparação com o grupo controle (Hernández, Lecube *et al*., 2002). Estudos também mostraram que a inibição química de iNOS ou o *knock out* para iNOS, na retina isquêmica preveni a angiogênese localmente na retina avascular, mediada pelo menos em parte, pela regulação negativa do receptor do fator de crescimento endotelial vascular VEGF 2 (VEGFR2). Ao mesmo tempo, a neovascularização da retina patológica foi consideravelmente mais forte nos animais que expressam iNOS, mostrando que a iNOS desempenha um papel crucial na doença neovascular da retina

(Sennlaub, Courtois *et al*., 2001). Estes dados sugerem que as altas concentrações de NO produzido principalmente pela iNOS podem contribuir para a patogênese de RD.

1.3.3. O Estresse Nitrosativo no Epitélio Pigmentado da Retina

O EPR da retina constitui parte da BHR externa e é responsável pelo estado "imune privilegiado" do olho e em resposta a citocinas inflamatórias como o TNF-α, produz NO (Holtkamp, Kijlstra *et al*., 2001). Não há muito estudos investigativos relacionados ao estresse nitrosativo promovido pela hiperglicemia ou concentrações elevadas de glicose no EPR e seu envolvimento na patogênese da RD.

Já foi descrito, que camundongos com DM induzidos por STZ e células ARPE-19 expostas sob alta concentração de glicose, apresentam redução na expressão e atividade do transportador de folato associado a níveis elevados de NO independente da ativação do c-GMP (Naggar, Ola *et al*., 2002). Outro estudo experimental *in vivo* demonstrou que em ratos com DM também induzidos por STZ, há um aumento nos níveis de NO na retina e no EPR e, no entanto, o aumento do transporte e consumo de arginina ocorre somente no EPR comparados aos controles sugerindo a importância do EPR no desenvolvimento da RD via NO (Salceda, Hernández-Espinosa *et al*., 2008). A elevada produção de metabólitos do NO acompanhada com aumento da expressão iNOS e nitrotirosina em ARPE-19 exposta a alta concentração de glicose esteve associada a ativação dos sistema p38MAPK e ERK (Yuan, Feng *et al.,* 2008).

Sendo assim, as informações descritas na literatura indicam que o EPR pode ser a fonte principal ou contribuir para o estresse nitrosativo presente na retina na

patogênese da RD. No entanto, mais estudos serão necessários para a compreensão dos mecanismos.

1.4. Mecanismos Proposto para Inibição da iNOS

Como discutido, o aumento da expressão da iNOS está implicado nos efeitos da hiperglicemia no EPR e esta relacionado a patogênese da RD e por isso do interesse como um alvo terapêutico. Muitos mecanismos têm sido propostos para a sua modulação, sejam direta ou indiretamente.

Dentre os diversos mecanismos, já foi demonstrado que mecanismos de modificação pós-translacional da proteína i-NOS, como auto S-nitrosilação, ocorrem para promover a sua inibição e auxiliar sua no controle da produção excessiva de NO em condições de estresse celular (Rosenfeld, Bonaventura *et al.*,, 2010). Um possível mecanismo também de modificação pós-translacional de proteína, que possivelmente inibiria a alta atividade da iNOS, seria a S-glutationilação. Em condições de estresse oxidativo, a S-glutationilação pode ocorrer através da troca de tiol-dissulfeto entre uma proteína alvo com a glutationa oxidada (GSSG) ou a da reação da glutationa reduzida (GSH) com os grupos tióis proteicos oxidados (Ying, Clavreul *et al*., 2007; Hill e Bhatnagar, 2007). Em um estudo recente com a isoforma e-NOS isolada, confirmou-se que o tratamento com GSSG induz a S-glutationilação da proteína eNOS resultando na diminuição de sua atividade e produção de NO promovido pelo seu desacoplamento em sua forma dímera. Através de sua cristalização e ensaios com espectrometria de massa foi possível identificar o sítio de S-glutationilação da proteína (PrS-SG), Cys 689 e Cys 908, no domínio redutase contendo flavina (FAD-FMN). A alteração destes resíduos

interferiu no alinhamento FAD-FMN interrompendo a transferência de elétrons entre as flavinas e aumentando a sua accessibilidade solvente, de modo que o O_2 pode obter acesso e aceitar um elétron da flavina reduzida, resultando na formação de $O_2^{\bullet-}$ (Chen, Wang *et al*., 2010). O aumento da S-glutationilação da eNOS e diminuição de sua atividade também foi demonstrado *in vivo* em tecido da aorta em ratos diabéticos (Schuhmacher, Oelze *et al*., 2011). Estes dados sugerem que a S-glutationilação da eNOS diminui a sua atividade e promove efeitos deletérios em sua função fisiológica como a vasodilatação. No entanto, a indução da S-glutationilação da iNOS pode ser vista como forma positiva, sendo que a sua inibição é considerada um alvo terapêutico na patogênese de diversas doenças.

Outra forma clássica de inibição da iNOS seria através da modulação do TNF-α. E uma maneira de promover esta modulação, seria através do uso de agonistas de receptores opióide. A família de receptores de opióide é composta por 3 tipos, os receptores μ-, δ- e k- que respondem a alcalóides opióides clássicos, tais como a morfina e a heroína, assim como a ligantes peptídicos endógenos como as endorfinas. Eles pertencem à superfamília de receptores acoplados à proteína G, e são excelentes alvos terapêuticos para o controle da dor (Pradhan, Befort *et al*., 2011). Recentemente foi demonstrado que a estimulação do receptor opióide com o agonista morfina promove a supressão de TNF-α. na retina em modelo de ratos com isquemia/reperfusão e o pré-tratamento com o antagonista, naloxone, reverte este efeito (Husain, Liou *et al*, 2011).

Baseado nestes achados, os dois mecanismos propostos acima têm como alvo terapêutico a inibição da iNOS, no entanto em mecanismos diferentes. O sucesso de ambos será dependente do "agente indutor" (tratamento) escolhido. No caso da

modificação pós-translacional, o agente deverá promover a S-glutationilação, e no caso da modulação do TNF-α, o agente devera estimula o receptor opióide.

1.4.1 A S-Nitrosoglutationa (GSNO) como Agente Indutor de S-glutationilação e Inibição da iNOS

A existência de formas de transporte mais estáveis do NO endógeno tem sido postulada para aumentar a meia vida do NO *in vivo* (Liu, Rudd *et al*., 1998). Tióis com baixo peso molecular, tais como a cisteína, glutationa reduzida (GSH) e penicilamina são os principais candidatos para carrear moléculas e podem formar SNO em reação com óxidos de nitrogênio (Stamler, Lamas *et al*., 2001). A S nitrosoglutationa (GSNO), formada pela reação de S- nitrosilação do NO com GSH no ambiente extracelular é o SNO mais abundante e é uma das formas mais importantes do NO *in vivo*. Devido à capacidade da GSNO modular sinalização celular através de modificações pós-translacional de proteínas S-nitrosilação e/ou S-glutationilação, a GSNO é um grande candidato para a indução de S-glutationilação da i-NOS.

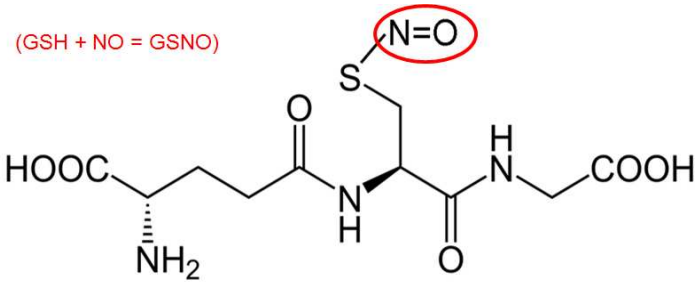

Figura 18. A molécula de GSNO obtida através da reação de S-nitrosilação entre a GSH e o NO.

A GSNO é um composto relativamente estável, e a sua degradação requer reações químicas e/ou enzimáticas, que podem ser tiol e metal-dependente (Hogg, 2002;

Singh, Wishnok *et al*., 1996; Zeng, Spencer *et al*., 2001). A degradação enzimática mais importante é a redução da GSNO a glutationa oxidada (GSSG) e amônia (NH_3) dependente da glutationa desidrogenase formaldeído ou álcool desidrogenase III (ADH III), também denonimada GSNO redutase (GSNO-R). Esta enzima oxida o NADH para NAD^+ e converte a GSNO em glutationa S-hidroxisulfonamida (GSNHOH), que por sua vez é convertida em GSSG.

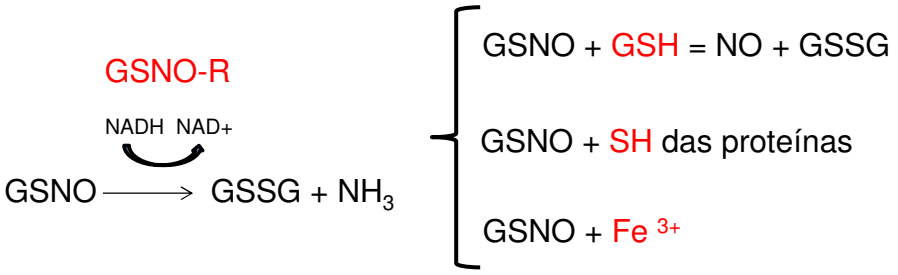

Figura 19. As diversas formas de degradação do GSNO. A GSNO-R é a principal enzima responsável pela sua denitrosilação, através do consumo de NADH, reduz o GSNO a GSSG e NH_3. O GSNO pode diretamente reagir com tióis como a GSH resultando na produção de NO e GSSG e também podem agir diretamente com os grupos tióis das proteínas. O GSNO possui alta afinidade com o Fe^{3+}.

A GSNO-R é altamente conservada entre bactérias e seres humanos e é amplamente expressa em organismos. Os níveis de GSNO-R influenciam significativamente o nível de proteínas S-nitrosiladas (Hedberg, Griffiths *et al*., 2003; Liu, Hausladen *et al*., 2001). Sua atividade redox depende das concentrações da razão $NADH/NAD^+$.

A GSNO tem sido utilizada como terapêutico em estudos com modelo de inflamação. Foi demonstrado que a administração do GSNO conferiu proteção em modelo experimental de isquemia cerebral através da regulação da expressão da iNOS e NF-kB (Khan, Sekhon *et al*.,2005). Há poucos estudos com a retina relacionados ao GSNO e nenhum demonstrando sua atuação na RD. Um estudo prévio demonstrou efeitos terapêuticos do GSNO em modelo experimental de uveite autoimune, onde a

administração oral promoveu a diminuição dos níveis de mediadores inflamatórios associados com a "manutenção" histológica e funcional da retina (Haq, Rohrer *et al*, 2007).

Baseado em todas estas informações e principalmente na sua capacidade de induzir modificações pós-translacionais de proteína como a S-glutationilação, o GSNO é um possivel candidato sintético para modular a expressão da iNOS em situações de estresse nitrosativo.

1.4.2. O Cacau como Agente Supressor de TNF-α e Inibidor da iNOS

Outro candidato proposto para atuar na inibição da iNOS via TNF-α, é o natural cacau, rico em flavonóides (a maior subclasse dos polifenóis) e com propriedades anti-inflamatórias (Selmi, Mao *et al.*, 2006). O cacau e seus derivados têm sido consumidos pelos humanos desde 460 AC e era considerado como um alimento dos deuses e a cura da humanidade (Dillinger, Barriga *et al.*, 2000).

O cacau tem despertado muita atenção devido ao seu significativo conteúdo de polifenóis. O cacau e seus produtos, ou seja, licor de cacau, cacau em pó e os chocolates podem apresentar propriedades antioxidantes dependente do conteúdo dos predominantes flavonóides, catequina e epicatequina. Além disso, a presença de metilxantinas, peptídeos, fibras e minerais pode sinergicamente aumentar ou reduzir as propriedades antioxidantes do cacau e seus produtos. Nos últimos dez anos, pelo menos 28 estudos em humanos foram realizados utilizando diferentes produtos derivados do cacau (Jalil e Ismail, 2008). Dentre elas, destacam-se o seu efeito protetor nas seguintes linhas de pesquisa: regulação da pressão arterial, diabetes, efeito anti-envelhecimento e prevenção de arteriosclerose (Latif, 2013).

Os dados epidemiológicos sobre os efeitos benéficos do chocolate veio da população indígena Kuna das ilhas do Panamá. Esta população era caracterizada por uma baixa prevalência de aterosclerose, diabetes tipo 2 e hipertensão. O "segredo" por trás disso era a ingestão diária da bebida caseira feita com cacau pelos índios Kuna. Estes traços desapareceram após a migração para as áreas urbanas no Panamá continental devido a alterações posteriores na dieta, como um menor consumo de cacau, sendo este industrializado (McCullough, Chevaux *et* al., 2006). Estudos demostram que 6,3 g (30 kcal) por dia de "chocolate escuro" contendo 30 mg de polifenóis são suficientes para reduzir a pressão arterial em pacientes hipertensos (Taubert, Roesen *et al*., 2007).

A epicatequina é o polifenol mais abundante encontrado no cacau e no "chocolate escuro" (com alta porcentagem de cacau) e é conhecida pelo seu papel antioxidante (Ramiro-Puig e Castell, 2009) e de proteção cardiovascular (Taubert, Roesen *et al*., 2007). Estudos *in vitro* demonstram a alta afinidade de flavonóides com receptores opióide (Katavic, Lamb *et al*., 2010). Já foi demonstrado que a epicatequina induz proteção cardíaca dependente da estimulação do receptor opióide-δ (Panneerselvam, Tsutsumi *et* al.,2010).

Sendo assim, o cacau enriquecido com polifenóis, é um candidato natural proposto para modular o TNF-α e controlar a expressão da iNOS via receptor opióide-δ.

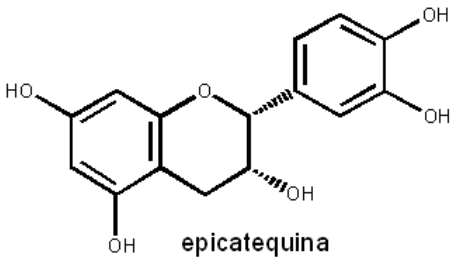

Figura 20. Estrutura molécular do flavonóide epicatequina encontrado no cacau.

1.4.3 Justificativa

Baseado nestes dados, a investigação do estresse nitrosativo no EPR é importante na compreensão da patogênese da RD em fases precoces. Novas modalidades terapêuticas para o tratamento da RD são desejáveis. Nos estudos desenvolvidos, investigamos a iNOS como um possível alvo terapêutico no desenvolvimento da RD e os mecanismos propostos para a sua inibição, modificação pós-translacional e/ou modulação são diferentes estratégias que no futuro poderão ser testadas.

2-OBJETIVOS

Como decrito na literatura, o DM promove o estresse nitrosativo através do aumento da expressão da proteína iNOS e produção de NO em modelo de RD. Este mecanismo pode estar associado as alterações precoces na BHR externa na condição de RD. O objetivo dessa pesquisa foi verificar os mecanismos nitrosoativos envolvidos na patogênese da RD e os possíveis alvo-terapêuticos para esta condição, em modelos *in vivo* e *in vitro.*

OBJETIVOS ESPECÍFICOS

ARTIGO I: O objetivo deste trabalho foi avaliar os efeitos do tratamento tópico (colírio) com um composto sintético, GSNO, em modelo de RD experimental *in vivo* na modulação da expressão da iNOS. Os mecanismos foram investigados através dos estudos *in vitro* com células ARPE-19 expostas a alta concentração de glicose.

ARTIGO II: O objetivo deste estudo foi avaliar o efeito do cacau com baixo ou alto teor de polifenol na proteção da integridade das junções intercelulares via modulação da expressão da iNOS em modelo *in vitro* com células ARPE-19 submetidas a concentrações elevadas de glicose.

3-CAPÍTULOS

3.1-CAPÍTULO I

ORIGINAL ARTICLE

S-Nitrosoglutathione inhibits inducible nitric oxide synthase upregulation by redox post-translational modification in experimental diabetic retinopathy

Mariana Aparecida B. Rosales[1], Kamila Cristina Silva[1], Diego A. Duarte[1], Marcelo G. de Oliveira[2], Gabriela Freitas Pereira de Souza[2], Rodrigo Ramos Catharino[3], Mônica Siqueira Ferreira[3], Jose B. Lopes de Faria[1], Jacqueline M. Lopes de Faria[1]

[1]Renal Pathophysiology Laboratory and Investigation on Diabetes Complications, School of Medical Sciences (FCM), University of Campinas (UNICAMP), Campinas, São Paulo, Brazil, Zip Code 13083-877.

[2]Institute of Chemistry, University of Campinas (UNICAMP), Campinas, São Paulo, Brazil, Zip Code 13083-887.

[3]INNOVARE Biomarkers Lab, Medicine and Experimental Surgery Department, FCM, University of Campinas (UNICAMP), Campinas, São Paulo, Brazil, Zip Code 13083-877.

Running head: iNOS post-translational modification by GSNO in DM retina.

Corresponding author: Jacqueline M. Lopes de Faria, MD, PhD; Faculty of Medical Sciences, University of Campinas (UNICAMP), Campinas, SP, Brazil. Phone: +55-19-35217499 / Fax: +55-19-35217366; email: jmlfaria@fcm.unicamp.br

Word count: 4249 words

Number of references: 54

Number of grayscale illustrations: 3

Number of color illustrations: 6

Abstract

Purpose: Diabetic retinopathy (DR) is associated with nitrosative stress. The purpose of this study was to evaluate the beneficial effects of S-nitrosoglutathione (GSNO) eye drop treatment on an experimental model of DR. ***Methods:*** Diabetes (DM) was induced in spontaneously hypertensive rats (SHR). Treated animals received GSNO eye drop (900nM or 10μM) twice daily in both eyes for 20 days. The mechanisms of GSNO effects were evaluated in human retinal pigment epithelium (RPE) cell line (ARPE-19). ***Results:*** In animals with DM, GSNO decreased inducible nitric oxide synthase (iNOS) expression and prevented tyrosine nitration formation, ameliorating glial dysfunction measured with glial fibrillary acidic protein, resulting in improved retinal function. In contrast, in non-diabetic animals, GSNO induced oxidative/nitrosative stress in tissue resulting in impaired retinal function. Nitrosative stress was markedly present in RPE layer accompanied by *c*-wave dysfunction and the *in vitro* study confirmed that high glucose (HG) condition, increased nitric oxide production, accompanied by iNOS upregulation and tyrosine nitration. Also, it was demonstrated decreased GSNO and reduced glutathione levels and GSNO reductase expression. Treatment with GSNO under HG condition counteracted nitrosative stress due to iNOS downregulation by S-glutathionylation. This post-translational modification was probably promoted by the release of oxidized glutathione through GSNO denitrosylation via GSNO-R. In contrast, in the normal glucose condition, GSNO treatment promoted nitrosative stress by NO formation. ***Conclusion:*** In this study, a new therapeutic modality (GSNO eye drop) targeting nitrosative stress by redox post-translational modification of iNOS was efficient against early damage in the retina due to experimental DR. The present work showed the potential clinical implications of balancing the S-nitrosoglutathione/glutathione system in treating DR.

Introduction

Diabetic retinopathy (DR) is the leading cause of blindness and visual disability in working-age adults[1]. The pathogenesis of DR is complex and multifactorial, and includes molecular alterations to reactive oxygen species (ROS) and reactive nitrogen species (RNS), elevated nitric oxide (NO) and superoxide production, expression of different isoforms of nitric oxide synthase (NOS), nitrate and polyADP-ribosylate proteins (PARP), and downregulation of antioxidant enzymes. Therefore, better understanding of these mechanisms is a valuable tool for the pharmacological treatment of DR[2].

NO formed by constitutive endothelial NOS (eNOS) and neuronal NOS (nNOS) plays an important role in regulating physiological functions from the cardiovascular system to the central and peripheral nervous systems. However, NO produced by inducible NOS (iNOS) in excessive amounts for long periods of time promotes nitrosative stress and results in cytotoxicities such as apoptosis, inhibition of mitochondrial respiration, regulation of oxidative phosphorylation, neurodegeneration, and circulatory failure[3-6]. This can be achieved through reaction with superoxide anions to yield peroxynitrite, which can produce toxic hydroxyl radicals and promote oxidative injury via the formation of peroxynitrous acid, a reactive nitrogen-containing species. Endogenous NO is unstable, and some of its main biological actions are mediated through S-nitrosylation[7],i.e., the covalent incorporation of nitric oxide moiety into thiol groups (C-SH or R-SH) to form S-nitrosothiol (SNO). S-nitrosylation promotes posttranslational modification of certain proteins and affects their activities such as transcription factors, enzymes, and structural proteins. Thus, S-nitrosylation demonstrates action in vasodilation, inflammation, and neurodegeneration[8,9].

In the diabetic setting, the increase in NO production as a result of iNOS induction is associated with inflammatory responses and oxidative stress, in retinas of experimental models[10]. Studies by our group showed an increase in iNOS protein expression in the retinas

of animals with short duration of experimental diabetes[11,12]. Retinas from donors with diabetes (DM) and nonproliferative DR (NPDR) showed higher iNOS immuno-reactivity localized on the inner nuclear layer, probably on Müller glial cells, compared to subjects without DM and without ocular disease[13]. In addition, NO stable end product concentrations (nitrites and nitrates) in the vitreous were significantly elevated in patients with proliferative DR (PDR) compared with the control group[14]. These data suggest that high concentrations of NO mainly produced by iNOS might contribute to the pathogenesis of DR.

The existence of more stable transport forms of endogenous NO has been postulated in view of the increased half-life of NO *in vivo*[15]. Low-molecular-weight thiols such as cysteine, reduced glutathione (GSH), and penicillamine are prime candidates for such carrier molecules, and they can form SNO on reaction with nitrogen oxides[16]. S-nitrosoglutathione (GSNO) is formed by the S-nitrosylation reaction of NO with GSH in the extracellular setting. GSNO is the most abundant endogenous SNO and the most important form of nitric oxide *in vivo*, due to GSNO's ability to modulate cellular signaling through posttranslational modifications of redox-sensitive proteins by S-nitrosylation and/or S-glutathionylation. The intracellular stability of GSNO is regulated by chemically driven degradation reactions-thiol and metal-mediated decomposition and enzymatically reactions[17-19]. The main enzymatic-dependent degradation described is the reduction of GSNO to oxidized glutathione (GSSG) and ammonia (NH_3) by glutathione-dependent formaldehyde dehydrogenase (or alcohol dehydrogenase III); also called GSNO reductase (GSNO-R). This enzyme uses the reducing power of NADH to convert GSNO to glutathione S-hydroxysulfenamide (GSNHOH), which in turn is converted into GSSG. GSNO-R turnover significantly influences the whole-cell level of S-nitrosation[20,21]. Its relative redox activities depend on substrate concentrations of nicotinamide adenine dinucleotide and its reduced form (NAD^+/NADH) ratio.

Previous studies showed that GSNO administration provided protection in an

experimental model of cerebral ischemia by downregulating the expression of iNOS and nuclear factor kappa B (NF-kB)[22]. The therapeutic effects of GSNO have been demonstrated in experimental autoimmune uveitis[23], in which the oral administration of GSNO significantly suppressed the levels of inflammatory mediators associated with maintaining normal retinal histology and function.

The outer blood retinal barrier (BRB) is formed by retinal pigment epithelial (RPE) cells, which consist of the tight junction proteins present in a monolayer epithelium and are implicated in the pathogenesis of DR[24]. RPE constitutes a site of immunosuppressive/inflammatory factor secretion inside the eye[25] such as iNOS and tumor necrosis factor-alpha (TNF-α)[26,27]. For this reason, human retinal pigment epithelial cell line (ARPE-19) cells constitute an adequate model for assessing nitrosative stress in vitro.

To our knowledge, no study has addressed the possible effects of GSNO in the development or progression of DR. Based on these observations, we hypothesized that diabetes increases iNOS protein expression and NO production, and that treatment with a GSNO compound could modulate iNOS expression/activity in the diabetic retina and further determine the importance of the S-nitrosoglutathione/glutathione system in DR pathogenesis. The hypothesis was tested with an in *vivo* model of diabetes and through *in vitro* exposure of ARPE-19 cells to a high glucose (HG) condition.

Material and Methods

Animals study

The animal study complies with the Statement for the Use of Animals in Ophthalmic and Vision Research (ARVO) in accordance with the local Committee for Ethics in Animal Research (1834-1/CEEA/IB/UNICAMP). Spontaneously hypertensive rats (SHR) were provided by Taconic (Germantown, NY) and bred in our animal facility. We have chosen to

use SHR rats because these animals display an earlier and extensive retinal changes after streptozotocin (STZ, 50 mg/kg; Sigma, St. Louis, MO) induction when compared with normotensive counterpart[28,29]. On the day of confirmation, the control (CT) and diabetic (DM) rats were randomly assigned to be treated with either eye drop vehicle only, hydroxypropyl methylcellulose (HPMC), low-dose eye drop GSNO (900nM), or high-dose eye drop GSNO (10μM) twice daily in both eyes. The preparation of GSNO eye drops was performed at the Chemistry Institute, State University of Campinas (UNICAMP). GSNO was synthesized by the equimolar reaction between glutathione (GSH) and sodium nitrite, in the dark, and remained dormant for 40 minutes to allow complete nitrosation of thiol. After this period, it was precipitated with acetone, filtered, and lyophilized in the dark. To prepare the eye drops, the GSNO was dissolved in a phosphate buffer and added to a solution vehicle (HPMC) at a final concentration of 10 μm or 900 nm of GSNO and 2% (w/w) of HPMC. The basal and final systolic blood pressures (SBP) were obtained by noninvasive tail cuff blood pressure amplifier with a built-in automatic cuff pump (Model 229; IITC Inc. Life Science, CA). Twenty days after DM induction, the rats were submitted to full-flash electroretinography and then euthanized.

ARPE-19 cell line culture

ARPE-19 was obtained from the Federal University of Rio de Janeiro (RJCB Collection). Cells were cultured in Dulbecco's Modified Eagle's Medium and Ham's F12 (DMEM: F12) supplemented with 10% FBS and 1% penicillin/streptomycin. ARPE-19 cell cultures were serum starved and then treated with normal glucose (NG), HG, with or without the following treatments. The cytotoxicity of the treatments with GSNO (from 10 μM to 10 nM) and NOS inhibitors (from 2 mM to 2 μM) after 24 hours in ARPE-19 cells was obtained by MTT cell viability assay[30]. We considered no cytotoxicity if cell death was below 10%

(data not shown). For NOS inhibitors, the cells were pre-treated for one hour with a non-selective L-NAME (Sigma-Aldrich, St. Louis, MO USA), and specific for iNOS, aminoguanidine (AG) (Sigma-Aldrich, St. Louis, MO USA) and N6-(1-iminoethyl)-lysine, hydrochloride (L-NIL) (Cayman Chemical, Ann Arbor, MI Ann Arbor, USA).

Full-flash electroretinogram (ERG) recording

Retinal function was measured in SHR animals as previously described, with some modification[31]. For retinal function analysis, we used -10 dB light stimulus for recordings of *a-* and *b-waves* and 0 dB for *c-wave* in which better signal responses are evoked.

Immunohistochemistry for glial fibrillary acidic protein (GFAP), nitrotyrosine (NT) and inducible nitric oxide synthase (iNOS) in retinal tissues and immunofluorescence of nitrotyrosine in ARPE-19 cells

Immunohistochemistry was performed as previously described by our group[31]. The retinal sections were incubated with goat polyclonal anti-GFAP (Santa Cruz Biotechnologies, Santa Cruz, CA) or rabbit polyclonal anti-NT (Upstate Cell Signaling Solutions, Lake Placid, NY) or rabbit polyclonal anti-iNOS (Santa Cruz) overnight at 4°C.

The immunofluorescence for ARPE-19 cells was performed as previously published[32]. Rabbit anti-NT (1:20) for overnight incubation at 4°C and secondary antibody Alexa 488 goat anti-rabbit (Invitrogen; San Diego, CA, USA) at1:200 for 1 h at room temperature were applied.

Western blotting analysis for inducible nitric oxide synthase (iNOS) in whole retinal tissue and in ARPE-19 cells

The western blotting was performed as previously described[31]. Membranes were

incubated with rabbit polyclonal iNOS antidoby (Cell Signaling Technology, USA).

Measuring intracellular ROS production in cells by H_2DCFDA and NO$^{\bullet}$ formation by DAF-2DA

As previously published[31,33], we measured the total intracellular ROS production by 2',7'-dichlorodihydrofluorescein diacetate (H_2DCFDA) and intracellular NO$^{\bullet}$ levels by diaminofluorescein diacetate (DAF-2DA).

Immuno-precipitation of S-nitrosoglutathione reductase (GSNO-R) and GSH/iNOS

The cells were lysed directly in a buffer containing 100 mM tris base, 10 mM sodium pyrophosphate, 100 mM sodium fluoride, 10 mM EDTA, 2 mM phenylmethylsulfonyl fluoride, 10 mM sodium ortovanadate, and 1% Triton X-100. Samples were incubated with rabbit anti-GSNO-R (ADH5 polyclonal antibody, Protein Tech Group, Chicago, IL, USA) or mouse monoclonal anti-glutathione (GSH) antibody (Virogen, USA) overnight, followed by the addition of protein A Sepharose for 1 h. After centrifugation, the pellets were washed in buffer (100 mM Tris Base, 2 mM sodium ortovanadate, 1 mM EDTA, and 0.5% Triton X-100). The immune-precipitated samples were prepared under reducing or non-reducing conditions as necessary and loaded onto SDS polyacrylamide gels. The membranes were blocked in nonfat milk and incubated with anti-GSNO-R or rabbit polyclonal anti-iNOS (Cell Signaling) and subsequently incubated with appropriate secondary antibodies. Equal loading and transfer were ascertained by ponceau for GSNO-R.

Determination of reduced glutathione (GSH) levels

Retinal GSH level was measured using the method described by Beutler et al.[34] with a few modifications[28].

Determination of GSNO by ultra high-performance liquid chromatography (UHPLC)

As described previously[35] and with some adaptations, for the measurement of GSNO, the cells were washed with ice-cold PBS once before lysis with an extraction buffer (25 mM ammonia sulfamate dissolved in *o*-metaphosphoric acid 5%). The lysate was sonicated for 30 seconds. Samples were centrifuged, and the supernatant collected and filtrated. GSNO measurement analyses were carried out on an Agilent 1290 Infinity UHPLC system (Agilent Technology, Waldbronn, Germany) by Liquid Chromatography with Diode Array Detection (LC/DAD). Chromatographic separation was achieved on a 2.6µm Kinetex-C18 column (50 x 2.1 mm) (Phenomenex, Torrance, CA, USA), operating at 25°C. Mobile phases were constituted with 100% 20mMKCl pH 2.5 (Ecibra, Curitiba, Brazil). The flow rate was 500 µL/min and injection volume was 3 µL. Chromatographic data were recorded and integrated using LCD ChemStation software.

Statistical analysis

The results were expressed as the means ± SD. The groups were compared by one-way analysis of variance (ANOVA), followed by the Fisher protected least-significant difference test. StatView statistics software was used for all comparisons, with a significance value of $P<0.05$.

Results

In vivo study

The physiological characteristics of the study animals are shown in Table 1.

GSNO eye drops prevented DM retinal function impairment and early markers of DR

A significant retinal function impairment was observed in *b* waves among CT high-

dose and DM rats compared to those treated with vehicle (P≤0.02) (Figure 1B). To assess the RPE function, we acquired c-wave responses (Figure 1C) and also a significant decrease in *c* wave amplitude in the CT high-dose and DM rats compared to the CT group (P≤0.02) was observed. Both doses of GSNO eye drops prevented this impairment in DM animals compared to the non-treated DM and CT high-dose groups (P<0.01) (Figure 1D).To evaluate early structural marker of DR, we assessed GFAP immunoreactivity (Figure 2A). There was a clear increase in retinal GFAP positivity in the DM rats in all layers of the retina compared to the CT group (P=0.02). The treatment with GSNO in both doses significantly decreased the GFAP expression in the DM groups (P<0.02) (Figure 2A,B).

GSNO eye drop reestablished the nitrosative status in retinas of DM rats

The nitrosative stress was estimated by nitrotyrosine expression, a product of tyrosine nitration mediated by RNS such as peroxynitrite anion and nitrogen dioxide (Figure 2C). We observed a GSNO-induced increase in NT expression in the CT treated groups (P≤0.03 vs CT group). The DM group also presented higher levels of NT compared to the CT group (P=0.007). Treatment with GSNO in the DM groups prevented the increase in NT production (P≤0.03) (Figure 2C,D).

To better understand the nitrosative stress mechanisms involved in producing NT in retinal tissue among different conditions, we evaluated the expression of iNOS (Figure 3A). There was no difference in iNOS expression among the CT low- and high-dose compared to the CT group (P≥0.1). Among the DM rats, there was a significant increase in iNOS expression compared to the CT groups (P=0.03) and it was observed an effective prevention in DM high-dose group (P=0.04) (Figure 3A,B). Immuno-reactivity for iNOS localization showed diffuse positivity among all retinal layers, markedly in RPE layer in DM compared to CT groups (P=0.0005); in DM high-dose group, the iNOS up regulation was prevented

(P=0.0004)(Figure 3C,D).

Collectively, these data suggest that the nitrosative stress observed in the CT animals treated with eye drops was GSNO-mediated. However, in the DM animals the nitrosative stress was associated with iNOS upregulation. The following *in vitro* experiments were designed in order to better understand the different effects of GSNO treatment eye drop in CT and DM animals.

In vitro study

To better understand the role of the S-nitrosoglutathione/glutathione system in the diabetic setting, we conducted experiments with ARPE-19 cells since RPE immuno-reactivity for iNOS was highly expressed in diabetic tissue.

GSNO counteracted the upregulation of ROS and RNS in cells exposed to HG, but promoted nitrosative stress in NG

We observed an increase in total ROS levels in response to HG compared to the NG condition (P=0.03). The treatments with HG plus GSNO in nanomolar concentrations were effective in counteracting the upregulation of ROS production ($P \leq 0.02$), but not in micromolar concentrations (P=0.09) (Figure 4A,C). Since nanomolar concentrations of GSNO were more efficient in protecting the cells against increased ROS production, the subsequent experiments were conducted only at 1 and 100 nM of GSNO. At NG condition, treatment with GSNO did not alter the levels of ROS production compared to NG (P=0.3) (Figure 4B,C).

As detected in ROS production, the intracellular $NO^{\bullet}$ production was increased in HG compared with the NG condition (P=0.0007); both doses of GSNO treatments prevented this increase in diabetic milieu condition ($P \leq 0.008$)(Figure 5A).

To investigate which isoform of NOS is the main source of the observed increased $NO^{\bullet}$ under the DM setting conditions, the cells cultured in the HG conditions were treated with L-NAME, a non-selective NOS inhibitor, and with specific blockers for the iNOS isoform, AG and L-NIL[36]. All treatments with AG or L-NAME similarly prevented the increase in $NO^{\bullet}$ production observed in the HG condition ($P<0.0001$). L-NIL at 500 μM and 2 mM concentrations also prevented these increases ($P<0.0001$) (Figure 5B), suggesting that the main source of NO production under HG conditions is iNOS, since blocking all isoforms of NOS with L-NAME added no further effect to that observed with iNOS selective blockers. In agreement, GSNO treatments in NG conditions did not alter the iNOS expression compared to control NG ($P=0.7$). In the HG condition, there was a significant increase in iNOS expression compared with the NG conditions ($P=0.02$). Treatment with GSNO at 1 and100 nM concentrations prevented this increment ($P\leq0.009$) (Figure 5C).

To estimate the oxidative/nitrosative damage in ARPE-19 cells, we assessed NT (Figure 6). Under NG conditions, the GSNO treatments (either 1 or 100 nM) did not significantly change the positivity of NT compared to NG ($P>0.05$). However, in the highest dose of the GSNO treatment there was a tendency to increase compared to NG ($P=0.07$). Higher positivity was clearly observed in cells exposed to HG compared to the NG condition ($P=0.0006$), and the presence of GSNO treatments counteracted this increase ($P\leq0.003$) (Figure 6 A,B).

These findings suggest that, under HG condition, there is an increase in RNS accompanied by upregulation of iNOS expression. The $NO^{\bullet}$ upregulation in HG was mediated by iNOS isoform and GSNO counteracted this effects. Based on this, these data indicate that GSNO under DM milieu is not a nitrosating agent but instead prevented RNS.

The dual effect of GSNO

To better understand whether GSNO itself can generate NO under NG conditions independently of iNOS, and whether in HG conditions GSNO can inhibit NO production via NOS system, we assessed NO•, GSNO and GSH levels under NG and HG condition.

In NG+GSNO condition, the NO levels increased when compared to NG alone (P=0.01). In the presence of iNOS inhibitor, the NO levels did not decrease compare to NG+GSNO (P=0.2). These observations indicate that in NG, GSNO acts as NO donor inducing nitrosative stress. Under the HG conditions, there was a marked increase in the NO levels compared with the NG condition (P=0.001). In the presence of GSNO alone or associated with AG, we observed similar decreases in the NO• intracellular levels compared with the HG conditions (P=0.002). The combination of AG in the presence of GSNO treatment did not further decrease NO• levels, demonstrating that in HG conditions GSNO counteracts NO• upregulation through iNOS inhibition (Figure 7A).

The redox state of the GSH/GSSG combination is an important indicator of the redox environment[37], and glutathione dysregulation is linked with the etiology and progression of human diseases[38]. We quantified the GSH levels in ARPE-19 cells, in the NG plus GSNO condition, we observed an increase in GSH levels compared with the NG condition (P=0.04). In the HG condition, the GSH levels were lower when compared to NG (P=0.04). The presence of GSNO in the HG conditions did not prevent this effect (P=0.9) (Figure 7B). In the NG conditions, the presence of GSNO resulting in GSH increase might be due to an increase in its synthesis through increased expression of gamma-glutamylcysteine synthetase[39] promoted by NO• generated by the GSNO+GSH=GSSG+NO• reaction[18] or might be metal-catalyzed[17] or thioredoxin-catalyzed[40] degradation-dependent.

We also evaluated the levels of endogenous GSNO in ARPE-19 cells with UHPLC method. Curiously, in NG condition treated with GSNO, the levels of GSNO decreased compared with NG condition (P=0.02). This intriguing observation indicates that exogenous

GSNO is rapidly catalyzed by either by enzymatic process or chemically reacting with thiol groups as GSH leading to total GSNO intracellular pool decreasing. The levels of GSNO are lower in HG compared with NG condition (P=0.005) and the treatment with GSNO under HG condition did not lead to an increase in GSNO levels (P=0.2) (Figure 7C). In the HG condition, GSNO improved nitrosative stress, not through the reestablishment of GSH and/or GSNO levels.

GSNO decreases NO• levels in HG by S-glutathionylation of iNOS

One possible mechanism by which GSNO displays different effects under NG or HG conditions is through GSNO-R, which reduces GSNO to GSSG. To address whether GSNO-R plays a role in decreasing NO levels under the HG plus GSNO treatment, we evaluated the expression of GSNO-R. There was no difference between NG and NG plus GSNO treatment (P=0.8); however, under HG, GSNO-R protein expression was markedly decreased (P=0.05). The HG plus GSNO treatment increased GSNO-R protein expression but did not reach conventional statistical significance (P=0.09) (Figure 8A). This increase in GSNO-R in cells exposed to HG treated with GSNO contributes to denitrosylation of GSNO leading to GSSG release. The decrease of endogenous GSNO under NG+GSNO treatment (Figure 7C) may be also explained by the denitrosylation promoted by GSNO-R (Figure 8A).

It was previously demonstrated that S-glutathionylation of eNOS regulates its activity[41]. To investigate whether similar post-translational modification could be involved in inhibition of iNOS by GSNO in HG conditions, we addressed the S-glutathionylation of iNOS. We observed that there was no expression of S-glutathionylated iNOS in NG alone or in NG plus GSNO. Under HG conditions, we observed a faint signal that was markedly increased in the presence of GSNO. This finding indicates that GSNO treatment promotes S-glutathionylation of iNOS (Figure 8B). To verify and confirm the specificity of iNOS

glutathionylation immuno-blotting, we treated the cells with GSSG 0.5 mM to induce S-glutathionylation or with the reducing agent dithiothreitol (DTT) 0.25 mM to reverse this reaction[41]. We observed that GSSG in NG conditions promoted S-glutathionylation of iNOS similar to that observed in the HG plus GSNO treatment; as expected, the presence of DTT reverse the S-glutathionylation of iNOS protein (Figure 8C). Taken together, these results suggest that nitrosative stress was prevented by GSNO treatment through iNOS inhibition by S-glutathionylation. The posttranslational modification was probably promoted by the release of GSSG through GSNO denitrosylation via GSNO-R. In contrast, in the NG condition, GSNO treatment promoted nitrosative stress through NO formation. These findings showed the potential clinical implications of balancing the S-nitrosoglutathione/glutathione system in treating DR.

Discussion

In this innovative study, we described that GSNO eye drop mitigated nitrosative stress and slowed the early structural changes present in the retina, thus improving retinal function in an experimental model of diabetes. Of interest, iNOS upregulation in the RPE layer in the DM animals may reveal the role of RPE in the pathogenesis of DR. In the ARPE-19 cells exposed to HG, treatment with GSNO alleviated oxidative and nitrosative stress by decreasing iNOS protein expression, thus reducing intracellular $NO^{\bullet}$ levels. In addition, GSNO-R expression was improved. Therefore, posttranslational modification (S-glutathionylation) of iNOS by GSNO in ARPE-19 cells under HG condition suggested its inhibition. This evidence further explains the protective mechanism of GSNO. Rosenfeld and colleagues have already identified a GSH binding site adjacent to the N-NO-pterin of iNOS[42]. However, under NG conditions, where the intracellular GSH pool is high, the GSNO compound acts as a donor of free NO.

Nitrosative stress is caused by overproduction of RNS. Diabetic stimuli may trigger generation of excess superoxide, which is rapidly converted to peroxynitrite (reaction of $O_2^{\bullet-}$ with $NO^{\bullet}$), hydroxyl radicals (Fenton reaction or the iron-catalyzed Haber–Weiss reaction), and hydrogen peroxide (reaction catalyzed by superoxide dismutase). Peroxynitrite can modify tyrosine residues in proteins to form nitrotyrosine. Nitrotyrosine is a well-accepted indicator of RNS generation, and this stable end product is involved in inactivating mitochondrial and cytosolic proteins, resulting in damage to cellular constituents. Moreover, nitrotyrosine can initiate lipid peroxidation, increase DNA damage, deplete intracellular GSH levels, and induce overexpression of proinflammatory factors and adhesion molecules. Therefore, nitration is being increasingly proposed as a contributor to tissue injury in human diseases[43,44].

It is becoming increasingly clear that iNOS activity is induced in rats and humans with DR[13,45,46]. Previous studies showed that $iNOS^{-/-}$ or the inhibition of iNOS in the ischemic retina prevented angiogenesis locally in the avascular retina, mediated at least in part by downregulation of vascular endothelial growth factor (VEGF) receptor 2 (VEGFR2). At the same time, pathological retinal neovascularization was considerably stronger in iNOS-expressing animals, showing that iNOS plays a crucial role in retinal neovasculardisease[47]. It was also shown that $iNOS^{-/-}$ mice display protection from retinal cell apoptosis in an ischemic proliferative retinopathy model[48]. Diabetic $iNOS^{-/-}$ mice showed downregulation of several inflammatory factors, nitration of proteins, superoxide production, and leucostasis, thus preventing the formation of acellular capillaries and pericyte ghosts[49]. Our data showed that the upregulation of iNOS expression in diabetes or HG conditions led to excessive NO generation. Furthermore, treatment with GSNO was highly associated with S-glutathionylation of iNOS, thus decreasing NO levels. When NO generation by iNOS is pharmacologically inhibited by the iNOS-specific inhibitor, AG, NO levels were significantly

decreased in the presence or absence of GSNO.

In NG situations, treatment with GSNO evoked an increase in nitrosative stress *in vitro* with higher levels of NO, although the GSH levels were upregulated in the ARPE-19 cells. Therefore, the presence of GSNO leads to GSH and NO production. This might be either spontaneous or metal-catalyzed[17] or thioredoxin-catalyzed[40] degradation-dependent. Under HG conditions, we observed an increase in oxidative/nitrosative stress and higher levels of NO• accompanied by decreases in the GSH and GSNO levels. The low GSH content in these cells may contribute to these effects. Cells exposed to HG showed decreased levels of GSNO-R protein expression, and the supplementation of GSNO at 100 nM improved GSNO-R protein expression and possibly increased the denitrosylation of GSNO, leading to GSSG generation (Figure 9). A previous work reported that GSSG induces S-glutathionylation of eNOS protein under oxidative stress, uncoupling it and thus altering its function[41] and other investigator demonstrated that this process was described in streptozotocin-induced animals[50]. The S-glutathionylation of NOS isoforms shows to be protective or not, dependent of the physiology function of the isoform. In this present work, S-glutathionylation of iNOS isoform is retinal protective.

GSNO-R acts only on GSNO, meaning that SNO proteins are not substrates, and it controls protein *S*-nitrosylation by influencing the cellular equilibrium between SNO proteins and GSNO[51,52].Others enzymatic systems such as human carbonyl reductase 1 (hCBR1), an NADPH-dependent short chain dehydrogenase/reductase has been demonstrated to reduce GSNO[53]. Previous studies using GSNO-R$^{-/-}$ mice showed increased levels of SNO proteins and decreased survival in mice when exposed to endotoxin, and these effects are attenuated by an inhibitor of iNOS[54]. Subsequent studies demonstrated that GSNO-R deficiency is linked to S-nitrosylation of the DNA repair enzyme[7]. In our in vitro model we described decrease expression of GSNO-R accompanied by reduction of GSNO levels in HG condition.

The present study showed for the first time the therapeutic effect of GSNO eye drop in counteracting nitrosative stress in an experimental model of DR, with consequent improved retinal function. GSNO supplementation prevented nitrosative stress by reducing NO generation through iNOS inhibition by S-glutathionylation under diabetic milieu conditions. The regulation of the S-nitrosoglutathione/glutathione system with RNS-based signaling pathways might be potential therapeutic targets in ocular diabetic complications.

Acknowledgments

This work was supported by the Fundação de Amparo à Pesquisa do Estado de São Paulo (Grants 2008/57560-0and2011/06719-1). M.A.B.R received a scholarship from Coordenação de Aperfeiçoamento de Pessoal de Nível Superior. The authors thank the staff of the Life Sciences Core Facility from the UNICAMP for support with confocal microscopy. The authors are very grateful to the personnel from the Renal Pathophysiology Laboratory, FCM, UNICAMP, for their invaluable help with this work.

References

1. Fong DS, Aiello L, Gardner TW, et al. American Diabetes Association. Retinopathy in diabetes. *Diabetes Care Suppl*. 2004;1:S84-87.

2. Zheng L, Kern TS. Role of nitric oxide, superoxide, peroxynitrite and PARP in diabetic retinopathy. *Front Biosci*. 2009;14:3974-3987.

3. Griffith OW, Stuehr DJ. Nitric oxide synthases: properties and catalytic mechanism. *Annu Rev Physiol*. 1995;57:707-736.

4. Knowles RG, Moncada S. Nitric oxide synthases in mammals. *Biochem J*. 1994;298:249-258.

5. Moncada S, Bolanos JP. Nitric oxide, cell bioenergetics and neurodegeneration. *Neurochem*. 2006;97:1676-1689.

6. Schmidt HH, Walter U. NO at work. *Cell* 1994;78:919-925.

7. Wei W, Li B, Hanes MA, Kakar S, Chen X, Liu L. S-nitrosylation from GSNOR deficiency impairs DNA repair and promotes hepatocarcinogenesis. *SciTransl Med*. 2010;2: 19ra13.

8. Hess DT, Matsumoto A, Kim SO, Marshall HE, Stamler JS. Protein S-nitrosylation purview and parameters. *Nat Rev Mol Cell Biol*. 2005;6:150-166.

9. Foster MW, McMahon TJ, Stamler JS. S-nitrosylation in health and disease. *Trends Mol Med*. 2003;9:160-168.

10. Du Y, Sarthy VP, Kern TS. Interaction between NO and COX pathways in retinal cells exposed to elevated glucose and retina of diabetic rats. *Am J Physiol Regul Integr Comp Physiol*. 2004;287:735-741.

11. Rosales MA, Silva KC, Lopes de Faria JB, Lopes de Faria JM. Exogenous SOD mimetic tempol ameliorates the early retinal changes reestablishing the redox status in diabetic hypertensive rats. *Invest Ophthalmol Vis Sci*. 2010;51:4327-4336.

12. Silva KC, Rosales MA, de Faria JB, de Faria JM. Reduction of inducible nitric oxide synthase via angiotensin receptor blocker prevents the oxidative retinal damage in diabetic hypertensive rats. *Curr Eye Res*. 2010;35:519-528.

13. Abu El-Asrar AM, Desmet S, Meersschaert A, Dralands L, Missotten L, Geboes K. Expression of the inducible isoform of nitric oxide synthase in the retinas of human subjects with diabetes mellitus. *Am J Ophthalmol*. 2001;132:551–556.

14. Hernández C, Lecube A, Segura RM, Sararols L, Simó R. Nitric oxide and vascular endothelial growth factor concentrations are increased but not related in vitreous fluid of patients with proliferative diabetic retinopathy. *Diabet Med*. 2002;19:655-660.

15. Liu Z, Rudd MA, Freedman JE, Loscalzo J. S-transnitrosation reactions are involved in the metabolic fate and biological actions of nitric oxide. *J Pharmacol Exp Ther*. 1998;284:526–534.

16. Stamler JS, Lamas S, Fang FC. Nitrosylation, the prototypic redox-based signaling mechanism. *Cell* 2001;106:675–683.

17. Hogg N. The biochemistry and physiology of S-nitrosothiols. *Annu Rev Pharmacol Toxicol*. 2002;42:585–600.

18. Singh SP, Wishnok JS, Keshive M, Deen WM, Tannenbaum SR. The chemistry of the S-nitrosoglutathione/glutathione system. *Proc Natl Acad Sci* USA 1996;93:14428–14433.

19. Zeng H, Spencer NY, Hogg N. Metabolism of S-nitrosoglutathione by endothelial cells. *Am J Physiol Heart Circ Physiol*. 2001;281:432–439.

20. Hedberg JJ, Griffiths WJ, Nilsson SJ, Hoog JO. Reduction of S-nitrosoglutathione by human alcoholdehydrogenase 3 is an irreversible reaction as analysed by electrospray mass spectrometry. *Eur J Biochem*. 2003;270:1249–1256.

21. Liu L, Hausladen A, Zeng M, Que L, Heitman J, Stamler JS. A metabolic enzyme for S-nitrosothiol conserved from bacteria to humans. *Nature* 2001;410:490–494.

22. Khan M, Sekhon B, Giri S, et al. S-Nitrosoglutathione reduces inflammation and protects brain against focal cerebral ischemia in a rat model of experimental stroke. J *Cereb Blood Flow Metab*. 2005;25:177-192.

23. Haq E, Rohrer B, Nath N, Crosson CE, Singh I. S-nitrosoglutathione prevents interphotoreceptor retinoid-binding protein (IRBP(161-180))-induced experimental autoimmune uveitis. *J Ocul Pharmacol Ther*. 2007;23:221-231.

24. Simo R, Villarroel M, Corraliza L, Hernandez C, Garcia-Ramirez M. The retinal pigment epithelium: something more than a constituent of the blood-retinal barrier—implications for the pathogenesis of diabetic retinopathy. *J Biomed Biotechnol*. 2010; 2010:190724.

25. Holtkamp GM, Kijlstra A, Peek R, de Vos AF. Retinal Pigment Epithelium-immune System Interactions: Cytokine Production and Cytokine-induced Changes. *Prog Retin Eye Res*. 2001;20:29-48.

26. Goureau O, Lepoivre M, Becquet F, Courtois Y. Differential regulation of inducible nitric oxide synthase by fibroblast growth factors and transforming growth factor b in bovine retinal pigmented epithelial cells: inverse correlation with cellular proliferation. *Proc. Natl. Acad. Sci. USA* 1993;90:4276-4280.

27. Liversidge J, Grabowski P, Ralston S, Benjamin N, Forrester JV. Rats retinal pigment epithelial cells express an inducible form of nitric oxide synthase and produce nitric oxide in response to inflammatory cytokines and activated T cells. Immunology 1994;83:404-409.

28. Pinto CC, Silva KC, Biswas SK, Martins N, de Faria JB, de Faria JM. Arterial hypertension exacerbates oxidative stress in early diabetic retinopathy. *Free Radic Res.* 2007;41:1151-1158.

29. Silva KC, Pinto CC, Biswas SK, de Faria JB, de Faria JM. Hypertension increases retinal inflammation in experimental diabetes: a possible mechanism for aggravation of diabetic retinopathy by hypertension. *Curr Eye Res*. 2007;32:533-541.

30. Mosmann T. Rapid colorimetric assay for cellular growth and survival: application to proliferation and cytotoxicity assays. *J Immunol Meth.* 1983;65: 55-63.

31. Silva KC, Rosales MA, Hamassaki DE, Saito KC, Faria AM, Ribeiro PA, Faria JB, Faria JM. Green tea is neuroprotective in diabetic retinopathy. *Invest Ophthalmol Vis Sci.* 2013;54:1325-1336.

32. Garcia-Ramírez M, Villarroel M, Corraliza L, Hernández C, Simó R. Measuring permeability in human retinal epithelial cells (ARPE-19): implications for the study of diabetic retinopathy. *Methods Mol Biol.* 2011;763:179-194.

33. Faria AM, Papadimitriou A, Silva KC, Lopes de Faria JM, Lopes de Faria JB. Uncoupling endothelial nitric oxide synthase is ameliorated by green tea in experimental diabetes by re-establishing tetrahydrobiopterin levels. *Diabetes* 2012;61:1838-1847.

34. Beutler E, Duron O, Kelly BM. Improved method for the determination of blood glutathione. *J Lab Clin Med.* 1963;16:882–888.

35. Yap, LP, Sancheti H, Ybanez MD, Garcia J, Cadenas E, Han D. Determination of GSH, GSSG, and GSNO using HPLC with electrochemical detection. *Methods Enzymol.* 2010;473: 137-147.

36. Moore WM, Webber RK, Jerome GM, Tjoeng FS, Misko TP, Currie MG. L-N6-(1-iminoethyl) lysine: a selective inhibitor of inducible nitric oxide synthase. *J Med Chem.* 1994;37:3886-3888.

37. Schafer FQ, Buettner GR. Redox environment of the cell as viewed through the redox state of the glutathione disulfide/glutathione couple. *Free Radic Biol Med.* 2001;30:1191–1212.

38. Ballatori N, Krance SM, Notenboom S, Shi S, Tieu K, Hammond CL. Glutathione dysregulation and the etiology and progression of human diseases. *Bio. Chem.* 2009;390: 191-214.

39. Moellering D, McAndrew J, Patel RP, et al. Nitric oxide-dependent induction of glutathione synthesis through increased expression of gamma-glutamylcysteine synthetase. *Arch Biochem Biophys.* 1998;358:74-82.

40. Nikitovic D, Holmgren A. S-Nitrosoglutathione is cleaved by the thioredoxin system with liberation of glutathione and redox regulating nitric oxide. *J Biol Chem.* 1996;271:19180–19185.

41. Chen CA, Wang, TY, Varadharaj, S, et al. S-glutathionylation uncouples eNOS and regulates its cellular and vascular function. *Nature* 2010;468:1115-1118.

42. Rosenfeld RJ, Bonaventura J, Szymczyna BR, et al. Nitric-oxide synthase forms N-NO-pterin and S-NO-cys: implications for activity, allostery, and regulation. *J Biol Chem.* 2010;285:31581-31589.

43. Pacher P, Beckman JS, Liaudet L. Nitric oxide and peroxynitrite in health and disease. *Physiol Rev.* 2007;87:315–424.

44. Pacher P, Obrosova IG, Mabley JG, Szabo C. Role of nitrosative stress and peroxynitrite in the pathogenesis of diabetic complications. Emerging new therapeutical strategies. *Curr Med Chem.* 2005;12:267–275.

45. Kowluru RA, Engerman RL, Kern TS. Abnormalities of retinal metabolism in diabetes or experimental galactosemia VIII. Prevention by aminoguanidine. *Curr Eye Res.* 2000;21:814-819.

46. do Carmo A, Lopes C, Santos M, Proença R, Cunha-Vaz J, Carvalho AP. Nitric oxide synthase activity and L-arginine metabolism in the retinas from streptozotocin induced diabetic rats. *Gen Pharmacol.* 1998;30:319–324.

47. Sennlaub F, Courtois Y, Goureau O. Inducible nitric oxide synthase mediatesthe change from retinal to vitreal neovascularization in ischemic retinopathy. *J Clin Invest.* 2001;107:717-725.

48. Sennlaub F, Courtois Y, Goureau O. Inducible nitric oxide synthase mediates the retinal apoptosis in ischemic proliferative retinopathy. *J Neurosci.* 2002;22:3987-3993.

49. Zheng L, Du Y, Miller C, et al. Critical role of inducible nitric oxide synthase in degeneration of retinal capillaries in mice with streptozotocin-induced diabetes. *Diabetologia* 2007;50:1987-1996.

50. Schuhmacher S, Oelze M, Bollmann F, et al. Vascular dysfunction in experimental diabetes is improved by pentaerithrityl tetranitrate but not isosorbide-5-mononitrate therapy. *Diabetes* 2011;60:2608-2616.

51. Foster MW, Liu L, Zeng M, Hess DT, Stamler JS. A genetic analysis of nitrosative stress. Biochemistry 2009;48:792–799.

52. Davis ME, Grumbach IM, Fukai T, Cutchins A, Harrison DG. Shear stress regulates endothelial nitric-oxide synthase promoter activity through nuclear factor kappaB binding. J *Biol Chem.* 2004;279:163–168.

53. Bateman RL, Rauh D, Tavshanjian B, Shokat KM. Human carbonyl reductase 1 is an S-nitrosoglutathione reductase. *J Biol Chem.* 2008;283:35756–35762.

54. Liu L, Yan Y, Zeng M, et al. Essential roles of S-nitrosothiols in vascular homeostasis and endotoxic shock. *Cell* 2004;116:617–628.

Table 1. Physiological Parameters of the Animals

Groups	Initial body weight (g)	Final body weight (g)	Systolic Blood Pressure (mmHg)	Glycated hemoglobin(% GHb)
CT (n=5)	170±16	215±18	191±18	9.25±1.13
CT-low dose (n=6)	178±13	245±10	184±5	9.67±0.76
CT-high dose (n=5)	163±14	240±8	182±4	9.81±0.72
DM n=6	166±22	127±13*	185±8	15.63±2.25*
DM-low dose(n=5)	169±9	123±14*	188±11	15.10±4.28*
DM-high dose (n=6)	173±16	136±14*	182±6	13.84±2.13*

The diabetic groups (DM) had lower final body weight and higher glycated hemoglobin levels compared to the control (CT) animals (*P<0.01). The treatment did not change any parameters.Legend of treatments:**CT:**non diabetic rats treated with vehicle of eye drop; **CT-low dose:** non diabetic rats treated with GSNO 900nM; **CT-high dose:**non diabetic rats treated with GSNO 10μM; **DM:**diabetic rats treated with vehicle of eye drop; **DM-low dose:**diabetic rats treated with GSNO 900nM; **DM-high dose:** diabetic rats treated with GSNO 10μM.

Figure legends

Figure 1. Retinal function evaluated by electroretinography. A. Representative waveforms of the *a*- and *b*-waves in the control (CT) and diabetic (DM) groups, which corresponds to the photoreceptor and inner retinal cell responses, respectively, in response to light stimulus intensity at -10dB. **B.** The bars represent the mean ± SD of the *b*-wave amplitude in μvolts. $^{*}P\leq0.02$ versus CT group; $^{\dagger}P\leq0.05$ versus DM and CT high-dose group. **C.** Waveforms of *c*-waves in normal and diabetic groups in response to light stimulus intensity at 0dB. **D.** The bars represent the mean ± SD of the *c*-wave amplitude in μvolts. $^{*}P\leq0.02$ versus CT group; $^{\dagger}P\geq0.01$ versus DM and CT high-dose group. There was no significant difference in *a*-waves and implicit *b*-wave time between the studied groups (data not shown)

Figure 2. Early marker of diabetic retinopathy and nitrosative stress of the studied groups. A. Photomicrograph representing immuno-localization of glial fibrillary acidic protein (GFAP) on retinal tissue. The GFAP in retinal tissue sections (5 μm) is shown in brown color (Magnification x400). **B.** Bars represent the mean ± SD of GFAP positivity analyses. The percentage of positivity per retinal field (mm^2) was transformed to changes/fold in relation to the media of control in each experiment to compare independent experiments. $^{*}P=0.02$ versus CT group; $^{\dagger}P\leq0.05$versus DM group. The treatment in the CT low- and high-dose groups did not alter GFAP immuno-reactivity compared to the CT group (P=0.2). **C.** Representative photomicrograph of nitrotyrosine (NT) immuno-reactivity. The presence of nitrotyrosine is shown in brown on retinal tissue sections (5 μm) (Magnification x400). The positivity was widely expressed among all retinal layers, and especially in RPE. **D.** The bars represent the mean ± SD of the percentage of positivity per retinal field (mm^2). $^{*}P\leq0.03$ versus CT group; $^{\dagger}P\leq 0.03$versus DM group. At least 3 independent experiments

were preformed for each assay. **RPE:** retinal pigment epithelium; **RCL**: rods and cones layer; **ONL**: outer nuclear layer; **OPL**: outer plexiform layer; **INL**: inner nuclear layer; **IPL**: inner plexiform layer; **GCL**: ganglion cell layer.

Figure 3. Evaluation of nitrosative stress of studied groups. A. Western blot for inducible nitric oxide synthase (iNOS) expression in total retinal lysate. **B.** Equal loading and transfer were ascertained by reprobing the membranes for ß-actin. The bars represent mean ±SD of band densities expressed in arbitrary units of densitometry. *P=0.03 versus CT group; †P=0.04 versus DM group. **C.** Representative photomicrograph of iNOS immuno-reactivity and localization on retinal tissue (Magnification x400). The presence of iNOS is shown in brown in all layers of the retina especially in RPE layer. **D.** The bars represent the mean ± SD of the percentage of positivity per retinal field (mm^2). *P=0.0005 versus CT group; †P=0.0004 versus DM group. At least 3 independent experiments were preformed for each assay. **RPE:** retinal pigment epithelium; **RCL**: rods and cones layer; **ONL**: outer nuclear layer; **OPL**: outer plexiform layer; **INL**: inner nuclear layer; **IPL**: inner plexiform layer; **GCL**: ganglion cell layer.

Figure 4. Total intracellular ROS production in ARPE-19 cells. Total ROS production was obtained by H_2DCFDA fluorescence. ARPE-19 cell cultures at 80% of confluence were serum starved, then exposed to glucose 5.5mM (normal glucose, NG); to NG plus GSNO at 1nM – 100µM (NG + GSNO); to glucose 30mM (high glucose, HG); and to HG plus GSNO at 1nM – 100µM (HG + GSNO) for 24 hours. NG + 24.5 mM of mannitol was used as an osmotic control.**A.** Bars represent the mean ± SD of fluorescence units obtained in ELISA reader and corrected by the number of cells at the end of each treatment. Mannitol was used for an osmotic control in this experiment to see if there is some effect of osmolarity. *P=0.03

versus NG; †P≤0.02 versus HG group. **B.** Total ROS production under normal glucose condition. **C.** Representative photomicrographs of qualitative H_2DCFDA assay indicating the levels of total ROS production in ARPE-19 cells using fluorescence microscope (Zeiss Axio Observer.A1 Inverted; Zeiss, Germany).

Figure 5. Intracellular nitric oxide ($NO^{\bullet}$) production and iNOS expression in ARPE-19 cells. ARPE-19 cell cultures at 80% of confluence were serum starved, then exposed to glucose 5.5mM (normal glucose, NG); to NG plus GSNO at 100nM (NG + GSNO); to glucose 30mM (high glucose, HG); and to HG plus GSNO at 1nM and 100nM (HG + GSNO) for 24 hours. NG + 24.5 mM of mannitol was used as an osmotic control.**A**. Detection of intracellular $NO^{\bullet}$ by DAF-2DA fluorescence. Bars represent the mean ± SD of the fluorescence units obtained via ELISA reader corrected by the number of cells at the end of each treatment. *P=0.0007 versus NG condition; †P≤0.008 versus HG treatment. **B.** $NO^{\bullet}$ production in the presence of total NOS (L-NAME) and specific for iNOS (AG and L-NIL) inhibitors in cell culture. *P<0.0001 versus NG; †P<0.0001 versus HG. The mannitol treatment did not change the levels of $NO^{\bullet}$ production (P=0.8). AG: aminoguanidine. **C.** Western blot for iNOS expression on total cell lysate. Exposed films were scanned with a densitometer (Bio-Rad) and analyzed quantitatively with Multi-Analyst Macintosh Software for Image Analysis Systems. Equal loading and transfer were ascertained by reprobing the membranes for ß-actin. The bars represent mean±SD of band densities expressed in arbitrary densitometric units. *P=0.02 versus NG condition; †P≤0.009 versus HG condition. At least 3 independent experiments were preformed for each assay.

Figure 6. Immunofluorescence of nitrotyrosine in ARPE-19 cell lines. ARPE-19 cell cultures at 80% of confluence were serum starved, then exposed to glucose 5.5mM (normal

glucose, NG); to NG plus GSNO at 1 and 100nM (NG + GSNO); to glucose 30mM (high glucose, HG); and to HG plus GSNO at 1 and 100nM (HG + GSNO) for 24 hours. **A.** Confocal images showing nitrotyrosine (NT) positivity and localization. The positivity of nitrotyrosine is shown in green (localized on the cytoplasm) and the nucleus is indicated with nuclear dye (DAPI) under a confocal laser scanning microscope (Zeiss, X630).**B.** The bars represent the mean ± SD of the score of positivity, from 0 for no positiveness to 4 for ≥80% of positiveness by blindness. $^{*}P=0.0006$ versus NG treatment; $^{\dagger}P\leq0.003$ versus HG treatment. At least 3 independent experiments were preformed.

Figure 7. Effects of GSNO under NG and HG conditions in ARPE-19 cells. ARPE-19 cell cultures at 80% of confluence were serum starved, then exposed to glucose 5.5mM (normal glucose, NG); to NG plus GSNO at 100nM (NG + GSNO); to glucose 30mM (high glucose, HG); and to HG plus GSNO at 100nM (HG + GSNO) for 24 hours. **A.** Detection of intracellular $NO^{\bullet}$ by DAF-DA fluorescence method in cells exposed to NG and HG in the presence or absence of specific iNOS inhibitor (AG). Bars represent the mean±SD of the fluorescence units corrected by the cell number. $^{*}P\geq0.001$ versus NG treatment; $^{\dagger}P=0.002$ versus HG condition. **B.** Measurement of GSH by colorimetric assay. Absorbance was read at 412 nm. GSH was used as an external standard for preparation of a standard curve. Bars represent the mean±SD of µmol of GSH corrected by protein cell lysate concentration (µg). $^{*}P<0.04$ versus NG; $^{\dagger}P<0.03$ versus NG. **C.** Measurement of endogenous GSNO by UHPLC method. Chromatography analyses of standard GSNO and levels of GSNO under different treatments, retention time=0.6 min. Bars represent the mean±SD of µmol of GSNO levels corrected by protein cell lysate concentration (µg) under different conditions. $^{*}P\leq0.02$ versus NG condition. At least 3 independent experiments were preformed.

Figure 8. GSNO promotes S-glutathionylation of iNOS. ARPE-19 cell cultures at 80% of

confluence were serum starved, then exposed to glucose 5.5mM (normal glucose, NG); to NG plus GSNO at 100nM (NG + GSNO); to glucose 30mM (high glucose, HG); and to HG plus GSNO at 100nM (HG + GSNO) for 24 hours. **A.** Immuno-precipitation of cell lysate with GSNO-R antibody incubated with GSNO-R antibody. The GSNO-R protein expression was measured by Western blot. Equal loading protein and transfer were confirmed by Ponceau. Bars represent the mean±SD expressed in arbitrary units of densitometry. $^{*}P=0.05$ versus NG. At least 3 independent experiments were preformed for each assay. **B.** Cell lysate was immuno-precipitated with the GSH protein complex antibody and immuno-blotted against iNOS. The GSH-protein complexes were blotted against iNOS. Equal loading protein was ascertained by reprobing the membranes for total GSH complex proteins. **C.** Controls for S-glutathionylation of iNOS were done by 0.5 mM GSSG (positive control) or GSSG plus the reduced agent DTT 0.25 mM (negative control) to reverse the reaction. The detection of S-glutationylated iNOS at 130 kDa was present in cells exposed to HG treated with GSNO; in cells exposed to NG in the presence of GSSG, the expression of S-glutationylated iNOS was equally increased as compared with HG plus GSNO, and DTT reversed this post-translational iNOS modification.

Figure 9. Schematic representation of possible mechanisms involved in nitrosative stress under normal or high glucose conditions in ARPE-19 cells.

In normal glucose condition plus GSNO: The high content of intracellular GSH can react with exogenous GSNO generating NO, thus promoting nitrosative stress. The exogenous and/or endogenous GSNO may be converted by GSNO-R or metal or other enzyme-catalyzed, leading to low levels of GSNO.

In high glucose condition: iNOS generates high levels ofNO accompanied by decrease of endogenous GSH, GSNO and GSNO-R levels, resulting in nitrosative stress. The low content

of GSH can explain the low levels of endogenous GSNO.

In high glucose condition plus GSNO: The effect of treatment was not due to endogenous GSH and GSNO reestablishment levels.GSNO-R expression is improved which denitrosylates exogenous GSNO generating GSSG + NH_3 formation; GSSG S-glutathionylates iNOS, reducing NO production thus preventing nitrosative stress.

Figure 1. Retinal function evaluated by electroretinography.

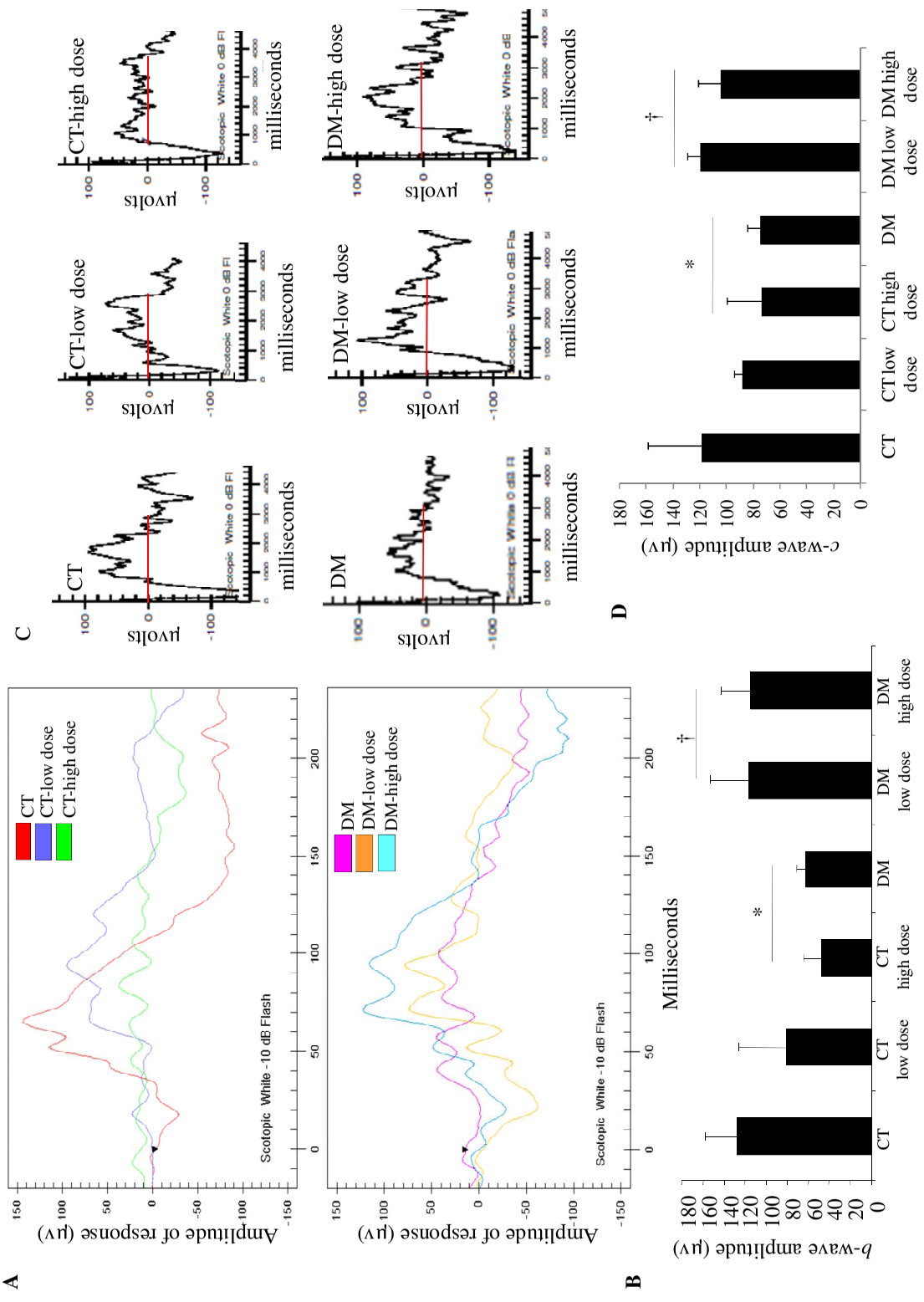

Figure 2. Early marker of diabetic retinopathy and nitrosative stress of the studied groups.

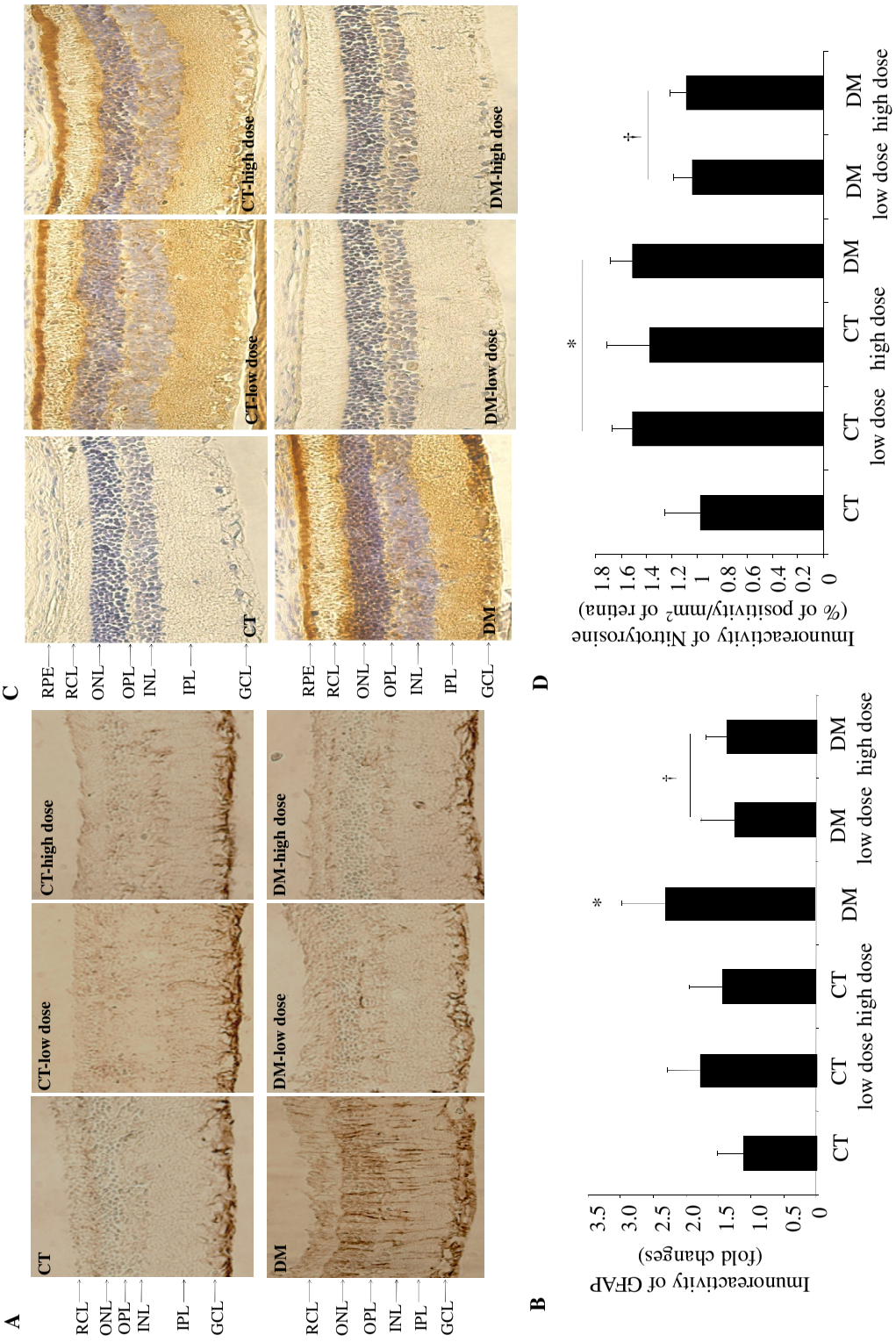

Figure 3. Evaluation of nitrosative stress of studied groups.

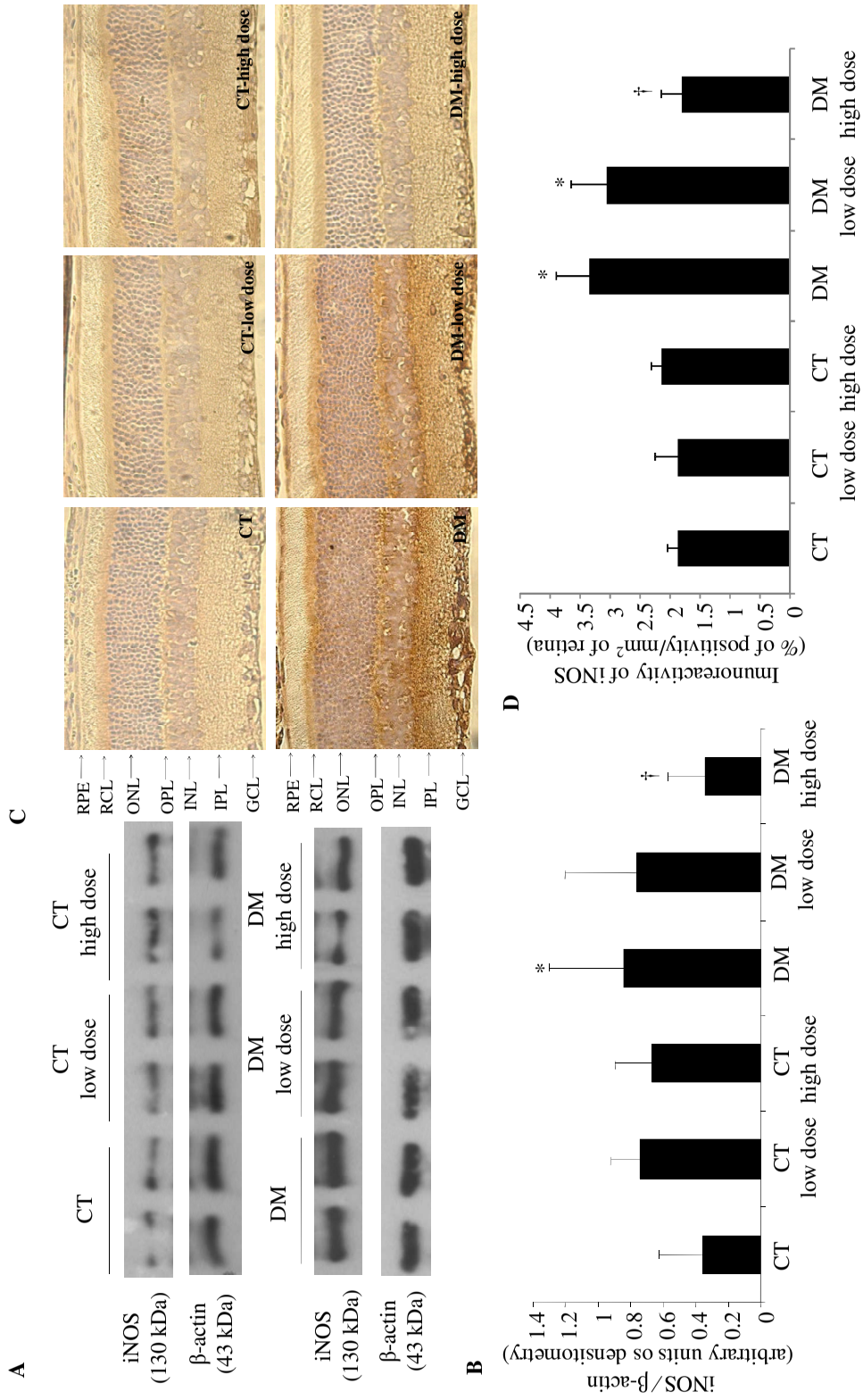

Figure 4. Total intracellular ROS production in ARPE-19 cells.

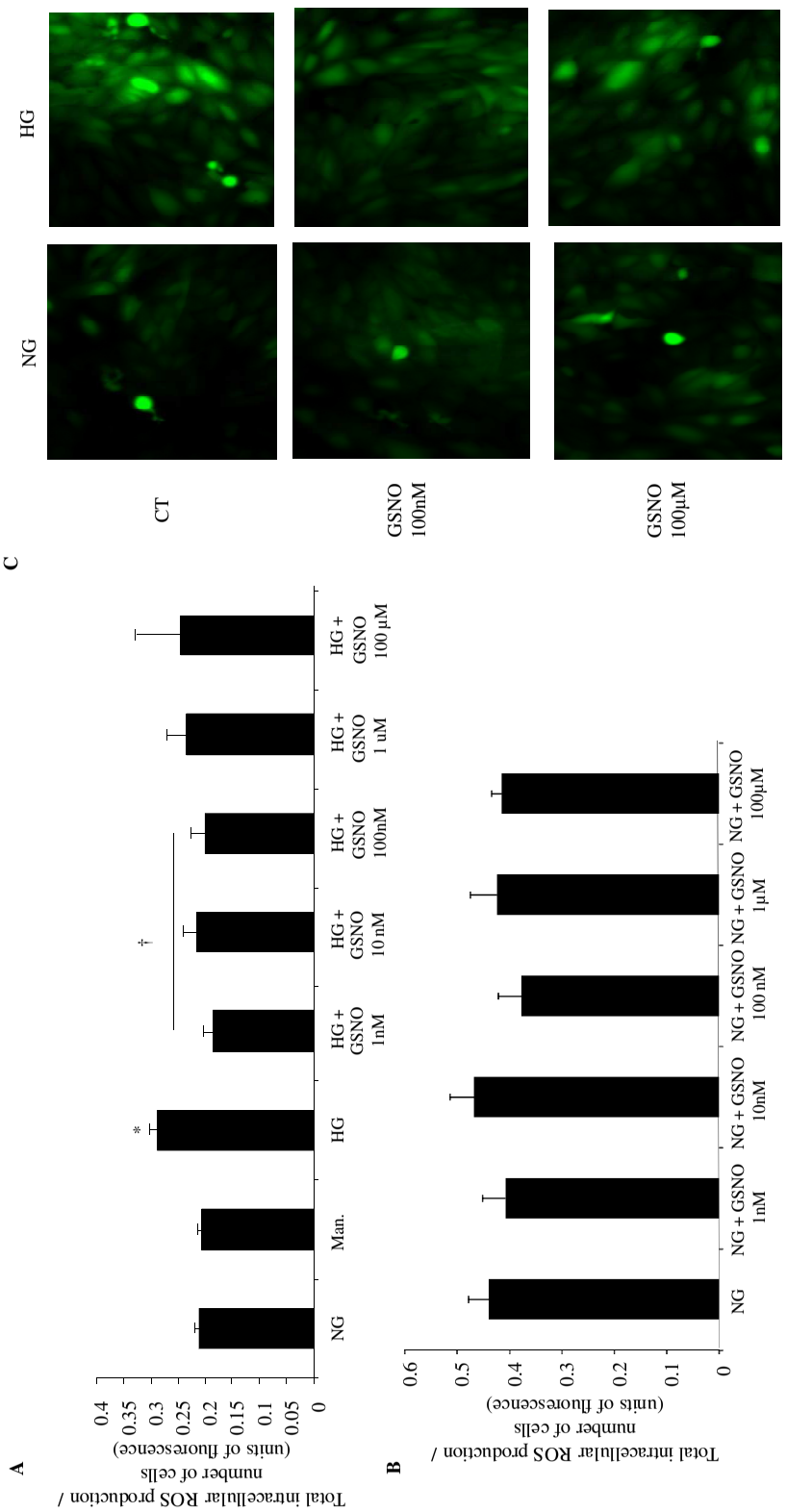

Figure 5. Intracellular nitric oxide (NO·) production and iNOS expression in ARPE-19 cells.

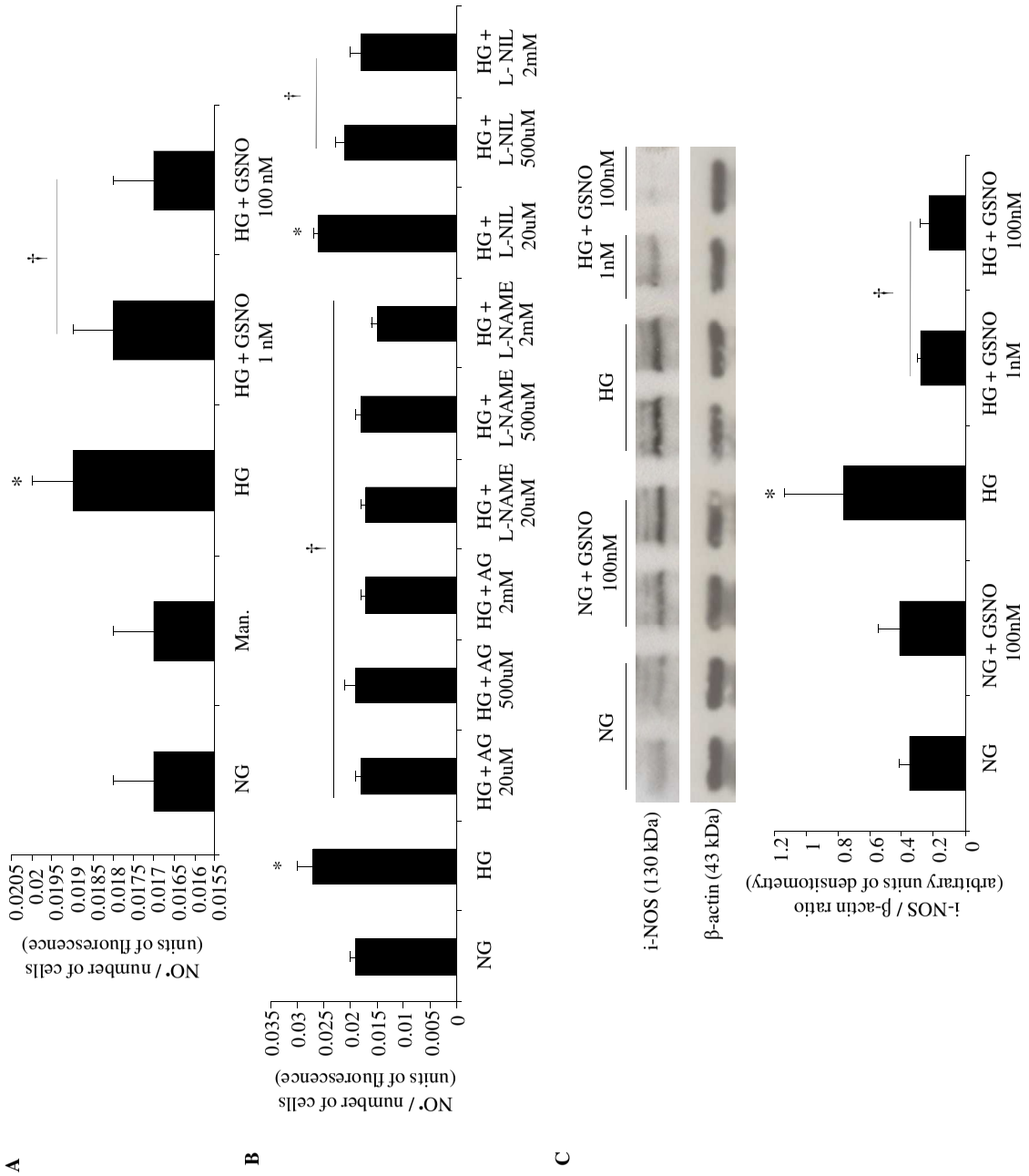

Figure 6. Immunofluorescence of nitrotyrosine in ARPE-19 cell lines.

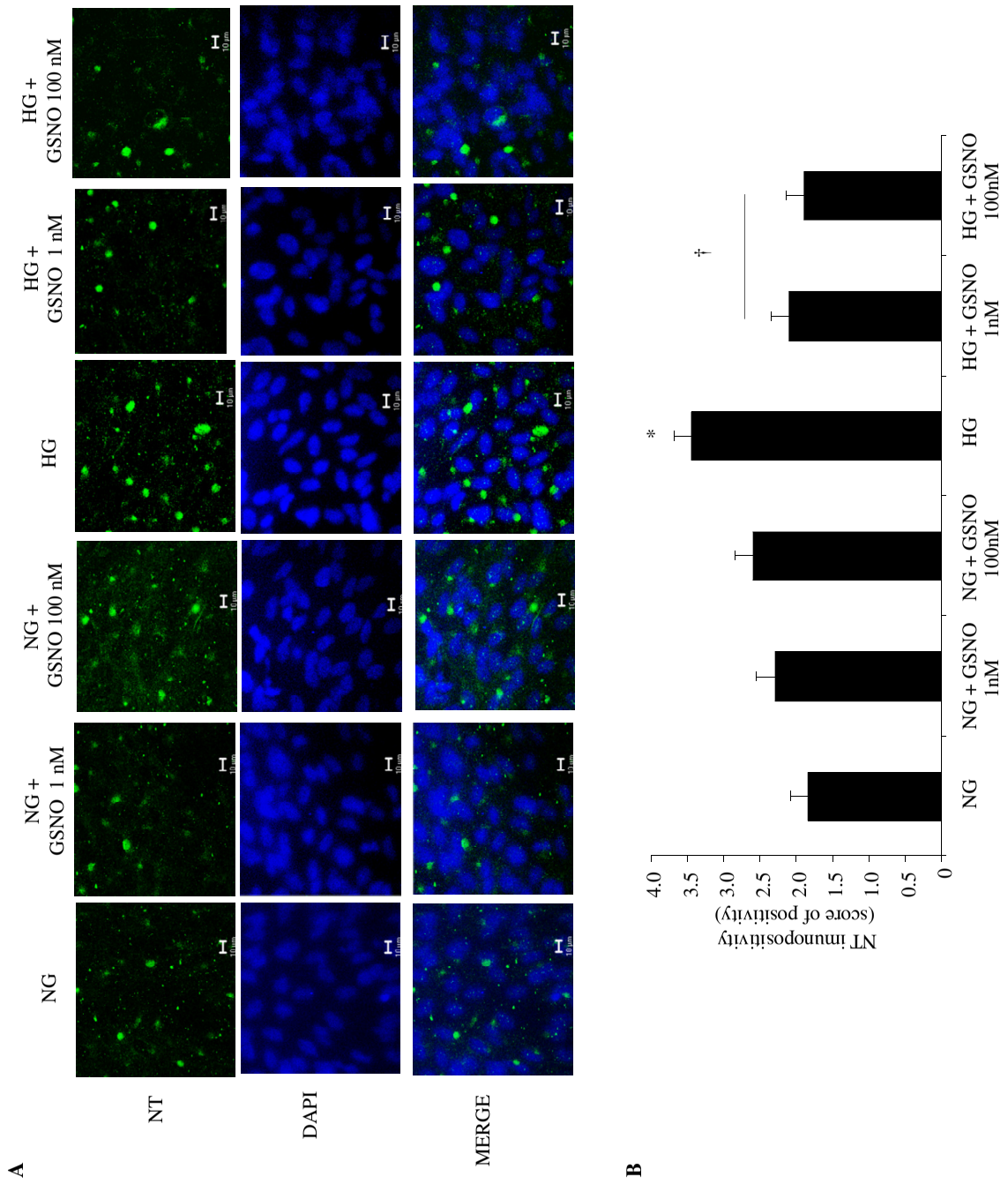

Figure 7. Effects of GSNO under NG and HG conditions in ARPE-19 cells.

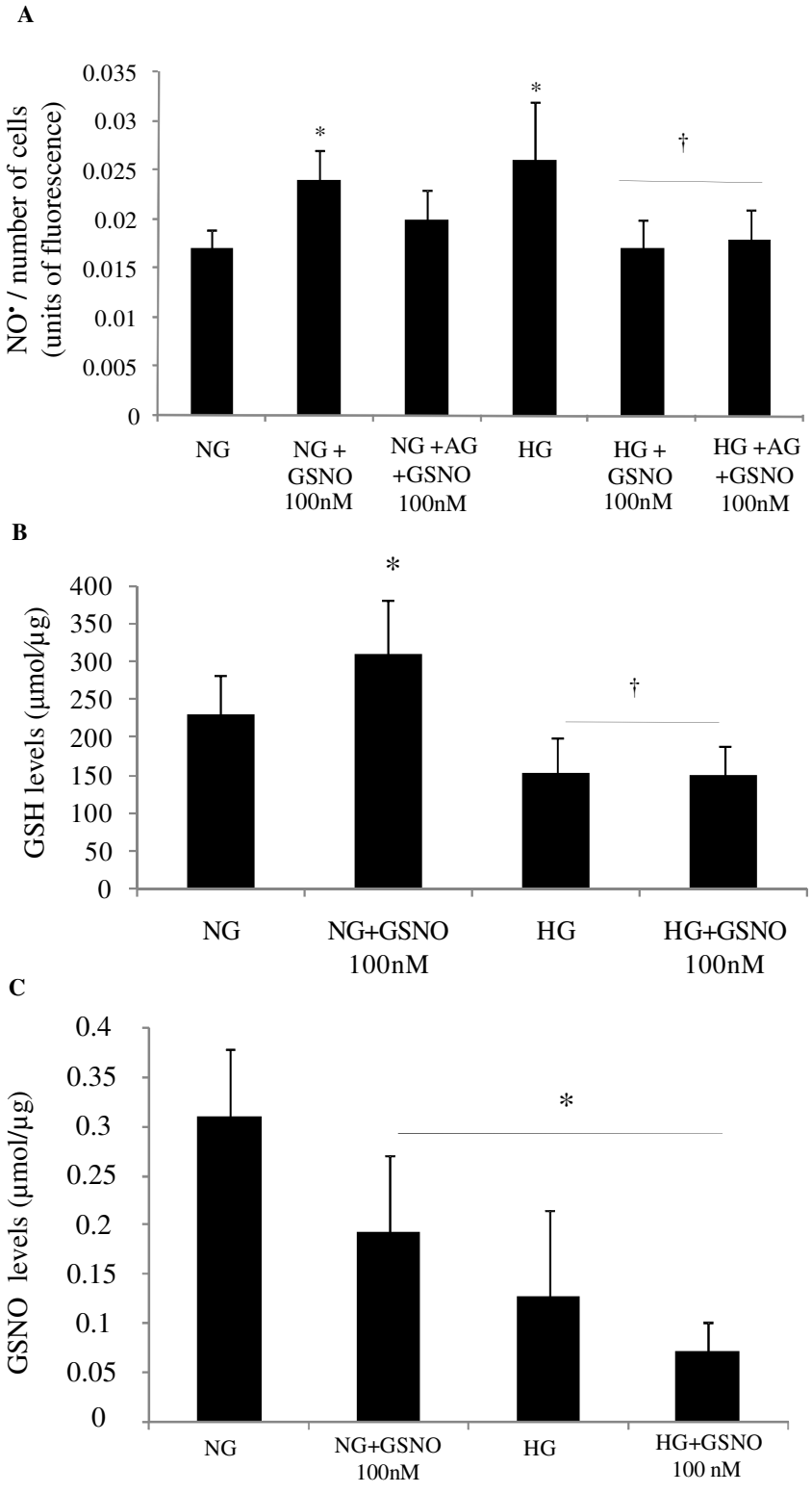

Figure 8. GSNO promotes S-glutathionylation of iNOS.

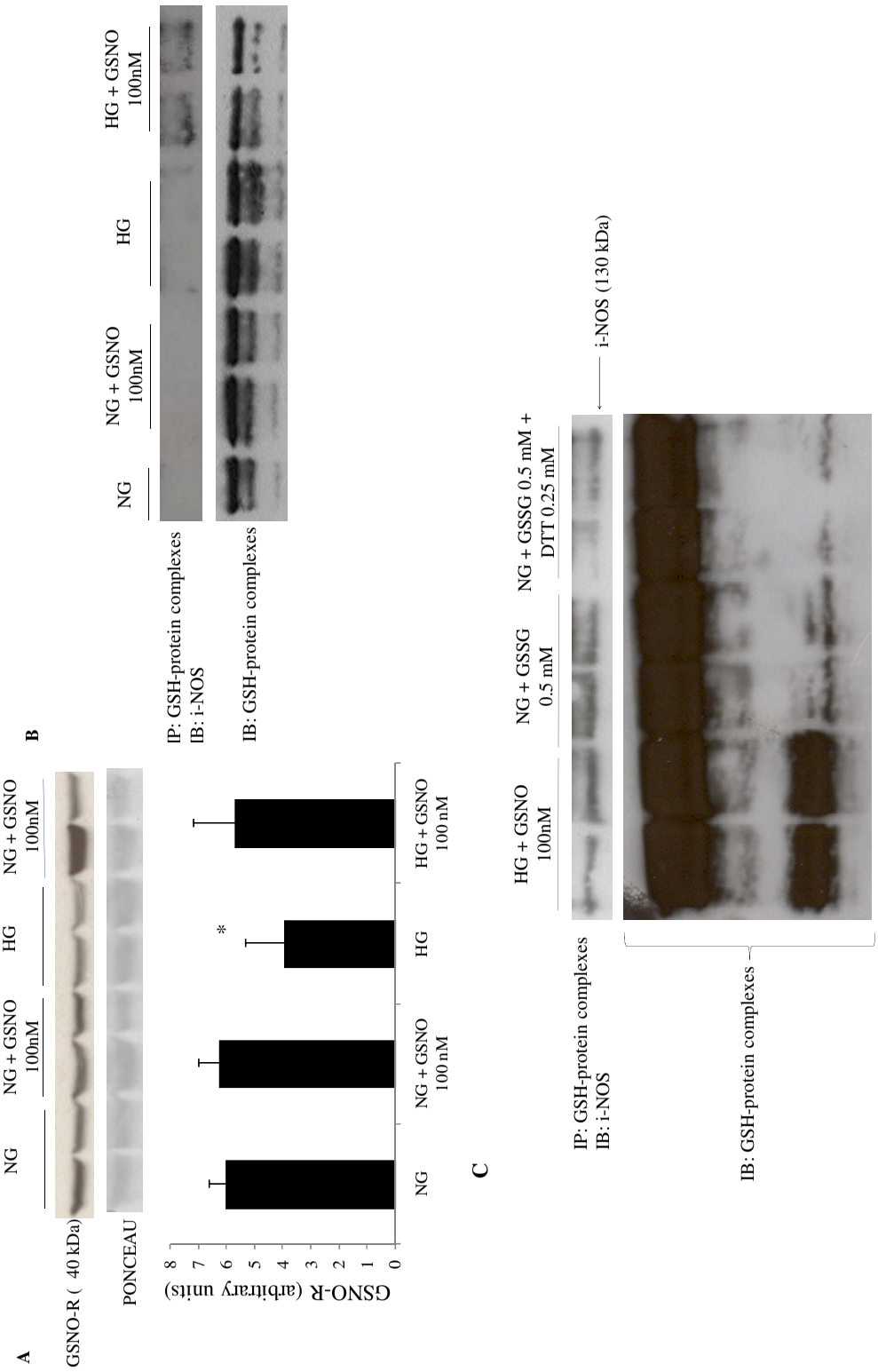

Figure 9. Schematic representation of possible mechanisms involved in nitrosative stress under normal or high glucose conditions in ARPE-19 cells.

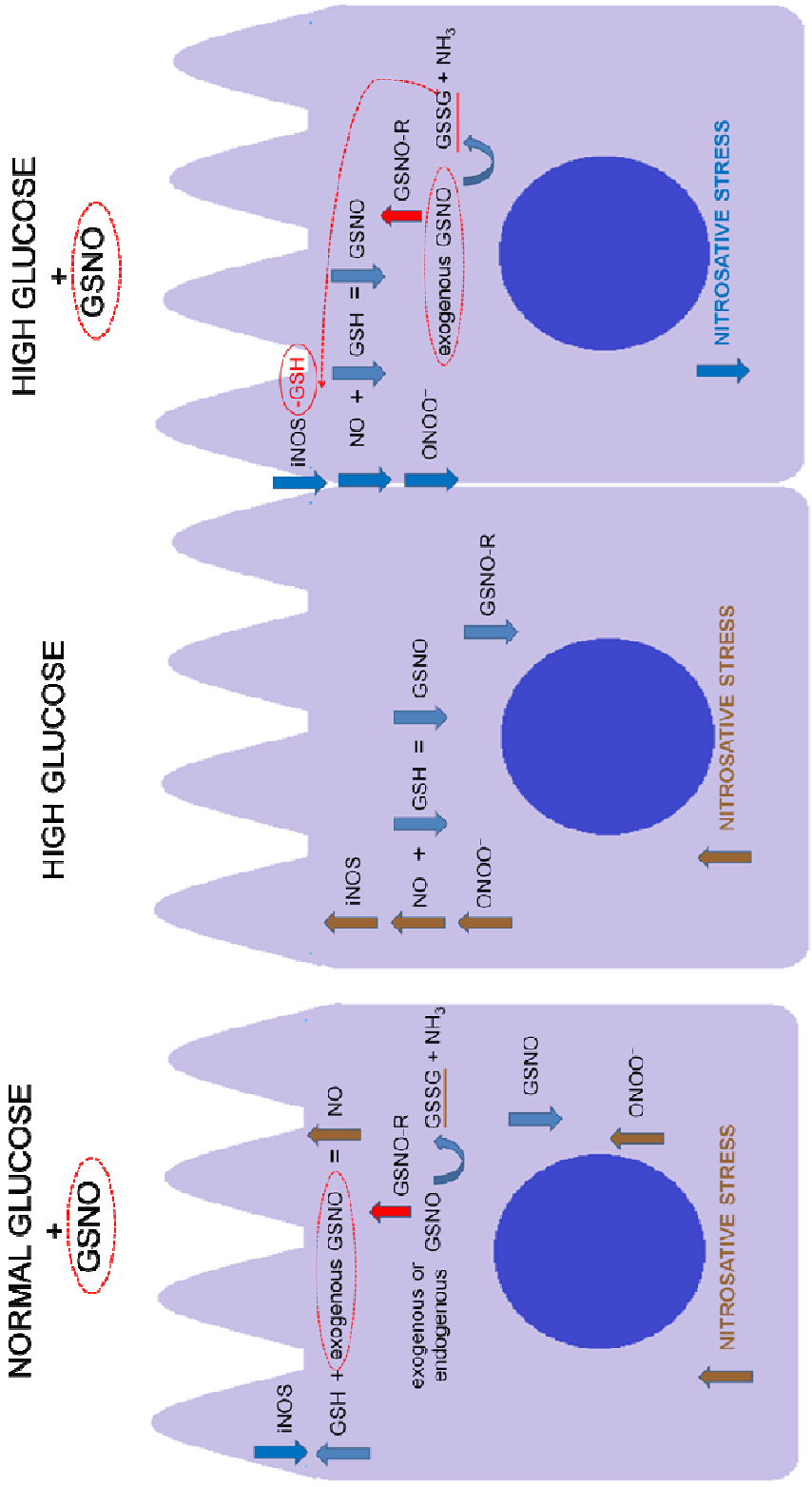

3.2-CAPÍTULO II

ORIGINAL ARTICLE

Endocytosis of tight junctions Caveolin-1 S-nitrosylation dependent is ameliorated by epicatechin through delta-opioid receptor on human retinal pigmented epithelium (ARPE-19) cells exposed to diabetic milieu conditions

Mariana Aparecida B. Rosales, Kamila Cristina Silva, Diego A. Duarte, Jose B. Lopes de Faria, Jacqueline M. Lopes de Faria

Renal Pathophysiology Laboratory and Investigation on Diabetes Complications, School of Medical Sciences (FCM), University of Campinas (UNICAMP), Campinas, São Paulo, Brazil, 13083-877.

Running head: Tight junctionsendocytosis inhibition by epicatechin on opioid receptor

Corresponding author: Jacqueline M. Lopes de Faria, MD, PhD; Faculty of Medical Sciences, University of Campinas (UNICAMP), Campinas, SP, Brazil. Phone: +55-19-35217499 / Fax: +55-19-35217366; email: jmlfaria@fcm.unicamp.br

Word count: 4.485

Number of references: 65

Number of grayscale illustrations: 5

Number of color illustrations: 4

Artigo II

ABSTRACT

Background: Retinal pigment epithelium cells (RPE) along with tight junctions (TJs) proteins constitute the outer blood retinal barrier (BRB). Contradictory findings suggest the role of outer BRB in the pathogenesis of diabetic retinopathy (DR). The aim of this study was to investigate whether the mechanisms involved in these alterations are nitrosative-sensitive, and if cocoa or epicatechin (EP), the predominant polyphenol found in cocoa, protects from thisdamage under diabetic (DM) milieu conditions. ***Methods*****:** Human RPE cells line (ARPE-19) were exposed to high glucose (HG) conditions (30 mM glucose) for 24 hours in the presence or absence of cocoa powder with 0.5% or 60.5% of polyphenol (low-polyphenol cocoa [LPC] and high-polyphenol cocoa [HPC]). ***Results:***Cells exposed to HG presented decreased claudin-1 and occluding TJs expressions and increased extracellular matrix accumulation (ECM); the levels of tumor necrosis factor-alpha (TNF-α) and inducible nitric oxide synthase (iNOS) were upregulated accompanied by an increased production of nitric oxide (NO) levels. This nitrosative stress resulted in S-nitrosylation of caveolin-1 (CAV-1), which in turn increased the CAV-1 traffic and its interactions with claudin-1 and occludin. In the presence of HPC or EC through its δ-opioid receptor (DOR) binding and stimulating capacities, this cascade is inhibited, thus decreasing TNF-α-induced iNOS upregulation and CAV-1 endocytosis. As a result, the TJs were restored, leading to prevention of paracellular permeability and resistance of ARPE-19 monolayer and decreased ECM accumulation.***Conclusion:*** These results reveal that TJs detriment in ARPE-19 cells exposed to DM milieu is througha CAV-1 S-nitrosylation dependent endocytosis mechanism and that HPC or its EP exerts the protective effects through its DOR-binding capacity. **Artigo II**

INTRODUCTION

Diabetic retinopathy (DR) is the most serious complication of diabetic (DM) eye disease and one of the most common causes of irreversible blindness worldwide (1). The retinal pigment epithelium (RPE) is a monolayer of pigmented cells that separates the neural retina from a network of fenestrated vessels called choriocapillaris, which is the major blood supplier for the photoreceptors, and therefore constitutes the outer blood-retinal barrier (BRB). It is increasingly recognizedthat impairment of the outer BRB plays an important role in the initiation and progress of early DR (2,3). The outer BRB is responsible for transport of nutrients, ions and water; absorption of light and protection against photo-oxidation; visual cycle and the phagocytosis of shed photoreceptor membranes and secretion of essential factors for the structural integrity of the retina. It also contributes to the immune-privileged status of the eye (4). Apart from these functions, the RPE stabilizes ion composition in the subretinal space, which is crucial for the maintenance of photoreceptor excitability. Any disturbance in function of these cells necessarily has detrimental consequences for the retina (2). It is well documented that defects in RPE function may underlie a number of sight-threatening conditions, such as age-related macular degeneration (5), proliferative vitreoretinopathy (6) and DR (7,8,2,3).It was reported that RPE dysfunction measured by c-wave amplitude of the electroretinogram (ERG) in experimental DM models is deeply reduced (9,10).However, the direct data for the effects of high glucose (HG) or hyperglycemia on the tight junctions (TJs) integrity and transport functions at the outer BRB are not completely understood.

Artigo II

TJs expressed in the outer BRB control fluids and solutes that enter the retina, and this sealing function, which is essential to retinal homeostasis, is impaired in DR (11). Our previous work showed that ARPE-19 cells exposed to HG displayed a decreasein claudin-1 expression (12), but the mechanisms were not addressed. It was shown that tumor necrosis factor-alpha (TNF-α) induced focal intrajunctional concentration of occludin followed by caveolin-1(CAV-1)–dependent endocytosis in the intestinal epithelial cells (13). CAV-1, the main scaffolding protein of caveolae, is composed of a lipophilic, hairpin-shaped, helical sequence embedded in the inner leaflet of the plasma membrane with both N- and C-terminal cytoplasmic domains. The N-terminus binds to signaling molecules that are required for CAV multimerization. Caveolae have been implicated in endocytosis, transcytosis, calcium signaling and numerous other signal transduction events. An understanding of CAV trafficking and caveola formation is crucial to understanding the possible role of CAV and caveolae (14). It has long been recognized that TJs are relatively cholesterol-rich (15), and the cholesterol-binding protein, CAV-1, was identified as a component of TJs membrane microdomains more than a decade ago by Nursratand coworkers (16). Many studies have provided compelling evidence that CAV-1is involved in regulating endothelial permeability (17). CAV-1 can be precipitated and binds independently to claudin-2 and occludin in MDCK II cells, suggesting a potential mechanism for selective retrieval of tight junction components(18).Thus, CAV-1 might have a more general role in regulating cell junctions, but its molecular regulation of epithelial cell adhesion and barrier function needs to be defined.

RPE contributes to the immune-privileged status of the eye as part of the blood-eye barrier and by the secretion of immunosuppressive/inflammatory factors inside the

eye (19).It was demonstrated that rat RPE cells express inducible nitric oxide synthase (iNOS) and produce nitric oxide (NO) in response to inflammatory cytokines and activated T cells (20,21).In addition, it was demonstrated that 48 hours of HG exposition causes an increase of iNOS expression in ARPE-19 cells(22).

Recently it was demonstrated that activation of opioid-receptors, particularly δ-opioid receptor (DOR),blocks pro-inflammatory cytokines such as TNF-α in the retina under ischemia/reperfusion conditions (23). Epicatechin (EC), the predominant flavonoid present in dark chocolate, is a well-known antioxidant agent (24). Structure-activity relationships of flavonoids with opioid receptor ligands show binding activity *in vitro* (25, 26).

Based on these, the purpose of this study was to evaluate the mechanism by which TJs are decreased in ARPE-19 cells under HG conditions and whether cocoa, through its EC content, could prevent this effect. Our data revealed that under HG, there was an increase in TNF-α levels and iNOS expression accompanied by an increased production of NO resulting in nitrosative imbalance. As a consequence, CAV-1 is S-nitrosylated, modulating the claudin/occludin CAV-1 interactions and CAV-1 traffic. EC, through its opioid receptor binding capacity, activates DOR-mediated downstream signaling, thus decreasing TNF-α-induced CAV-1 endocytosis. As a result, the TJs claudin-1 and occludin were restored, leading to reestablishment of paracellular permeability and resistance of ARPE-19 monolayer capacities.

MATERIAL AND METHODS

Characteristics of Low- and High-Polyphenol-Content Cocoa

The cocoa powder with different amounts of polyphenol was provided by Barry Callebau®. The composition of cocoa was the same in both preparations, with the only difference in the amounts of polyphenol—0.5% for low-polyphenol cocoa (LPC) and 60.5% for high-polyphenol cocoa (HPC). The quantitative characterization of high polyphenol cocoa (HPC) compounds determined by Ultra High-Performance Liquid Chromatography (UHPLC) is shown in supplementary figure 1.

ARPE-19 Cell Line Culture

Human RPE cell line (ARPE-19) cell cultures at 70-90% of confluence were serum starved with FBS concentration to 1%, then were exposed to normal glucose (5.5mM=NG) or high glucose (30mM=HG); or HG plus cocoa containing low (0.5%) or high (60.5%) amounts of polyphenols (LPC or HPC) at 100ng⁄ml (HG + LPC or HG+HPC, respectively) for 24 hours in the presence or absence of NOS non-selective inhibitor L-NAME and iNOS specific inhibitor aminoguanidine (AG) (2mM-2 μM), epicatechin (EC) (0,38nM-380nM), naltrindole (Nalt) (10nM-100μM) (Sigma-Aldrich, St. Louis, MO USA); GSNO (10nM-10μM) synthesized at the Chemistry Institute, State University of Campinas (UNICAMP) as previously described (27)and TNF-α (10-100ng⁄ml) (Calbiochem-Novabiochem, La Jolla, CA). The citotoxicity of treatments on ARPE-19 cells was determined by a thiazolyl blue tetrazolium bromide (MTT) colorimetric assay (28). Concentrations that cause less than 10% of cell toxicity were chosen for the experimental treatments.

Immunofluorescence

The immunofluorescence for ARPE-19 cells was performed as previously

published (29). The cover glasses with fixed cells were incubated with the appropriate primary antibodies—anti claudin-1, occludin, ZO-1 (Zymed Lab Gibco; Invitrogen, San Diego, CA, USA); FN (Calbiochem-Novabiochem, La Jolla, CA); Col-IV (Southern Biotech) and CAV-1 (Santa Cruz Biotechnologies, Santa Cruz, CA)—overnight at 4°C, and the appropriate secondary antibodies were applied for 1 h at room temperature.

Western Blotting Analysis

Western blotting was performed as previously described (12).Membranes were incubated with the appropriate primary antibodies—anti-claudin-1, occludin-1, ZO-1 (Zymed Lab Gibco, Invitrogen, San Diego, CA, USA); FN (Calbiochem-Novabiochem, La Jolla, CA); Col-IV (Southern Biotech) and iNOS (Cell Signaling Technology, USA)—overnight at 4°C, and the appropriate secondary antibodies were applied for 1 h at room temperature. Equal loading and transfer were ascertained by reprobing the membranes for ß-actin.

Measurement of Permeability to Dextran and Paracellular Epithelial Electrical Resistance (TER)

TJs integrity in cell culture is generally measured using transepithelial electrical resistance (TER) and/or paracellular tracer flux (29) as previously described with some modifications. ARPE-19 cellswere placed onTranswell-Clear Polyester Membrane Insert (HTS, Costar; Corning Inc, NY, USA).At day 5, a monolayer structure wasobserved and the complete medium wasreplaced by a medium with the treatments. The permeability of the RPE cells was determined by measuring the apical-to-basolateral movements of fluorescein isothiocyanate (FITC) dextran 40 kDa (100 ug/

mL) (Sigma, Saint Louis, Missouri, USA). Samples were measured at 485 nm of excitation and 528 nm of emission with a microplate fluorescence reader (SynergyMx, Biotek, USA).

For TER measurement, ARPE-19 5-day monolayer cells wereobtained in the same transwell membrane insert as described above.TER values were obtained using an epithelial voltmeter (MILLICELLERS; Millipore, Billerica, MA, USA) with STX100C (for 24-well format) electrode (World Precision Instruments, Sarasota, FL, USA) according to the manufacturer's instructions. Resistance measurements were calculated by subtracting the resistance of the filter alone (background) from the values obtained with the filters with RPE cells.

Measurement Intracellular ROS Production in Cells by Dichlorodihydrofluorescein Diacetate (DCF) and $NO^{\bullet}$ Formation by Diaminofluorescein Diacetate (DAF)

Cells were grown on a 96-well plate and incubated for 30 min with 10 μM of 2',7'-dichlorodihydrofluorescein diacetate (H_2DCFDA) for total intracellular ROS production, and diaminofluorescein diacetate (DAF-2DA) for intracellular $NO^{\bullet}$ levels in Hank's buffer. The amount of fluorescence of DCF or DAF was measured using a fluorescence microplate reader (SynergyMx, Biotek, USA) at excitation and emission wavelengths of 485 and 528 nm, respectively. The relative fluorescence values were corrected by the number of cells in each treatment.

Immunoprecipitation

Cells were washed after treatments with ice-cold PBS and lysed directly in a buffer containing 100 mM tris base, 10 mM sodium pyrophosphate, 100 mM sodium

fluoride, 10 mM EDTA, 2 mM phenylmethylsulfonyl fluoride, 10 mM sodium ortovanadate and 0.1mg⁄ml aprotinin. After centrifugation at 11.000 rpm for 15 min at 4°C, the supernatants were collected and Protein A-sepharose (GE Healthcare Life Sciences) was added (10% of total volume) and incubated for 15 min at 4ºC to remove unspecific binds. Then, the samples were centrifuged at 11.000 rpm for 10 min at 4°C and the protein content was determined by Bradford method (30). 500µg of samples were incubated with mouse anti-caveolin-1(Santa Cruz Biotechnologies, Santa Cruz, CA) or anti-S-Nitroso-Cysteine antibody (Sigma-Aldrich, St. Louis, MO USA) overnight, followed by the addition of protein A-sepharose for 2 h. After centrifugation, the pellets were washed in PBS containing 1 mM EDTA. The immunoprecipitated samples were prepared under reducing or non-reducing conditions as necessary. The Western blotting was performed as described above and incubated with rabbit anti-claudin-1 or occludin for immunoprecipitated samples and subsequently incubated with appropriate secondary antibodies.

Albumin Endocytosis Assay

ARPE-19 cells were submitted to treatments with concomitant addition of BSA conjugated with Alexa 594 (50 µg /ml, Life Technologies, Gaithersburg, MD) in the medium as previously described with some modifications (31). Cells on coverslips were washed with Hank's buffer and fixed with cold methanol (-20ºC) for 10 min at room temperature. Cells were then blocked and incubated in rabbit polyclonal caveolin-1 antibody overnight at 4°C, and then incubated for 1 h with the appropriate secondary antibody.

Artigo II

Human TNF-α Levels

The quantitative levels of human TNF-α in cell culture supernatant of ARPE-19 cells after 24 hours of treatments were determined by Invitrogen Human Tumor Necrosis Factor-Alpha Ultra Sensitive (Hu TNF-α US) colorimetric ELISA Kit (Invitrogen, Carlsbad, CA) according to the manufacturer's instructions.

Fluorometric Measurement of CAV-1 S-Nitrosylation by Diaminonaphthalene(DAN) Assay

S-Nitrosylation of CAV-1 was measured as previously described with some modifications (32).Samples were immunoprecipitated with mouse anti-caveolin-1. The immunoprecipitates were washed with PBS containing 1 mM EDTA. The pellets were resuspended in 500 µl of PBS+EDTA and incubated with 200µM $HgCl_2$ and 200µM diaminonaphthalene (DAN) for 30 min in the dark at room temperature followed by the addition of 0.1 N NaOH of final concentration. In the DAN assay, NO is displaced from S-NO bonds on S-nitrosylated proteins by $HgCl_2$. A fluorescent triazole generated from the reaction between DAN and NO released from *S*-nitrosylated CAV-1 was recorded using a spectrofluorometer (Hitachi, model F-4500, Tokyo, Japan) operating at excitation and emission wavelengths of 375 and 450 nm, respectively, with slit widths of2.5 nm.

Statistical Analysis

Results are presented as folders of increment to independently compare experiments and expressed as the means ± SD. The groups were compared by one-way analysis of variance (ANOVA), followed by the Fisher protected least-significant difference test. StatView statistics software was used for all comparisons, with a significance value of $P \leq 0.05$.

RESULTS

High-Polyphenol Cocoa Preserved the Integrity of Tight Junctions of ARPE-19 CellsExposed to Diabetic Milieu Conditions

In order to investigate the integrity of the ARPE-19 cells monolayer, we evaluated the expression of the TJs proteins claudin-1, occludin and ZO-1. ARPE-19 cells exposed to HG conditions for 24 hours showed a decrease in the expression of claudin-1 and occludin proteins compared to NG ($P \leq 0.03$)(Figure 1A,C). In addition, the immunofluorescence showed the loss of these proteins on the cell membrane under HG treatment (Figure 1B, D). This decrease was prevented by HPC ($P \leq 0.03$) but not by LPC ($P > 0.2$) compared to HG conditions (Figure 1A-D).

In contrast, an increasewas detected in ZO-1 expression under HG compared to NG conditions ($P = 0.03$); the treatment with HPC significantly prevented this alteration compared to HG ($p = 0.001$) (Figure 1E,F). The LPC treatment showeda tendency to decrease compared to HG, but it did not reachstatistical significance ($P = 0.09$).

High-Polyphenol Cocoa Prevented Extracellular Matrix Accumulation in CellsExposed to HG Conditions

The RPE cells play a crucial role in the survival of photoreceptors, choriocapillaris and choroid, through the release of growth factors and production of extracellular matrix (ECM) (4,33). Besides the changes and disorganization on TJs proteins observed under HG conditions, the ARPE-19 monolayer barrier depends upon the ECM accumulation. After 24 hours under HG, the cells upregulates the production of collagen IV and fibronectin proteins when compared to NG conditions ($P \leq 0.02$), and

the treatment with HPC protected from this alteration (P≤0.05) (Figure 2). In light of the findings that ARPE-19 cells exposed to HG for 24 hours showed a profound disturbance on TJs proteins expression accompanied by accumulation of ECM proteins, and that HPC prevented these abnormalities, we assessed the functional features (permeability and resistance) of this monolayer barrier.

High-Polyphenol Cocoa Protected the Barrier Features of ARPE-19 Cell Monolayer Under HG Medium

To investigate whether the above changes could influence the functional features of these cells, we assessed the ARPE-19 monolayer barrier by measuring the paracellular permeability apical-basolateral movements of FITC-dextran and its transepithelial resistance (TER). The cells grown underHG conditions showed significant lower dextran diffusion accompanied by higher TER compared to NG (p≤0.04). Similar to the previous results, only HPC significantly protected the barrier function (p≤0.05) from these abnormalities (Figure 3A,B). One possible mechanism by which the TJs claudin-1 and occludin expressions are decreased in HG medium could

be a mechanism dependent on CAV-1 endocytosis phenomenon. *In vitro* studies have reported occludin endocytosis via macropinocytosis, clathrin-coated pits and caveolae (34,35,36).To test this hypothesis, we assessed CAV-1⁄claudin-1 and CAV-1⁄occludin immunocomplexes.

High-Polyphenol Cocoa Prevented Caveolin-1/Claudin and Caveolin-1/Occludin Complexes in ARPE-19 Cells Under Diabetic Milieu Conditions

In HG conditions, there was a clear augment of CAV-1/claudin-1 and CAV-1/occludin

1/occludin bindings compared to NG ($p \leq 0.04$); the presence of HPC prevented these interactions compared to HG ($p \leq 0.04$) (Figure 4A,B). Through immunolocalization of the CAV-1 protein on the ARPE-19 monolayer, we observed a uniform distribution of CAV-1 in all parts of the cell, membrane, cytoplasm and nucleus in NG conditions. When the cells were exposed to HG, there was a massive internalization of CAV-1 forming roundish structures in the cytoplasm compatible with caveossome. These structures are associated with endocytosis. The use of LPC seems to attenuate this process, but it was clearly prevented on HPC treatment (Figure 4C).

Collectively, these results suggest that in DM milieu conditions, the decrease in TJs claudin-1 and occludin of ARPE-19 cells is associated with caveossome formation.The protective effect of HPC was at least partly dependent on the amount of polyphenols present in the cocoa treatment.

Epicatechin, the Main Compound of Cocoa Polyphenols, Counteracts to Nitrosative Stress, Preventing CAV-1 S-nitrosylation

It was described that TNF-α stimulates occludin endocytosis via caveolin in intestinal epithelial cells (37), but the mechanism by which TNF-α induces increase of internalization and traffic of CAV-1 is unclear. Post-translational modifications of CAV-1 in N-terminal near the scaffolding domain, such as ubiquitination (38) and phosphorylation (31), were involved in exacerbated traffic. As TNF-α increases NO production by regulating iNOS, we verify whether $NO^{\bullet}$ directly modifies the assembly and mobility of CAV-1 by S-nitrosylation, thus regulating vesicular trafficking in ARPE-19 cells.

Artigo II

First we evaluate the oxidative and nitrosative stress in our system. In cells exposed to HG, an increase in total ROS production was observed compared to NG ($P \leq 0.0001$). This effect was prevented by the LPC ($P=0.01$) and was even more significantly decreased with HPC treatment compared to HG ($P \leq 0.0001$) or LPC conditions ($P=0.01$). To test the effect of EC, the most abundant polyphenol present in cocoa, we used the corresponding percentage found in LPC and HPC doses, 0.15 and 12%, respectively. Only the EC concentration correspondent to the percentage present in HCP was able to abrogate the increase in ROS production ($P=0.0005$) compared to HG (Figure 5A). This demonstrates that the high amount of polyphenols present in our HPC counteracts the increase of ROS production in ARPE-19 cells exposed to HG. Following, the NO pathways that could be involved in ROS production in HG conditions were investigated by theH_2DCFDA method. The presence of HPC or unspecific NOS blocker (L-NAME) was able to prevent increased ROS levels compared to HG ($P \leq 0.02$). Concomitant treatments of L-NAME+HPC or L-NAME+EC under HG conditions showed no additive effect. The difference between HG+L-NAME+HPC and HG+L-NAME+EC ($P=0.05$) suggests that other cocoa compounds might exert a protective effect through different pathways (Figure 5B).

Then, we evaluated the production of intracellular NO by theDAF-2DA method and the specific effect of EC on its production. We observed an increase in NO production in cells exposed to HG compared to the CT ($P=0.008$). Just HPC or the corresponding EC content were able to prevent this increment ($P \leq 0.005$) (Figure 5C). These data suggest a specific effect of EC on the NO system. In order to confirm the

source of NO, we assessed the iNOS expression. As expected, iNOS was found upregulated under HG conditions (P=0.003), and in the presence of HPC, this alteration was abolished (P=0.007) (Figure 5D).

As the nitrosative stress induced by iNOS is present in this system, we investigated whether CAV-1 would possibly be nitrosylated by the excessive amounts of NO. The nitrosylated CAV-1 was assessed by immunoprecipitation experiments and analyzed by spectrofluorometry with the DAN method and Western blot (Figure 6A,B). In Figure 6A, the NO released from S-nitrosylated CAV-1 detected by DAN was quantified. It showed that in cells incubated with a NO donor (NG+GSNO), a positive control or HG there was a clear induction of S-nitrosylation on the CAV-1 molecule ($P<0.0001$). HPC, EC alone or AG equally prevented this process ($P\leq0.002$) compared to HG. The presence of iNOS inhibitor AG with HPC showed an additional effect compared to HPC alone (P=0.05). This latter result suggests that other cocoa compounds might act in this pathway. However, HG+AG+EC treatment did not offer an additional effect compared to HG+EC (P=0.6), meaning that the main action of EC is in the prevention of CAV-1*S*-nitrosylation via iNOS downregulation (Figure 6A). In line with fluorimetric assays, a significant increased expression of S-nitrosylated CAV-1 was detected under HG compared to NG ($P<0.0001$), and there was no difference between the protective effect of HPC or EC compared to HG (P=0.5). The treatment HG+AG+HPC again presented an additional effect compared to HG+HPC (P=0.04), and there was no difference between HG+EC and HG+AG+EC treatments (P=0.2) (Figure 6B).

Artigo II

To further understand whether the nitrosylation of the CAV-1 molecule interferes inthe interaction between CAV-1 and the TJs and the CAV-1 internalization, we studied the endocytosis of CAV-1.

Epicatechin Prevents CAV-1 Endocytosis Process, and This Effect Is Dependent of TNFa-iNOS Upregulation Through δ-Opioid Receptor

We measured the TNF-α levels in the supernatant of these cells and observed an increase in cells exposed to HG compared to NG (P=0.002), and both HPC and EC similarly prevented this increment (P≤0.03) (Figure 7A). As activation of opioid receptors can reduce TNF-α production in the retina model of ischemic/reperfusion (23),we used DOR blocker naltrindole (Nalt) to test this hypothesis on ARPE-19 under HG conditions. In the presence of Nalt, the effects of HPC or EC were abolished compared to controls (P≤0.0008) (Figure 7A), indicating that EC modulates TNF-α via DOR receptor. Then, we confirm whether TNF-α can induce iNOS upregulation in our *in vitro* model and if the DOR receptor is involved in this modulation. As expected, the iNOS expression increased when stimulated with TNF-α compared to NG (P=0.0006); the treatment with EC prevented this stimulus (P=0.001); the presence of Nalt abrogated this effect compared to NG+TNF-α+EC (P=0.0002). As expected, ARPE-19 cells under HG conditions increased iNOS expression (P=0.008 vs. NG conditions), and the presence of EC prevented this alteration, leading to normal levels (P=0.02); DOR blocker Nalt abrogates the effects of EC protection compared to HG+TNF-α+EC (P=0.04) (Figure 7B).

To test whether EC prevents CAV-1 endocytosis via DOR receptor, we

performed the albumin endocytosis assay. The process of endocytosis of CAV-1 was observed in a low degree under NG, while it was greatly increased under HG conditions. The treatment with HPC or EC decreased CAV-1 endocytosis, and in the presence of the DOR blocker, this effect was abolished. These findings indicate that the protective effect of EC is at least in part via DOR receptor blockage preventing caveolin transcellular trafficking (Figure 8).

Collectively, these data strongly suggest that the beneficial effects of polyphenols, especially epicatechin, on ARPE-19 cells under DM milieu conditions are via δ-opioid receptor binding, thus decreasing iNOS-TNF-α-dependent upregulation. As a consequence, the NO intracellular production is ameliorated and CAV-1 nitrosylation is prevented, restoring CAV-1 trafficking.

DISCUSSION

In the present study we provide evidence that the process by which claudin-1 and occludin TJs decrease in ARPE-19 cell monolayer exposed to DM milieu conditions is through the CAV-1 endocytosis associated with a profound unbalance in paracellular resistance and permeability. In addition an increase in ZO-1 expression and ECM accumulations was observed. The CAV-1 endocytosis process is dependent of stimulation by TNF-α, which in turn upregulates iNOS expression. The NO production is increased, resulting in S-nitrosylation of CAV-1. The treatment with HPC or EC abolished this effect through direct interaction on DORin ARPE-19 cells. These results reveal for the first time to the best of our knowledge the protective role of EC in

preventing nitrosative posttranslational modification of CAV-1 on ARPE-19 cells, thus restoring the properties of the ARPE-19 barrier exposed to HG conditions.

Most of the research on the physiopathology of DR has focused on the impairment of the neuroretina and the breakdown of the inner BRB. By contrast, the effects of DM on the RPE and in particular on its secretory and transport activity have received less attention. In one direction, the RPE transports electrolytes and water from the subretinal space to the choroid, and in the opposite direction, the RPE transports glucose, retinol, ascorbic acid and fatty acids from the choriocapillaries to the photoreceptors. Both directions showed changes under HG conditions (2). To transport glucose, the RPE contains high amounts of glucose transporters in both apical and basolateral membranes. Both GLUT1 and GLUT3 are highly expressed in the RPE (39,40,41).Recently it has been demonstrated that HG promoted alterations in transport such as downregulation of GLUT-1 (42); alterations in transport of retinol due to a downregulation of the interstitial retinol binding protein (IRBP); impairment of the transport of ascorbic acid limiting the RPE's antioxidant defense (43, 44). There is a large amount of water produced in the retinal tissue, mainly as a consequence of the large metabolic turnover in neurons and photoreceptors. The Na^+-K^+-ATPase, located in the apical membrane, provides energy for the transepithelial transport (45).Constant elimination of water from the subretinal space produces an adhesion force between the retina and the RPE that is lost by inhibition of Na^+-K^+-ATPase by ouabain (46). In cultured bovine RPE cells, it has been demonstrated that HG induces a loss of Na^+/K^+ATPase function, thus decreasing the permeability (47).

TJs constitute the barrier between the subretinal space and the choriocapillaris.

The effects of TJs expression in permeability function have some contradictory findings. It was described that HG concentrations result in a reduction of permeability accompanied by increased TER in human ARPE-19 cells that was unrelated to claudin-1 overexpression mRNA levels (48).However, ARPE-19 cells under endoplasmic reticulum stress induced by tunicamycin or thapsigargin presented a significant increase of ZO-1, occludin and claudin-1 associated with an increase of TER (49).In addition, hyperglycemia could impair the transport of water from subretinal space to the choriochapilaris and, consequently, might contribute to DME development (2). On the other hand, a microscopic imaging assay for directly visualizing macromolecules leaked through the outer BRB in rodents demonstrated the importance of outer BRB breakdown in DM induced by STZ and ischemia experimental model (3).

Nitrosative stress is an early event present on pathogenesis of DR (50). In this present work, the iNOS activation leading to increased NO levels posttranslationally altered CAV-1 molecules, thus increasing the communication with claudin-1 and occludin. Recently, it was demonstrated the pivotal role of CAV-1–dependent occludin endocytosis induced by TNF-α in regulating TJs in intestine epithelial cells (13). Other work showed that phosphorylation of CAV-1 increases its association with vascular endothelial(VE)-cadherin/catenin complexes in response to the pro-inflammatory mediator thrombin. As a consequence, the association of catenin with VE-cadherin is weakened and the junction-associated actin filaments is lost, thus compromising the barrier function (51). Abnormalities in gene expression of CAV-1 have been linked to DR (52), but the possible implications of the CAV-1/caveolae in the outer retina need to be better understood. In RPE cells, caveolae exhibit a unique bipolar distribution (53),

but their functions in either the apical or basolateral RPE membrane domains have not been elucidated. A previous work showed that ablation of CAV-1 resulted in reduced inner and outer retinal functions and *Cav-1* KO retinas also displayed unusually tight adhesion with the RPE, suggesting alterations in outer retinal fluid homeostasis. These findings demonstrate that the reduced retinal function resulting from CAV-1 ablation involves impairment of subretinal and/or RPE ion/fluid homeostasis (54).Post-translational modifications of CAV-1 in N-terminal near the scaffolding domain were involved in exacerbated traffic, such as ubiquitination (55) and phosphorylation (31).In line with our present data, these authors demonstrated that CAV-1 SNO is an important mechanism of caveolae trafficking regulation in endothelial cells.

The opioid receptor family comprises three members—the μ-, δ- and k-opioid receptors—which respond to classical opioid alkaloids such as morphine and heroin as well as to endogenous peptide ligands like endorphins. They belong to the G-protein-coupled receptor (GPCR) superfamily, and are known as excellent therapeutic targets for pain control (56). Activation of one or more opioid receptors by morphine can reduce ischemic/reperfusion injury by the suppression of TNF-α production in the retina. Naloxone, an opioid antagonist, reversed the morphine-induced suppression of TNF-α production *in vitro* (23). EC, the predominant flavonoid component present in cocoa and dark chocolate, is a well-known antioxidant associated with a lower risk of stroke and heart failure (57,58,59). Moreover, EC-induced cardiac protection dependent on DOR receptor stimulation was shown (26).Herein, we demonstrated that the increase of TNF-α levels on ARPE-19 cells exposed to HG is abolished when the cells were treated with HPC or the corresponding amount of EC, neutralizing the HG effect; this

action was abrogated in the presence of Nalt, a DOR blocker. This set of experiments clearly demonstrated that EC protects the ARPE-19 monolayer barrier/permeability through stimulation of DOR, thus modulating the TNF-α actions. It was reported the crystal structure of the mouse DOR, bound to the subtype-selective antagonist Nalt (60), and it was showed that blocking the DOR with oral administration with Nalt resulted in a decrease of the EC protective effect on the mitochondrial structure in mice cardiac protection (61).

In conclusion, we identified EC as a negative regulator of CAV-1 nitrosylation in ARPE-19 cells under DM milieu conditions through the activation of δ-opioid receptor. Because CAV-1 plays an important role in major diseases such as cancer (62), atherosclerosis (63), DM complications (64)and inflammation (65), our findings might provide insights not only into the regulatory mechanism of claudin-1 and occluding by CAV-1 internalization in ARPE-19 cells exposed to HG conditions, but also into the above pathological conditions.

Acknowledgments

This work was supported by the Fundação de Amparo à Pesquisa do Estado de São Paulo (Grants 2008/57560-0 and 2011/06719-1). M.A.B.R. received a scholarship from Coordenação de Aperfeiçoamento de Pessoal de Nível Superior. The authors thank the staff of the Life Sciences Core Facility from the UNICAMP for support with confocal microscopy. The authors are very grateful to the personnel from the Renal Pathophysiology Laboratory, FCM, UNICAMP, for their invaluable help with this work.

ArtigoII

FIGURE LEGENDS

Figure 1. Expression of claudin-1, occludin and ZO-1 tight junctions proteins in ARPE-19 cells under HG conditions and the effects of LPC and HPC treatments. The expression of tight junctions was evaluated after 24 hours in NG, HG, HG+HPC or LPC (100ng⁄ml) treatments. **A,C,E.** Western blot for claudin-1, occludin and ZO-1 expression, respectively, in total cell lysate. Equal loading and transfer were ascertained by reprobing the membranes for ß-actin. The arbitrary unit of densitometry was transformed to folders of increment in relation to the media of NG in each experiment to compare independent experiments. The bars represent mean ±SD. $^{*}P\leq0.03$ versus NG; $^{\#}P\leq0.03$ versus HG. **B,D,F.** Confocal immunofluorescence images showing claudin-1,occludin and ZO-1 expression and localization. The marked TJs are shown in green (located on cell membrane), and the nucleus is indicated in red with propidium iodide (PI) under confocal microscopic field (X630).

Figure 2. HPC prevents the ECM accumulation in ARPE-19 cells under 24 hours in HG. The expression of ECM accumulation was evaluated after 24 hours in NG, HG, HG+HPC or LPC (100ng⁄ml) treatments. **A,C.** Western blot for fibronectin and collagen-IV expression, respectively, in total cell lysate. Equal loading and transfer were ascertained by reprobing the membranes for ß-actin. The arbitrary unit of densitometry was transformed to folders of increment in relation to the media of NG in each experiment to compare independent experiments. The bars represent mean ±SD. $^{*}P\leq0.02$ versus NG;$^{\#}PP\leq0.05$versus HG. **B,D.** Immunofluorescence images showing fibronectin and collagen-IV expression and localization. Fibronectin was

marked in red and its nuclei by DAPI, and collagen-IV was marked in red and its nuclei with propidium iodide (PI), both localized on the membrane under microscopic field (X630).

Figure 3. HPC-protected RPE dysfunctionin ARPE-19 cells under 24 hours in HG. **A.** The permeability and transepithelial electrical (TER) of the RPE cells was determined after 24 hours in NG, HG, HG+HPC or LPC (100ng⁄ml) treatments. For permeability, the apical-to-basolateral movements of FITC dextran (40 kDa) were measured. 200 µL of samples were collected from the basolateral side at 30, 60, 120 and 240 minutes after adding the molecules. A minimum ofthree cultures wasused for each measurement. **B.**For TER measurement, resistance wascalculated by subtracting the resistance of the filteralone (background) from the values obtained with the filters withRPE cells and expressed in ohms-cm^2.TER changes were monitored before and after 24 hours of treatments. The bars represent mean ±SD in both experiments.$^{*}P\leq0.04$versus NG; $^{\#}P\leq0.05$versus HG.

Figure 4. HPC-prevented CAV-1⁄claudin and occludin complexes and CAV-1 internalization. The expression of CAV-1⁄claudin or occludin complexes and CAV-1 expression were evaluated after 24 hours in NG, HG, HG+HPC or LPC (100ng⁄ml) treatments. **A, B.** Immunoprecipitation of cell lysate with CAV-1 antibody incubated with claudin-1 or occludin antibodies, respectively. The CAV-1⁄claudin or occludin complex expressions were measured by Western blot. Equal loading and transfer were ascertained by reprobing the membranes forCAV-1.The arbitrary unit of densitometry was transformed to folders of increment in relation to the media of NG in each

Artigo II

experiment to compare independent experiments.The bars represent mean ±SD in both experiments.*P≤0.04versus NG; #P≤0.04versus HG.**C.** Immunofluorescence images showing CAV-1 expression and localization. CAV-1 was marked in green and its nuclei with propidium iodide (PI) under microscopic field (X630).

Figure 5. Epicatechin, the main compound of HPC, counteracts nitrosative stress. Measurements ofintracellular ROS and NO productions after 24 hours in NG, HG, HG+HPC or LPC (100ng⁄ml); HG+EC correspondent to percentage found in LPC and HPC, 0.25% and12%, respectively. **A,B.**Total intracellular ROS production obtained by H_2DCFDA fluorescence method.**A.** The effects of epicatechin (EC) amounts on ROS production. Bars represent the mean ± SD of fluorescence units obtained in ELISA reader and corrected by the number of cells at the end of each treatment. Mannitol was used for an osmotic control in this experiment to see if there is some effect of osmolarity. *P≤0.0001versus NG;#P≤0.01 versus HG group. **B.** The NOS non-selective inhibitor L-NAME (2 mM) was used to test EC role in downregulating ROS production via NO system. Bars represent the mean ± SD of fluorescence units obtained in ELISA reader and corrected by the number of cells at the end of each treatment.*P≤0.03versus NG;#P≤0.02versus HG; †P=0.05 versus HG+L-NAME+EC. **C.** Intracellular NO production measured by DAF-2DA method. Bars represent the mean ± SD of fluorescence units obtained in ELISA reader and corrected by the number of cells at the end of each treatment.*P=0.008versus NG;#P≤0.005 versus HG. **D.** Western blot for iNOS expression in total cell lysate. Equal loading and transfer were ascertained by reprobing the membranes for ß-actin. The arbitrary unit of densitometry was transformed to folders of increment in relation to the media of NG in each experiment to

compare independent experiments. The bars represent mean ±SD.*P=0.003versus NG;#P=0.007versus HG.

Figure 6. Epicatechin counteracts nitrosative stress and prevented S-nitrosylation of CAV-1. Measurement of CAV-1 S-nitrosylation after 24 hours in NG, HG, HG+HPC (100ng⁄ml), HG+EC (12ng⁄ml).The specific iNOS blocker aminoguanidine (AG) was used in a concentration of 2mM to access the protective effects of EC via downregulation iNOS. **A**. Fluorometric Measurement of CAV-1 S-nitrosylation by diaminonaphthalene (DAN) assay. GSNO (1μM) was usedas a positive control on induction of CAV-1 S-nitrosylation. The fluorescence units obtained via ELISA reader weretransformed to folders of increment in relation to the media of NG in each experiment to compare independent experiments. Bars represent the mean ± SD.*P<0.0001 versus NG conditions; #P≤0.002versus HG treatment; †P=0.05 versus HG+HPC.**B.** Expression of S-nitrosylated CAV-1. Western blot of cell lysate immune precipitated with S-Nitroso-Cysteine (SNO-Cys) antibody and immunoblotted for anti-CAV-1.Equal loading and transfer were ascertained by reprobing the membranes for SNO-Cys antibody.The arbitrary unit of densitometry was transformed to folders of increment in relation to the media of NG in each experiment to compare independent experiments.The bars represent mean ±SD in both experiments.*P<0.0001versus NG; #P≤0.002 versus HG; †P=0.04 versus HG+HPC.

Figure 7. Epicatechin prevents TNFα-iNOS upregulation through δ-opioid receptor (DOR). A. Measurement of TNF-α levels in the supernatant of ARPE-19 cells by ELISA assay. We used specific DOR blocker naltrindole (Nalt) in a concentration of 10μM to investigate whether the effects of EC are dependent on DOR receptor.

The absorbance values were corrected by protein concentration and expressed as pg⁄ml⁄µg. *P=0.002 versus NG; #P≤0.03 versus HG; †P≤0.0008 versus HG+HPC and HG+EC, respectively.**B.** Western blot for iNOS expression in total cell lysate. TNF-α treatment, in a concentration of 40ng⁄ml, was used to induce iNOS expression. Equal loading and transfer were ascertained by reprobing the membranes for ß-actin. The arbitrary unit of densitometry was transformed to folders of increment in relation to the media of NG in each experiment to compare independent experiments. The bars represent mean ±SD.*P≤0.01versus NG; #P≤0.02versus;†P=0.04 versus HG+EC.

Figure 8. Epicatechin prevents CAV-1 endocytosis process through δ-opioid receptor blockage. Albumin (BSA) Endocytosis Assay. Immunofluorescence images showing endocytosis of BSA conjugated with Alexa 594 (red), CAV-1 localization (green) and its nuclei with DAPI (blue) under microscopic field (X630).

Legends:

NG: normal glucose; **NG+GSNO**: normal glucose + GSNO; **HG:** high glucose; **HG+LPC:** high glucose + low polyphenol cocoa; **HG+HPC:** high glucose + high polyphenol cocoa; **HG+EC:**high glucose + epicatechin; **HG+EC (%LPC):** high glucose + epicatechin 0.25ng⁄ml; **HG+EC (%HPC):** high glucose + epicatechin 12ng⁄ml; **HG+L-NAME:** high glucose + L-NAME; **HG+L-NAME+HPC:** high glucose + L-NAME+high polyphenol cocoa; **HG+L-NAME+EC:** high glucose + L-NAME+epicatechin; **HG+AG:** high glucose + aminoguanidine; **HG+AG+HPC:**high glucose + aminoguanidine + high polyphenol cocoa; **HG+AG+EC:**high glucose + aminoguanidine + epicatechin; **NG+TNF-α:** normal glucose + TNF-α; **NG+TNF-**

α+EC: normal glucose + TNF-α + epicatechin; **NG+TNF-α+Nalt+EC:** normal glucose high polyphenol cocoa; **HG+Nalt+EC:** high glucose + naltrindole + epicatechin.

REFERENCES

1- Frank RN Diabetic retinopathy. N Engl J Med 350: 48–58, 2004.

2- Simo R, Villarroel M, Corraliza L, Hernandez C, Garcia-Ramirez M. The retinal pigment epithelium: something more than a constituent of the bloodretinal barrier–implications for the pathogenesis of diabetic retinopathy. J Biomed Biotechnol: 2010:190724, 2010.

3- Xu HZ, Le YZ. Significance of outer blood-retina barrier breakdown in diabetes and ischemia. Invest Ophthalmol Vis Sci 52(5): 2160-4, 2011.

4- Strauss O. The retinal pigment epithelium in visual function. Physiol Rev 85: 845–881, 2005.

5- Eagle RC Jr. Mechanisms of maculopathy. Ophthalmology 91(6):613-25, 1984.

6- Dorey CK, Wu G, Ebenstein D, Garsd A, Weiter JJ. Cell loss in the aging retina: relationship to lipofuscin accumulation and macular degeneration. Invest OphthalmolVis Sci 30: 1691–1699, 1989.

7- Vinores SA, Gadegbeku C, Campochiaro PA, Green WR. Immunohistochemical localization of blood-retinal barrier breakdown in human diabetics. Am J Pathol 134: 231–235, 1989.

8- Hewitt AT, Adler R. The retinal pigment epithelium and interphotoreceptor matrix: structure and specialized functions. Retina: Basic Science and Inherited Retinal Disease. 1: 58–71, 1994.

9- Pautler EL, Ennis SR. The effect of induced diabetes on the electroretinogram components of the pigmented rat. Invest Ophthalmol Vis Sci 19(6): 702-5, 1980.

10- Samuels IS, Lee CA, Petrash JM, Peachey NS, Kern TS. Exclusion of aldose reductase as a mediator of ERG deficits in a mouse model of diabetic eye disease. Vis Neurosci 29(6): 267-74, 2012.

11- Villarroel M, García-Ramírez M, Corraliza L, Hernández C, Simó R High glucose concentration leads to differential **expression** of **tight junction** proteins in human

Artigo II

retinal pigment epithelial **cells.**Endocrinol Nutr 56(2): 53-8, 2009.

12- Silva KC, Rosales MA, Hamassaki DE, Saito KC, Faria AM, Ribeiro PA, Faria JB, Faria JM. Green tea is neuroprotective in diabetic retinopathy.Invest Ophthalmol Vis Sci 54(2): 1325-36, 2013.

13- Marchiando AM, Shen L, Graham WV, Weber CR, Schwarz BT, Austin JR 2nd, Raleigh DR, Guan Y, Watson AJ, Montrose MH, Turner JR. Caveolin-1-dependent occludin endocytosis is required for TNF-induced tight junction regulation in vivo. J Cell Biol 189(1): 111-26, 2010.

14- Parton RG, Simons K. The multiple faces of caveolae. Nat Rev Mol Cell Biol 8: 185–194, 2007.

15- Feltkamp, CA, Van der Waerden AW. Junction formation between cultured normal rat hepatocytes. An ultrastructural study on the presence of cholesterol and the structure of developing tight-junction strands. J. Cell Sci.63**:** 271–286, 1983.

16- Nusrat A, Parkos CA, Verkade P, Foley CS, Liang TW, Innis-Whitehouse W, Eastburn KK, Madara JL.Tight junctions are membrane microdomains. J Cell Sci 113:1771–1781, 2000.

17- Schubert W, Frank PG, Razani B, Park DS, Chow CW, Lisanti MP. Caveolae-deficient endothelial cells show defects in the uptake and transport of albumin in vivo. J Biol Chem 276: 48619–48622, 2001.

18- Itallie CM, Anderson JM. Caveolin binds independently to claudin-2 and occludin. Ann N Y Acad Sci 1257: 103-7, 2012.

19- Holtkamp GM, Kijlstra A, Peek R, de Vos AF. Retinal Pigment Epithelium-immune System Interactions: Cytokine Production and Cytokine-induced Changes. Prog Retin Eye Res 20: 29-48, 2001.

20- Goureau O, Lepoivre M, Becquet F, Courtois Y. Differential regulation of inducible nitric oxide synthase by fibroblast growth factors and transforming growth factor b in bovine retinal pigmented epithelial cells: inverse correlation with cellular proliferation. Proc Natl Acad Sci U SA 90: 4276-4280, 1993.

21- Liversidge J, Grabowski P, Ralston S, Benjamin N, Forrester JV. Rats retinal pigment epithelial cells express an inducible form of nitric oxide synthase and produce nitric oxide in response to inflammatory cytokines and activated T cells. Immunology 83: 404-409, 1994.

22- Yuan Z, Feng W, Hong J, Zheng Q, Shuai J, Ge Y. p38MAPK and ERK promote nitric oxide production in cultured human retinal pigmented epithelial cells induced by high concentration glucose. Nitric Oxide 20: 9-15, 2009.

Artigo II

23- Husain S, Liou GI, Crosson CE. Opioid-receptor-activation: Suppression of ischemia/reperfusion-induced production of TNF-alpha in the retina. Invest Ophthalmol Vis Sci 52: 2577-83, 2011.

24- Ramiro-Puig E, Castell M. Cocoa: antioxidant and immunomodulator. Br J Nutr 101: 931–940, 2009.

25- Taubert D, Roesen R, Lehmann C, Jung N, Schomig E. Effects of low habitual cocoa intake on blood pressure and bioactive nitric oxide: a randomized controlled trial. JAMA298: 49–60, 2007.

25- Katavic PL, Lamb K, Navarro H, Prisinzano TE. Flavonoids as opioid receptor ligands: identification and preliminary structure-activity relationships. J Nat Prod 70: 1278–1282, 2007.

26- Panneerselvam M, Tsutsumi YM, Bonds JA, Horikawa YT, Saldana M, Dalton ND, Head BP, Patel PM, Roth DM, Patel HH.Dark chocolate receptors: epicatechin-induced cardiac protection is dependent on delta-opioid receptor stimulation. Am. J. Physiol. Heart Circ. Physiol 299: H1604–H1609, 2010.

27- Costa IS, de Souza GF, de Oliveira MG, Abrahamsohn Ide A. S-nitrosoglutathione (GSNO) is cytotoxic to intracellular amastigotes and promotes healing of topically treated Leishmania major or Leishmania braziliensis skin lesions. J Antimicrob Chemother 68(11): 2561-8, 2013.

28- Mosmann T. Rapid colorimetric assay for cellular growth and survival: application to proliferation and cytotoxicity assays. J Immunol Meth 65: 55-63, 1983.

29- Garcia-Ramírez M, Villarroel M, Corraliza L, Hernández C, Simó R. Measuring permeability in human retinal epithelial cells (ARPE-19): implications for the study of diabetic retinopathy. Methods Mol Biol 763: 179-194, 2011.

30- Bradford MM. A rapid and sensive method for the quantification of microgram quantities of protein utilizing the principle of protein dye binding. Anal Biochem.72: 248–254, 1976.

31- Takeuchi K, Morizane Y, Kamami-Levy C, Suzuki J, Kayama M, Cai W, Miller JW, Vavvas DG. AMP-dependent kinase inhibits oxidative stress-induced caveolin-1 phosphorylation and endocytosis by suppressing the dissociation between c-Abl and Prdx1 proteins in endothelial cells. J Biol Chem 288(28): 20581-91, 2013.

32- Azad N, Vallyathan V, Wang L, Tantishaiyakul V, Stehlik C, Leonard SS, Rojanasakul Y S-nitrosylation of Bcl-2 inhibits its ubiquitin-proteasomal degradation. A novel antiapoptotic mechanism that suppresses apoptosis. J Biol Chem 281(45): 34124-34, 2006.

33- Elner VM, Burnstine MA, Strieter RM, Kunkel SL, Elner SG. Cell-associated human retinal pigment epithelium interleukin-8 and monocyte chemotactic protein-1: immunochemical and in-situ hybridization analyses. Exp Eye Res 65: 781–789, 1997.

34- Ivanov AI, Nusrat A, Parkos CA. Endocytosis of epithelial apical junctional proteins by a clathrin-mediated pathway into a unique storage compartment. Mol Biol Cell 15: 176–188, 2004b.

35- Bruewer M, Utech M, Ivanov AI, Hopkins AM, Parkos CA, Nusrat A. Interferon-gamma induces internalization of epithelial tight junction proteins via a macropinocytosis-like process. FASEB J 19: 923–933, 2005.

36- Shen L, Turner JR. Actin depolymerization disrupts tight junctions via caveolae-mediated endocytosis. Mol Biol Cell 16: 3919–3936, 2005.

37- Marchiando AM, Shen L, Graham WV, Weber CR, Schwarz BT, Austin JR 2nd, Raleigh DR, Guan Y, Watson AJ, Montrose MH, Turner JR. Caveolin-1-dependent occludin endocytosis is required for TNF-induced tight junction regulation in vivo. Cell Biol 189(1): 111-26, 2010.

38- Kirchner P, Bug M, Meyer H. Ubiquitination of the N-terminal region of caveolin-1 regulates endosomal sorting by the VCP/p97 AAA-ATPase. J Biol Chem 288(10): 7363-72, 2013

39- Ban Y, Rizzolo LJ. Regulation of glucose transporters during development of the retinal pigment epithelium. Developmental Brain Research 121: 89–95, 2000.

40- Bergersen LJ, Jóhannsson E, Veruki ML, Nagelhus EA, Halestrap A, Sejersted OM, Ottersen OP.Cellular and subcellular expression of monocarboxylate transporters in the pigment epithelium and retina of the rat. Neuroscience 90: 319–331, 1999.

41- Senanayake PD, Calabro A, Hu JG, Bonilha VL, Darr A, Bok D, Hollyfield JG. Glucose utilization by the retinal pigment epithelium: evidence for rapid uptake and storage in glycogen, followed by glycogen utilization. Experimental Eye Research 83: 235–246, 2006.

42- Kim DI, Lim SK, Park MJ, Han HJ, Kim GY, Park SH. The involvement of phosphatidylinositol 3-kinase/Akt signaling in high glucose-induced downregulation of GLUT-1 expression in ARPE cells. Life Sciences 80:626–632, 2007.

43- Salceda R, Contreras-Cubas C. Ascorbate uptake in normal and diabetic rat retina and retinal pigment. Comp Biochem Physiol C Toxicol Pharmacol. 146:175-179, 2007.

44- Minamizono A, Tomi M, Hosoya K.I. Inhibition of dehydroascorbic acid transport across the rat blood-retinal and -brain barriers in experimental diabetes. Biological andPharmaceutical Bulletin 29: 2148–2150, 2006.

Artigo II

45- Marmorstein AD. The polarity of the retinal pigment epithelium. Traffic 2: 867–872, 2001.

46- Frambach DA, Roy CE, Valentine JL, Weiter JJ. Precocious retinal adhesion is affected by furosemide and ouabain. Current Eye Research 8: 553–556, 1989.

47- Crider JY, Yorio T, Sharif NA, Griffin BW. The effects of elevated glucose on Na+/K+-ATPpase of cultured bovine retinal pigment epithelial cells measured by a new nonradioactive rubidium uptake assay. Journal of Ocular Pharmacology and Therapeutics 13: 337–352, 1997.

48- Villarroel M, Garcia-Ramirez M, Corraliza L, Hernandez C, Simo R. Effects of high glucose concentration on the barrier function and the expression of tight junction proteins in human retinal pigment epithelial cells. Exp Eye Res 89: 913–920, 2009.

49- Yoshikawa T, Ogata N, Izuta H, Shimazawa M, Hara H, Takahashi K. Increased expression of tight junctions in ARPE-19 cells under endoplasmic reticulum stress. Curr Eye Res 36: 1153-63, 2011.

50- Zheng L, Du Y, Miller C, Gubitosi-Klug RA, Ball S, Berkowitz BA, Kern TS. Role of inducible nitric oxide synthase in degeneration of retinal capillaries in mice with streptozotocin-induced diabetes.Diabetologia 50: 1987-96, 2007.

51- Kronstein R, Seebach J, Grossklaus S, Minten C, Engelhardt B, Drab M, Liebner S, Arsenijevic Y, Taha AA, Afanasieva T, Schnittler HJ. Caveolin-1 opens endothelial cell junctions by targeting catenins. Cardiovasc Res 93:130-140, 2012.

52- Klaassen I, Hughes JM, Vogels IMC, Schalkwijk CG, Van Noorden CJF, Schlingemann RO. Altered expression of genes related to blood–retina barrier disruption in streptozotocin induced diabetes. Experimental Eye Research 89: 4–15, 2009.

53- Mora, RC, Bonilha VL, Shin BC, Hu J, Cohen-Gould L, Bok D, Rodriguez-Boulan E. Bipolar assembly of caveolae in retinal pigment epithelium. Am. J. Physiol. Cell Physiol 290:832–843, 2006.

54- Li X, McClellan ME, Tanito M, Garteiser P, Towner R, Bissig D, Berkowitz BA, Fliesler SJ, Woodruff ML, Fain GL, Birch DG, Khan MS, Ash JD, Elliott MH. Loss of caveolin-1 impairs retinal function due to disturbance of subretinal microenvironment. J Biol Chem 287: 16424-16434, 2012.

55- Kirchner P, Bug M, Meyer H. Ubiquitination of the N-terminal region of caveolin-1 regulates endosomal sorting by the VCP/p97 AAA-ATPase. J Biol Chem 288: 7363-72, 2013.

Artigo II

56- Pradhan, AA, Befort K, Nozaki C, Gaveriaux-Ruff C, Kieffer BL. The delta opioid receptor: an evolving target for the treatment of brain disorders. Trends Pharmacol. Sci 32: 581–590 2011.

57- Engler MB, Engler MM. The emerging role of flavonoid-rich cocoa and chocolate in cardiovascular health and disease. Nutr Rev64: 109–118, 2006.

58- Ramiro-Puig E, Castell M. Cocoa: antioxidant and immunomodulator. Br J Nutr 101: 931–940, 2009.

59- Steffen Y, Schewe T, Sies H. Myeloperoxidase-mediated LDL oxidation and endothelial cell toxicity of oxidized LDL: attenuation by (-)-epicatechin. Free Radic Res 40: 1076–1085, 2006.

60- Granier S, Manglik A, Kruse AC, Kobilka TS, Thian FS, Weis WI, Kobilka BK. Structure of the δ-opioid receptor bound to naltrindole. Nature 485: 400–404, 2012.

61- Panneerselvam M, Ali SS, Finley JC, Kellerhals SE, Migita MY, Head BP, Patel PM, Roth DM, Patel HH. Epicatechin regulation of mitochondrial structure and function is opioid receptor dependent. Mol Nutr Food Res 57(6):1007-14, 2013.

62- Yu S, Fan J, Liu L, Zhang L, Wang S, Zhang J. Caveolin-1 up-regulates integrin α2,6-sialylation to promote integrin α5β1-dependent hepatocarcinoma cell adhesion. FEBS Lett 587(6): 782-7, 2013.

63- Rodriguez-Feo JA, Hellings WE, Moll FL, De Vries JP, van Middelaar BJ, Algra A, Sluijter J, Velema E, van den Broek T, Sessa WC, De Kleijn DP, Pasterkamp G. Caveolin-1 influences vascular protease activity and is a potential stabilizing factor in human atherosclerotic disease. PLoS One 3(7): e2612, 2008.

64- Cassuto J, Dou H, Czikora I, Szabo A, Patel VS, Kamath V, Belin de Chantemele E, Feher A, Romero MJ, Bagi Z. Peroxynitrite Disrupts Endothelial Caveolae Leading to eNOS Uncoupling and Diminished Flow-Mediated Dilation in Coronary Arterioles of Diabetic Patients. Diabetes Dec 18. [Epub ahead of print], 2013.

65- Wang Y, Wang X, Lau WB, Yuan Y, Booth DM, Li J, Scalia R, Preston KJ, Gao E, Koch WJ, Ma XL. Adiponectin Inhibits TNF-α-Induced Vascular Inflammatory Response via Caveolin-Mediated Ceramidase Recruitment and Activation. Circ Res Jan 7. [Epub ahead of print], 2014.

Artigo II

Figure 1. Expression of claudin-1, occludin and ZO-1 tight junctions proteins in ARPE-19 cells under HG conditions and the effects of LPC and HPC treatments.

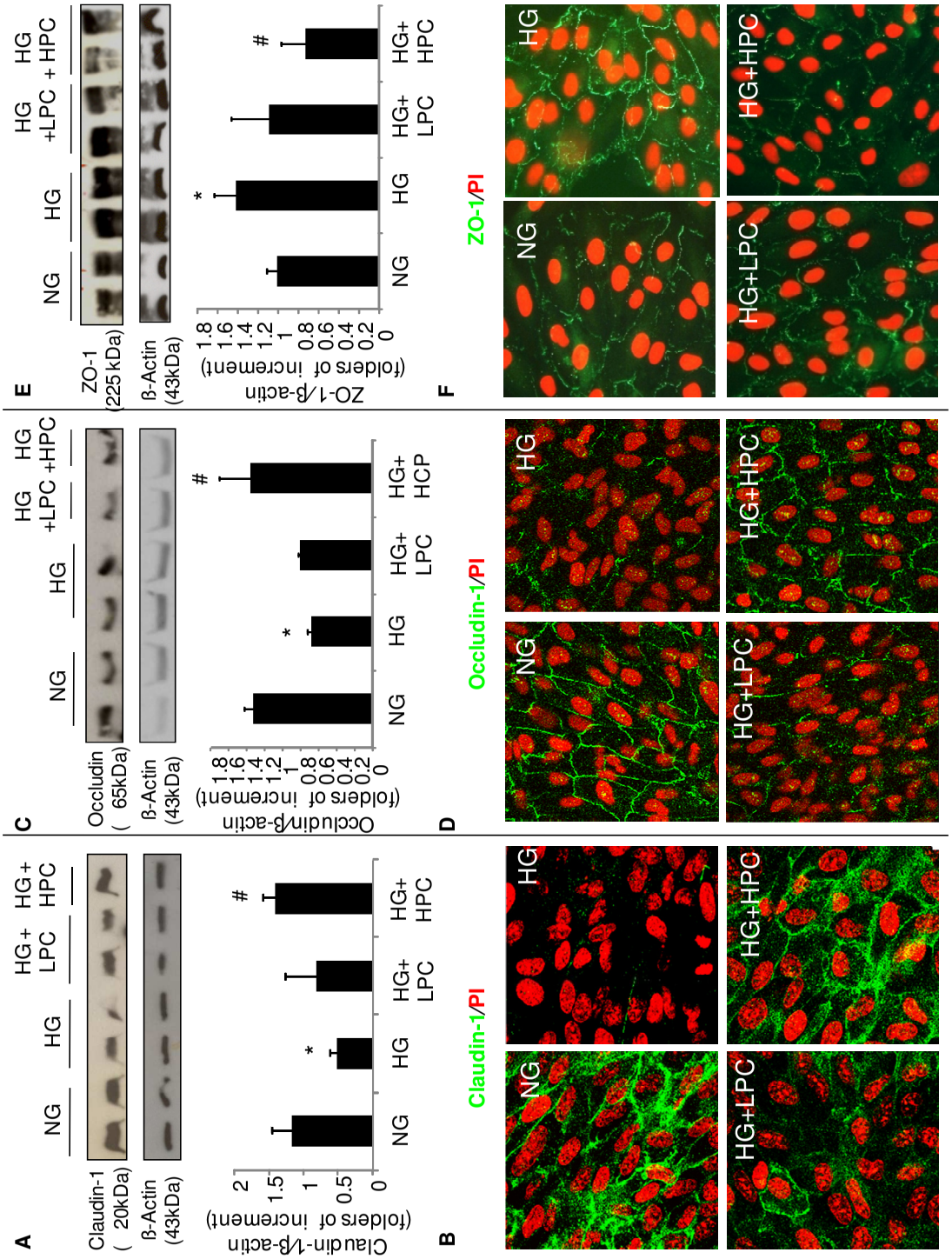

Figure 2. HPC prevents the ECM accumulation in ARPE-19 cells under 24 hours in HG.

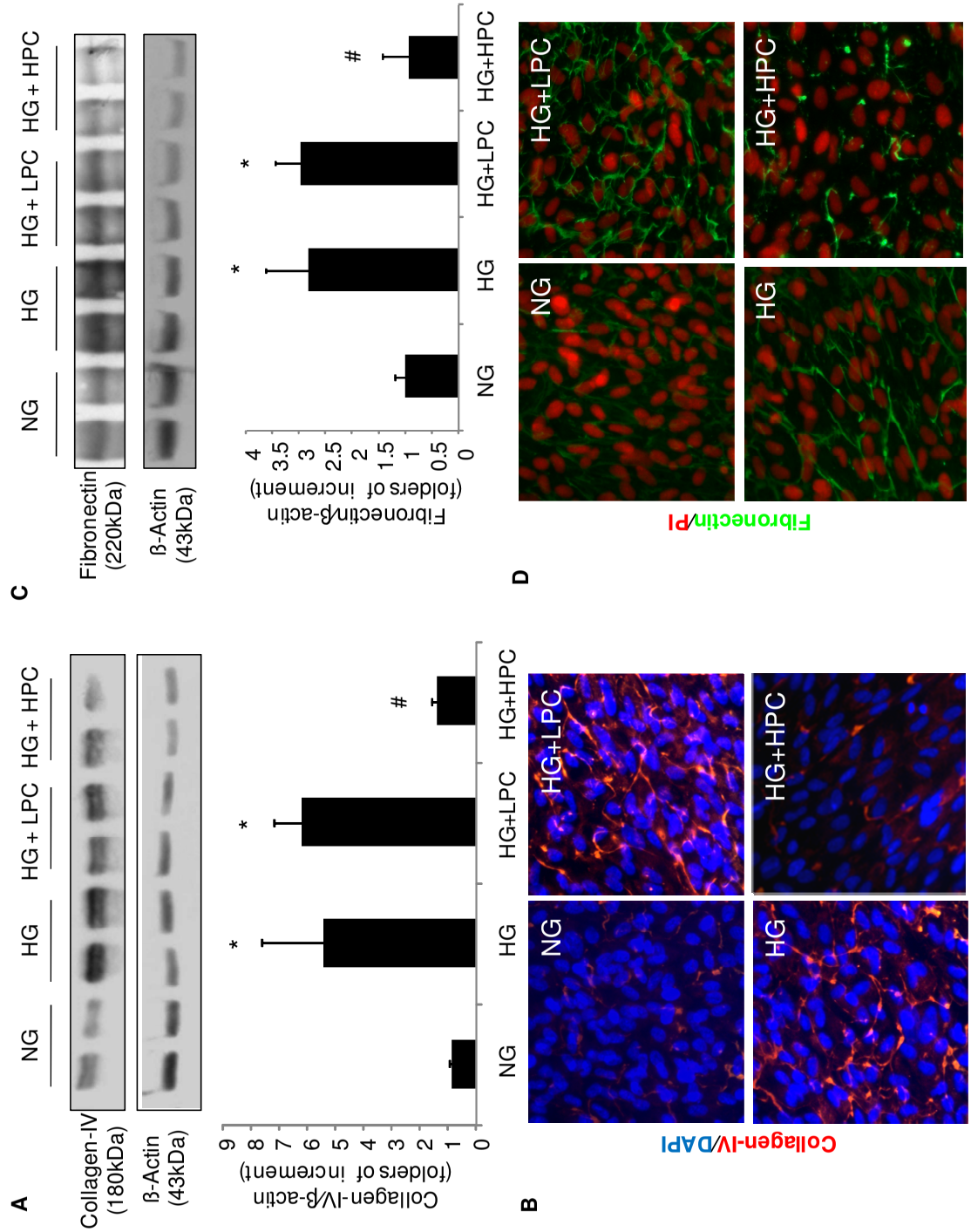

Figure 3. HPC-protected RPE dysfunction in ARPE-19 cells under 24 hours in HG.

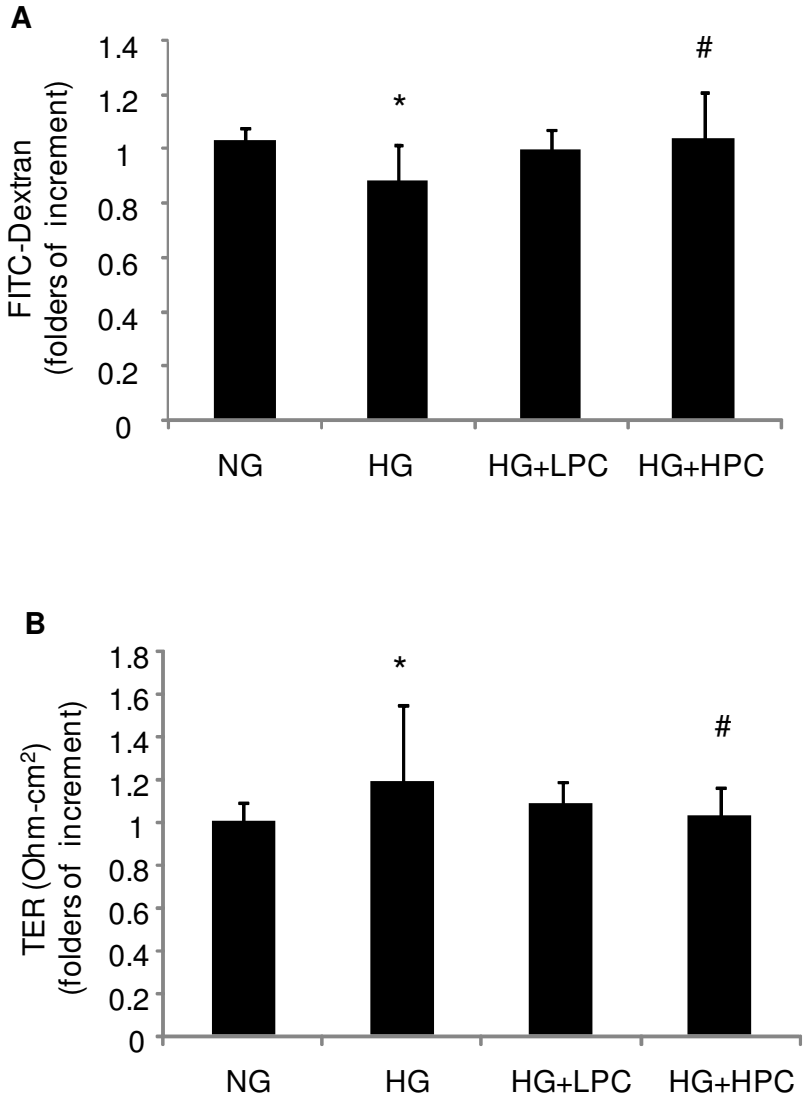

Artigo II

Figure 4. HPC-prevented CAV-1/claudin and occludin complexes and CAV-1 internalization.

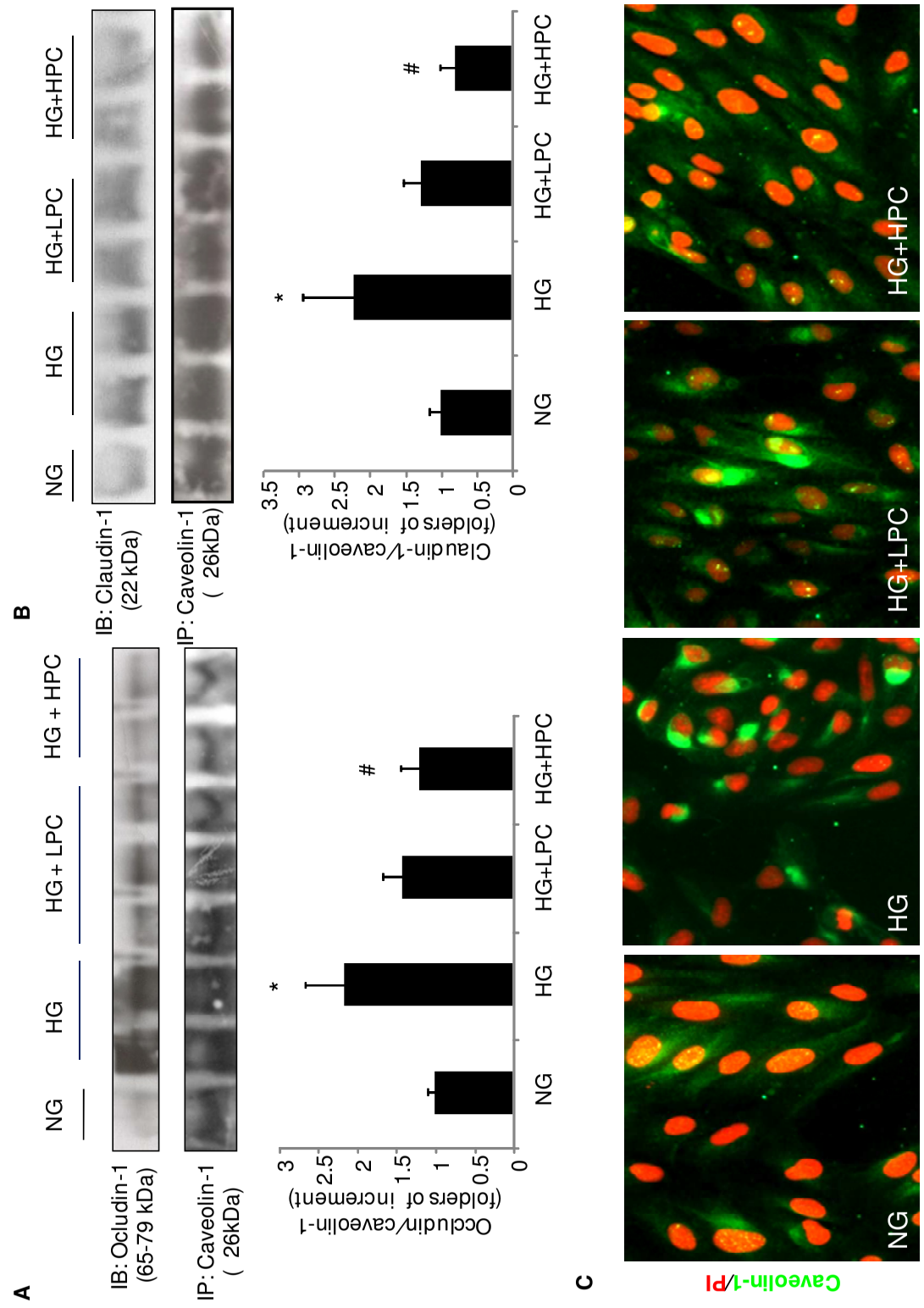

Artigo II

Figure 5. Epicatechin, the main compound of HPC, counteracts nitrosative stress.

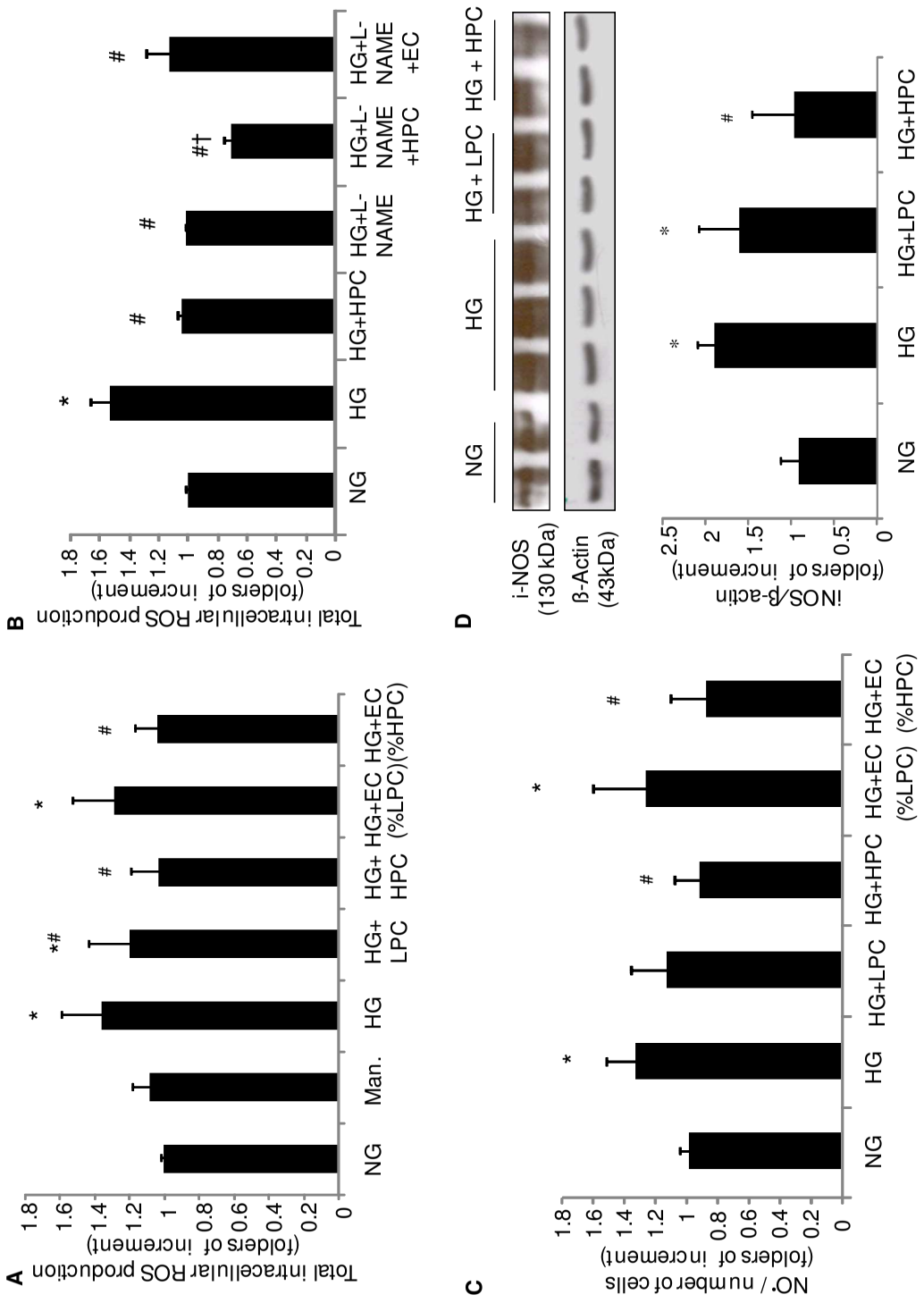

Figure 6. Epicatechin counteracts nitrosative stress and prevented S-nitrosylation of CAV-1.

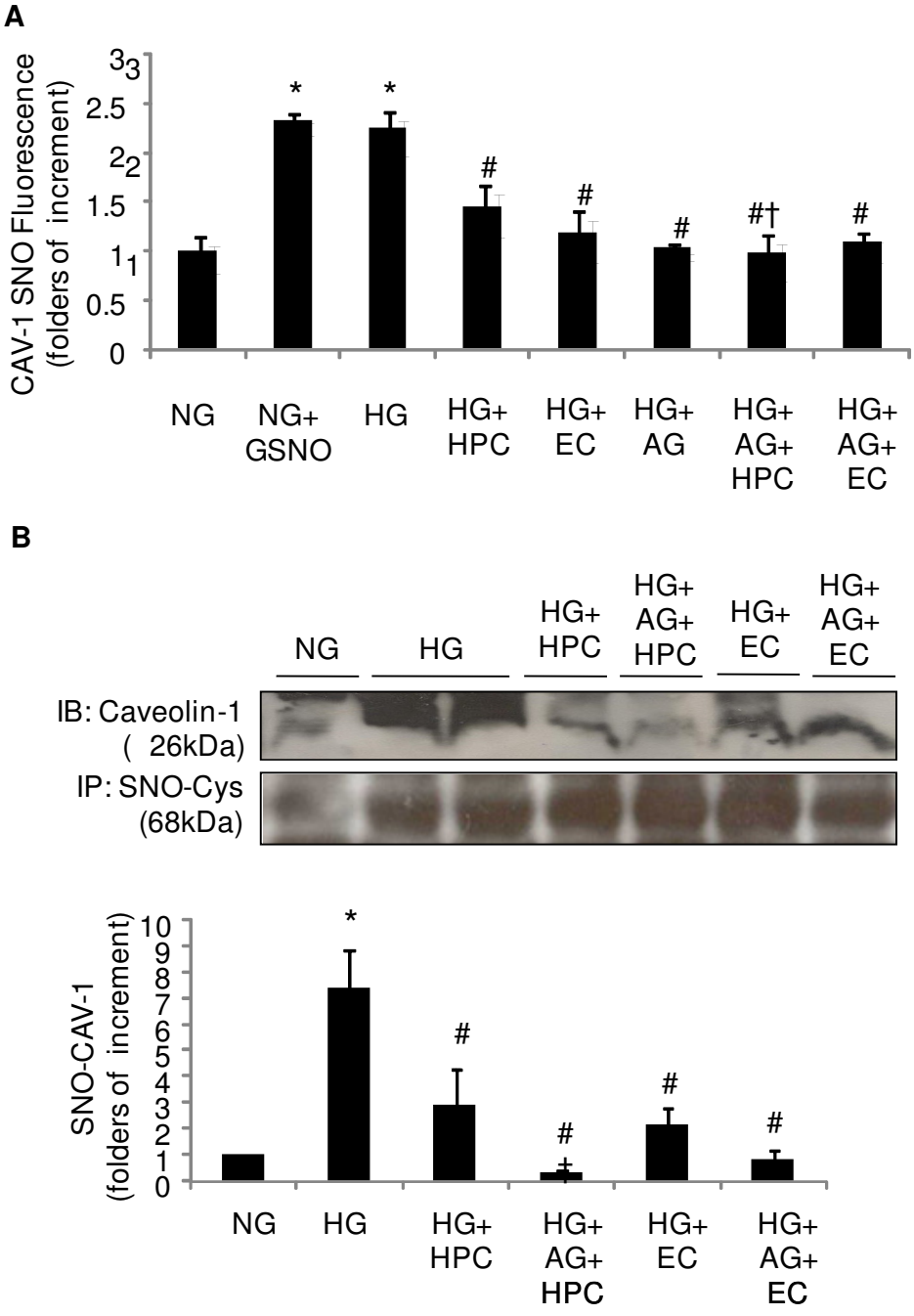

Figure 7. Epicatechin prevents TNFα-iNOS upregulation through δ-opioid receptor (DOR).

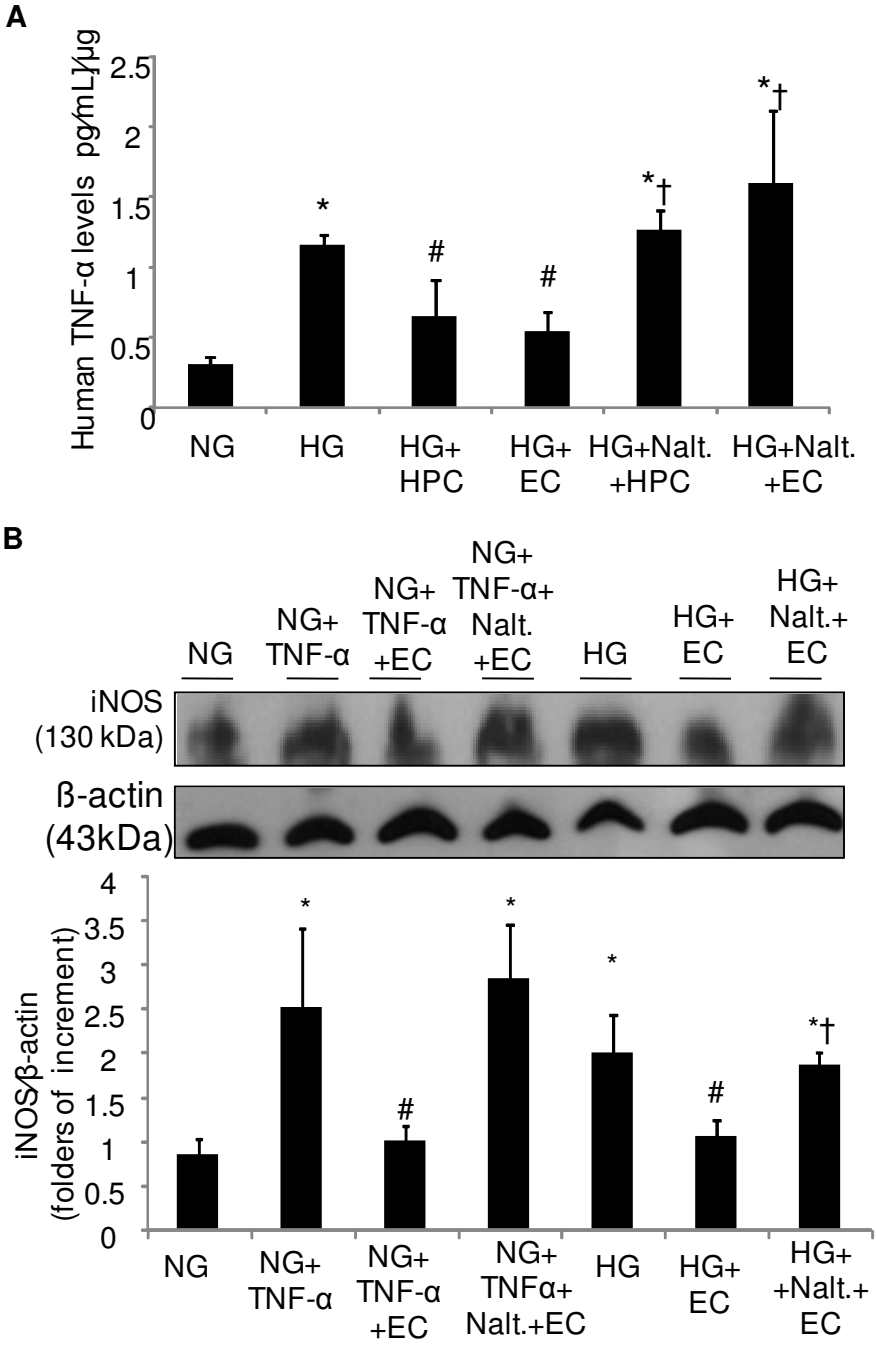

Figure 8. Epicatechin prevents CAV-1 endocytosis process through δ-opioid receptor blockage.

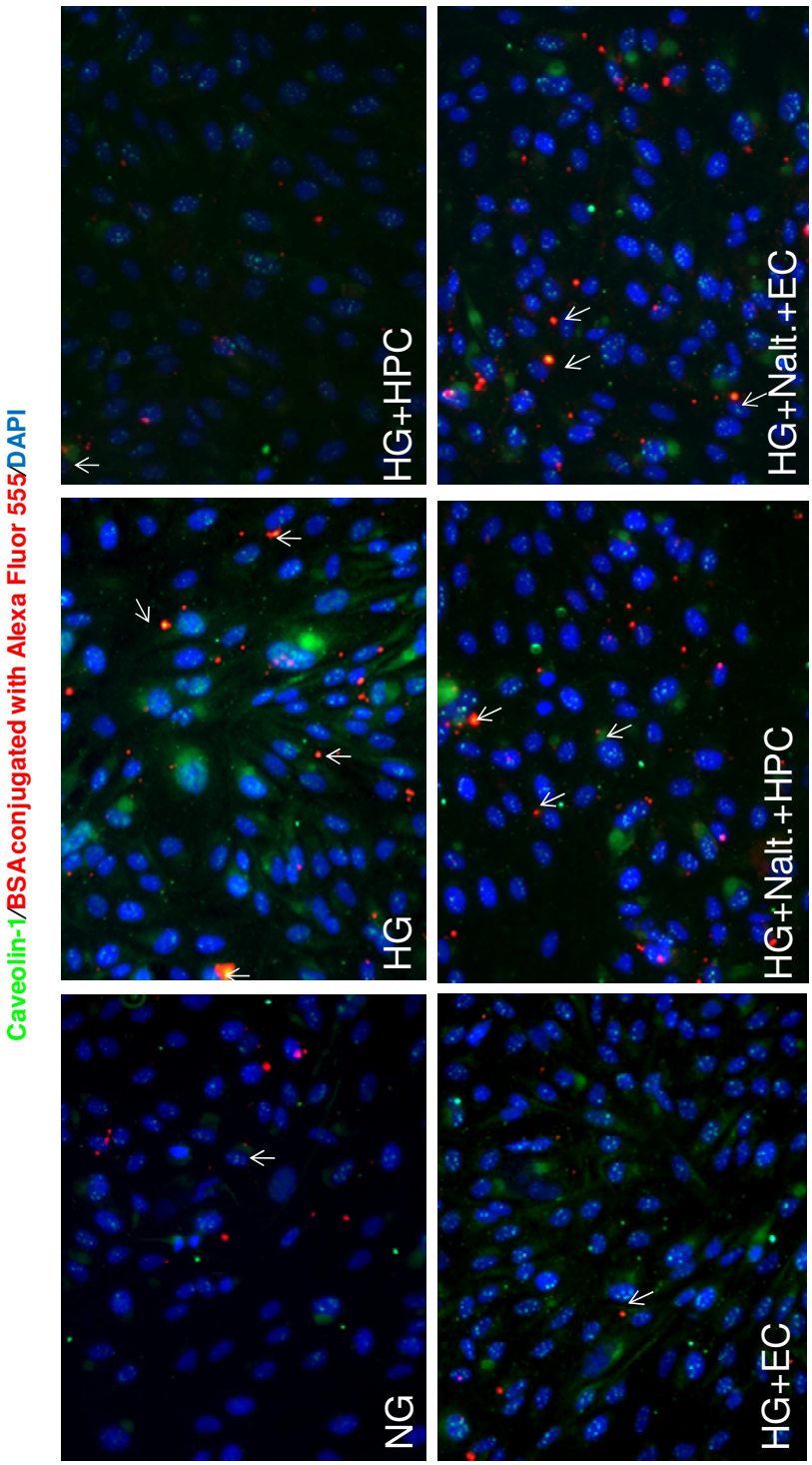

Artigo II

Supplementary figure 1.

Compounds	**Quantity (%)**
Polyphenols	**60.5**
Catechin	1
Epicatechin	12
Epigallocatechin	0.58
Epigallocatechin gallate	0.25
Gallocatechin gallate	3
Epicatechin gallate	1.12
Procyanidine B1	0.2
Procyanidine B2	4.1
Procyanidine B3	0.2
Carbohydrates	**12**
Solubre fibres	5.5
Proteins	**9.5**
Xanthines	**9.42**
Theobromine	8
Caffeine	1.42
Others	**8.58**

Supplementary figure 1: Quantitative characterization of high polyphenol cocoa (HPC) compounds determined by UHPLC. The polyphenols (catechin, epicatechin, epigallocatechin, epigallocatechin gallate, gallocatechin gallate, epicatechin gallate) and xanthines were quantified by our group. The remainder of the compounds was determined by Barry Callebau®. Among the polyphenols, epicatechin (EC) was presented in a higher percentage, 12%.

Artigo II

4. CONCLUSÕES GERAIS

Como descrito na literatura e também observado em nossos trabalhos, o aumento da expressão da iNOS está presente nas fase precoces da RD. Seu envolvimento na patogênese da RD faz com que esta enzima seja alvo terapêutico para prevenção. Até o momento não há tratamento farmacológico e principalmente não invasivo para a RD, e o uso de tratamentos tópicos como o colírio ou o consumo de compostos naturais, seriam de grande interesse.

No estudo do Artigo I, escolhemos a formulação de um colírio de GSNO devido a sua capacidade de modulação de proteínas através de modificações pós-translacional, S-nitrosilação e/ou S-glutationilação. O GSNO é conhecido por ser um doador de NO, no entanto se comportou de maneira diferente dependente da presença ou ausência do diabetes. No animal controle induziu o estresse oxidativo/nitrosativo no tecido da retina resultando em alterações funcionais. Nos animais com DM, o tratamento com colírio de GSNO reduziu a elevação da expressão da iNOS e preveniu a nitração da tirosina, melhorando a disfunção glial resultando na melhora da função retiniana. A presença do estresse nitrosativo esteve presente em todas as camadas das células da retina e foi mais acentuado no EPR. A onda "c" também apresentou alterações, afirmando o envolvimento da BHR externa. Baseado nestas observações, investigamos *in vitro* os efeitos do GSNO dependente das concentrações de glicose na linhagem celular humana ARPE-19. Nas células expostas a alta concentração de glicose, foi observado um aumento na produção de superóxido e NO acompanhado do aumento da expressão da iNOS, nitração da tirosina e diminuição nos níveis endógenos de GSNO assim como na expressão de GSH e GSNO-R. O tratamento com GSNO preveniu o estresse nitrosativo (diminuição de iNOS, NO e nitração de tirosina) e a diminuição dos níveis de GSNO-R, mas não restaurou os níveis de GSH ou GSNO. Este efeito foi provavelmente através da inibição da iNOS através da S-glutationilação promovida pela GSSG liberada através da

denitrosilação do GSNO exógeno via GSNO-R. Em contraste, em condições de glicose normal, o tratamento com GSNO promoveu o estresse nitrosativo através do aumento da produção de NO independente da iNOS. Neste caso, o nitrosotiol GSNO atuou como um doador direto de NO através de reações com grupos tióis. Curiosamente, os níveis endógenos não aumentam com o tratamento, sugerindo o seu consumo. Este estudo demonstra a importância da iNOS e a relevância do sistema S-nitrosoglutationa/glutationa na patogênese da RD. Além disso, através de técnica de alta precisão pudemos quantificar os níveis endógenos de GSNO o que aprofundou o entendimento do papel do NO em condições que mimetizam o DM.

No Artigo II, nós demonstramos o papel do cacau enriquecido com polifenóis na proteção da integridade das junções intercelulares em células ARPE-19 expostas à alta concentração de glicose. Através do Artigo I, observamos que o alvo terapêutico é a iNOS e neste estudo, investigamos a participação da iNOS na regulação das junções intercelulares e dos possíveis mecanismos protetores do cacau. Neste trabalho demonstramos que a diminuição da expressão das junções intercelulares claudina-1 e ocludina em células ARPE-19 sob alta concentração de glicose estiveram associadas à interação com a CAV-1. O aumento do tráfego da CAV-1 foi dependente de sua S-nitrosilação. O cacau com alto teor de polifenol ou a epicatequina diminuíram a expressão da iNOS através da modulação do TNF-α via DOR. Este efeito foi revertido com o uso do antagonista, naltrindole, demonstrando a alta especificidade da epicatequina com o DOR e o seu mecanismo de ação.

Em ambos os estudos, os tratamentos aplicados foram primários, ou seja, preventivos. Futuros estudos clínicos serão necessários para a avalição dos efeitos dessas modalidades terapêuticas em pacientes diabéticos com RD não proliferativa leve.

5. REFERÊNCIAS BIBLIOGRÁFICAS

Abu El-Asrar AM, Desmet S, Meersschaert A, Dralands L, Missotten L, Geboes K. Expression of the inducible isoform of nitric oxide synthase in the retinas of human subjects with diabetes mellitus. Am J Ophthalmol 132: 551–556, 2001.

Adamis AP, Shima DT, Yeo KT, Yeo TK, Brown LF, Berse B, D'Amore PA, and Folkman J. Synthesis and secretion of vascular permeability factor/vascular endothelial growth factor by human retinal pigment epithelial cells. Biochem Biophys Res Commun 193: 631–638, 1993.

Adler AJ, Southwick RE. Distribution of glucose and lactate in the interphotoreceptor matrix. Ophthalmic Res 24: 243–252, 1992.

Adorante JS, Miller SS. Potassium-dependent volume regulation in retinal pigment epithelium is mediated by Na,K,Cl cotransport. J Gen Physiol 96: 1153–1176, 1990.

Alder VA, Su EN, Yu DY, Cringle SJ, Yu PK. Diabetic retinopathy: early functional changes. Clin Exp Pharmacol Physiol 24: 785-8, 1997.

Anderson RE, O'Brien PJ, Wiegand RD, Koutz CA, and Stinson AM. Conservation of docosahexaenoic acid in the retina. Adv Exp Med Biol 318: 285–294, 1992.

Arden GB. Comments on "A new view of diabetic Retinopathy" by A.J. Barber. Prog Neuropsychopharmacol Biol Psychiatry 28: 747-748, 2004.

Augusto O. Radicais Livres Bons, Maus e Naturais. Oficina De Textos, 2006.

Baehr W, Wu SM, Bird AC, Palczewski K. The retinoid cycle and retina disease. Vis Res 43: 2957–2958, 2003.

Ban Y, Rizzolo LJ. Differential regulation of tight junction permeability during development of the retinal pigment epithelium. Am J Physiol Cell Physiol 279: C744 C750, 2000.

Ban Y, Rizzolo LJ. Regulation of glucose transporters during development of the retinal pigment epithelium. Developmental Brain Research 121: 89–95, 2000.

Bauer PM, Yu J, Chen Y, Hickey R, Bernatchez PN, Looft-Wilson R et al. Endothelialspecific expression of caveolin-1 impairs microvascular permeability and angiogenesis. Proc Natl Acad Sci U S A 102: 204–209, 2005.

Bazan NG, Gordon WC, Rodriguez de Turco EB. Docosahexaenoic acid uptake and metabolism in photoreceptors: retinal conservation by an efficient retinal pigment epithelial cell-mediated recycling process. Adv Exp Med Biol 318: 295-306, 1992.

Bergersen LJ, Jóhannsson E, Veruki ML, Nagelhus EA, Halestrap A, Sejersted OM, Ottersen OP.Cellular and subcellular expression of monocarboxylate transporters in the pigment epithelium and retina of the rat. Neuroscience 90: 319–331, 1999.

Bok D. The retinal pigment epithelium: a versatile partner in vision. J Cell Sci Suppl 17: 189–195, 1993.

Braga, VM. Cell-cell adhesion and signaling. Curr Opin Cell Biol 14: 546-556, 2002.

Bragge P, Gruen RL, Chau M, et al. Screening for presence or absence of diabetic retinopathy – a meta-analysis. Arch Ophthalmol 129: 435–444, 2011.

Calcutt NA, Cooper ME, Kern TS, Schmidt AM. Therapies for hyperglycaemia-induced diabetic complications: from animal models to clinical trials. Nat Rev Drug Discov 8: 417-429, 2009.

Chen CA, Wang TY, Varadharaj S, Reyes LA, Hemann C, Talukder MA, Chen YR, DruhanLJ,Zweier JL. S-glutathionylation uncouples eNOS and regulates its cellular and vascular function. Nature 468: 1115-1118, 2010.

Chen XL, Zhang XD, Li YY, Chen XM, Tang DR, Ran RJ. Involvement of HMGB1 mediated signalling pathway in diabetic retinopathy: evidence from type 2 diabetic rats and ARPE-19 cells under diabetic condition. Br J Ophthalmol 97: 1598-603, 2013.

Chen YH, Chen JY, Chen YW, Lin ST, Chan HL. High glucose-induced proteome alterations in retinal pigmented epithelium cells and its possible relevance to diabetic retinopathy. Mol Biosyst 8: 3107-24, 2012.

Chen YH, Chou HC, Lin ST, Chen YW, Lo YW, Chan HL. Effect of high glucose on secreted proteome in cultured retinal pigmented epithelium cells: its possible relevance to clinical diabetic retinopathy. J Proteomics 77: 111-28, 2012.

Cormack DH. Fundamentos de histologia. Guanabara Koogan; 1996. p.90-93.

Crider J.Y, Yorio T, Sharif NA, Griffin BW. The effects of elevated glucose on Na+/K+-ATPpase of cultured bovine retinal pigment epithelial cells measured by a new nonradioactive rubidium uptake assay. Journal of Ocular Pharmacology and Therapeutics. 13: 337–352, 1997.

DCCT Research Group. The effect of intensive treatment of diabetes on the development and progression of long-term complications in insulin dependent diabetes Mellitus. N Engl J Med 329: 977-986, 1993.

Dillinger TL, Barriga P, Escarcega S, Jimenez M, Salazar Lowe D, and Grivetti LE. Food of the gods: cure for humanity? A cultural history of the medicinal and ritual use of chocolate. J Nutr 130: 2057S–7072S, 2000.

Dorey CK, Wu G, Ebenstein D, Garsd A, Weiter JJ. Cell loss in the aging retina: relationship to lipofuscin accumulation and macular degeneration. Invest Ophthalmol Vis Sci 30: 1691–1699, 1989.

Dornonville de la Cour M. Ion transport in the retinal pigment epithelium. A study with double barrelled ion-selective microelectrodes. Acta Ophthalmol Suppl 209:1-32, 1993.

Du Y, Sarthy VP, Kern TS. Interaction between NO and COX pathways in retinal cells exposed to elevated glucose and retina of diabetic rats. Am J PhysiolRegulIntegr Comp Physiol 287: 735-741, 2004.

Duarte DA, Silva KC, Rosales MA, Lopes de Faria JB, Lopes de Faria JM. The concomitance of hypertension and diabetes exacerbating retinopathy: the role of inflammation and oxidative stress. Curr Clin Pharmacol 8: 266-77. 2013.

Dunn KC, Aotaki-Keen AE, Putkey FR, Hjelmeland LM. ARPE-19, a human retinal pigment epithelial cell line with differentiated properties. Exp Eye Res 62: 155-l69, 1996.

Dunn KC, Marmorstein AD, Bonilha VL, Rodriguez-Boulan E, Giordano F, Hjelmeland LM. Use of the ARPE-19 cell line as a model of RPE polarity: basolateral secretion of FGF5. Invest Ophthalmol Vis Sci 39: 2744-9, 1998.

Eagle RC Jr. Mechanisms of maculopathy. Ophthalmology 91: 613–625, 1984.

Feldman GJ, Mullin JM, Ryan MP. Occludin: Structure, function and regulation. Adv Drug Deliv Rev 57: 883-917, 2005.

Feltkamp, CA, Van der Waerden AW. Junction formation between cultured normal rat hepatocytes. An ultrastructural study on the presence of cholesterol and the structure of developing tight-junction strands. J. Cell Sci. 63: 271–286, 1983.

Feng Y, Venema VJ, Venema RC, Tsai N, Behzadian MA, Caldwell RB. VEGF-induced permeability increase is mediated by caveolae. Invest Ophthalmol Vis Sci 40: 157–167, 1999.

Ferrari CKB, França EL, Honorio-França AC. Nitric oxide, health and disease. J Appl Biomed 7: 163–173, 2009.

Finnemann SC, Bonilha VL, Marmorstein AD, Rodriguez-Boulan E. Phagocytosis of rod outer segments by retinal pigment epithelial cells requires avB5 integrin for binding but not internalization. Proc NatlAcad Sci 94: 12932-12937, 1997.

Finnemann SC. Focal adhesion kinase signaling promotes phagocytosis of integrin bound photoreceptors. EMBO J 22: 4143–4154, 2003.

Fong DS, Aiello LP, Ferris FL, Klein R. Diabetic retinopathy. Diabetes Care 27: 2540-2553, 2004.

Forrester JV, Xu H. Good news-bad news: the Yin and Yang of immune privilege in the eye. Front Immunol 3: 338, 2012.

Frambach DA, Valentine JL, and Weiter JJ. Furosemide-sensitive Cl transport in bovine retinal pigment epithelium. Invest Ophthalmol Vis Sci 30: 2271–2274, 1989.

Frank RN. Diabetic retinopathy. N Engl J Med 350: 48-58, 2004.

Goldstein IM, Ostwald P, Roth S. Nitric oxide: a review of its role in retinal function and disease. Vision Res. 36: 2979–2994, 1996.

González-Mariscal L, Tapia R, Chamorro D. Crosstalk of tight junction components with signaling pathways. Biochim Biphys Acta 1778: 729-756, 2008.

Griffith OW, Stuehr DJ. Nitric oxide synthases: properties and catalytic mechanism Annu Rev Physiol 57: 707-736, 1995.

Gundersen D, Orlowski J, and Rodriguez-Boulan E. Apical polarity of Na,K-ATPase in retinal pigment epithelium is linked to a reversal of the ankyrin-fodrin submembrane cytoskeleton. J Cell Biol 112: 863–872, 1991.

Hamann S. Molecular mechanisms of water transport in the eye. Int Rev Cytol 215: 395–431, 2002.

Haq E, Rohrer B, Nath N, Crosson CE, Singh I. S-nitrosoglutathione prevents interphotoreceptor retinoid-binding protein (IRBP(161-180))-induced experimental autoimmune uveitis. J Ocul Pharmacol Ther 23: 221-31, 2007.

Hedberg JJ, Griffiths WJ, Nilsson SJ, Hoog JO. Reduction of S-nitrosoglutathione by human alcoholdehydrogenase 3 is an irreversible reaction as analysed by electrospray mass spectrometry. Eur J Biochem 270: 1249–1256, 2003.

Heegand S. Morphology of the vitreoretinal bander region. Acta Ophtalmol Scand 222: 1-31, 1997.

Hernández C, Lecube A, Segura RM, Sararols L, Simó R. Nitric oxide and vascular endothelial growth factor concentrations are increased but not related in vitreous fluid of patients with proliferative diabetic retinopathy. Diabet Med 19: 655-660, 2002.

Hess DT, Matsumoto A, Nudelman R, Stamler, JS. Nat. S-nitrosylation: spectrum and specificity. Cell Biol 3: E46-49, 2001.

Hewitt AT, Adler R. The retinal pigment epithelium and interphotoreceptor matrix: structure and specialized functions. Retina:Basic Science and Inherited Retinal Disease 1: 58–71, 1994.

Hill BG, Bhatnagar A. Role of glutathiolation in preservation, restoration and regulation of protein function. IUBMB Life 59: 21–26, 2007.

Hogg N. The biochemistry and physiology of S-nitrosothiols. Annu Rev Pharmacol Toxicol 42: 585–600, 2002.

Holtkamp GM, Kijlstra A, Peek R, de Vos AF. Retinal Pigment Epithelium-immune System Interactions: Cytokine Production and Cytokine-induced Changes. ProgRetin Eye Res 20: 29-48, 2001.

Husain S, Liou GI, Crosson CE. Opioid-receptor-activation: Suppression of ischemia/reperfusion-induced production of TNF-alpha in the retina. Invest Ophthalmol Vis Sci 52: 2577-83, 2011.

Ihnat MA, Thorpe JE, Kamat CD, Szabó C, Green DE, Warnke LA, Lacza Z, Cselenyák A, Ross K, Shakir S, Piconi L, Kaltreider RC, Ceriello A. Reactive oxygen species mediate a cellular 'memory' of high glucose stress signalling. Diabetologia 50: 1523-31, 2007.

Ishida K, Panjwani N, Cao Z, Streilein JW. Participation of pigment epithelium in ocular immune privilege. 3. Epithelia cultured from iris, ciliary body, and retina suppress T-cell activation by partially non-overlapping mechanisms. Ocul Immunol Inflamm 11: 91–105, 2003.

Jackson GR, Barber AJ. Visual dysfunction associated with diabetic retinopathy. Curr Diab Rep 10: 380-4, 2010.

Jalil AM, Ismail A. Polyphenols in cocoa and cocoa products: is there a link between antioxidant properties and health? Molecules 13: 2190-219, 2008.

Kachi S, Yamazaki A, Usukura J. Localization of caveolin-1 in photoreceptor synaptic ribbons. Invest Ophthalmol Vis Sci 42: 850–852, 2001.

Katavic PL, Lamb K, Navarro H, Prisinzano TE. Flavonoids as opioid receptor ligands: identification and preliminary structure-activity relationships. J Nat Prod 70: 1278–1282, 2007.

Khan M, Sekhon B, Giri S, Jatana M, Gilg AG, Ayasolla K, Elango C, Singh AK, Singh I. S-Nitrosoglutathione reduces inflammation and protects brain against focal cerebral ischemia in a rat model of experimental stroke. J Cereb Blood Flow Metab 25: 177-192, 2005.

Kim DI, Lim SK, Park MJ, Han HJ, Kim GY, Park SH. The involvement of phosphatidylinositol 3-kinase /Akt signaling in high glucose-induced downregulation of GLUT-1 expression in ARPE cells. Life Sci 80: 626-32, 2007.

Kirchner P, Bug M, Meyer H. Ubiquitination of the N-terminal region of caveolin-1 regulates endosomal sorting by the VCP/p97 AAA-ATPase. J Biol Chem 288: 7363-72, 2013.

Kita M and Marmor MF. Effects on retinal adhesive force in vivo of metabolically active agents in the subretinal space. Invest Ophthalmol Vis Sci 33: 1883–1887, 1992.

Klaassen I, Hughes JM, Vogels IMC, Schalkwijk CG, Van Noorden CJF, Schlingemann RO. Altered expression of genes related to blood–retina barrier disruption in streptozotocin induced diabetes. Experimental Eye Research 89: 4–15, 2009.

Klein R, Klein BE, Moss SE, Cruickshanks KJ. The Wisconsin epidemiologic study of diabetic retinopathy: XVII. The 14-year incidence and progression of diabetic retinopathy and associated risk factors in type 1 diabetes. Ophthalmology 105: 1801-1815, 1998.

Klein R, Klein BE, Moss SE, Davis MD, DeMets DL. The Wisconsin Epidemiologic Study of Diabetic Retinopathy. IX. Four-year incidence and progression of diabetic retinopathy when age at diagnosis is less than 30 years. Arch Ophthalmol 107(2): 237-43, 1989.

Kniesel U and Wolburg H. Tight junction complexity in the retinal pigment epithelium of the chicken during development. Neurosci Lett 149: 71–74, 1993.

Knowles RG and Moncada S. Nitric oxide synthases in mammals. Biochem J 298: 249-258, 1994.

Latif R. Chocolate/cocoa and human health: a review. Neth J Med 71: 63-8, 2013.

Li X, McClellan ME, Tanito M, Garteiser P, Towner R, Bissig D, Berkowitz BA, Fliesler SJ, Woodruff ML, Fain GL, Birch DG, Khan MS, Ash JD, Elliott MH. Loss of caveolin-1 impairs retinal function due to disturbance of subretinal microenvironment. J Biol Chem 287: 16424-34, 2012.

Liu L, Hausladen A, Zeng M, Que L, Heitman J, Stamler JS. A metabolic enzyme for S-nitrosothiol conserved from bacteria to humans. Nature 410: 490–494, 2001.

Liu L, Yan Y, Zeng M., Zhang J, Hanes MA, Ahearn G, McMahon TJ, Dickfeld T, Marshall HE, Que LG, Stamler JS. Essential roles of S-nitrosothiols in vascular homeostasis and endotoxic shock. Cell 116: 617–628, 2004.

Liu Z, Rudd MA, Freedman JE, Loscalzo J. S-transnitrosation reactions are involved in the metabolic fate and biological actions of nitric oxide. J Pharmacol Exp Ther 284: 526–534, 1998.

Lopes de Faria JM, Silva KC, Lopes de Faria JB. Parte VII – Diabete Melito - Capítulo livro 61 Retinopatia Diabética. Endocrinologia 2ª edição, 2014.

Lopes de Faria JB, Silva KC, Lopes de Faria JM. The contribution of hypertension to diabetic nephropathy and retinopathy: the role of inflammation and oxidative stress. Hypertens Res 34: 413-22, 2011.

Mannick JB, Schonhoff, CM. Arch. Nitrosylation: the next phosphorylation? Biochem. Biophys 408: 1–6, 2002.

Marchiando AM, Shen L, Graham WV, Weber CR, Schwarz BT, Austin JR 2nd, Raleigh DR, Guan Y, Watson AJ, Montrose MH, Turner JR. Caveolin-1-dependent occludin endocytosis is required for TNF-induced tight junction regulation in vivo. J Cell Biol 189: 111-26, 2010.

Marmor MF. Control of subretinal fluid: experimental and clinical studies. Eye 4: 340–344, 1990.

Marmor MF. Mechanisms of fluid accumulation in retinal edema.Doc Ophthalmol 97: 239–249, 1999.
Marmorstein AD. The polarity of the retinal pigment epithelium. Traffic 2: 867–872, 2001.

McCullough ML, Chevaux K, Jackson L, et al, Hypertension, the Kuna, and the epidemiology of flavanols. J Cardiovasc Pharmacol 47: S103-9, 2006.

Miller SS and Steinberg RH. Active transport of ions across frog retinal pigment epithelium. Exp Eye Res 25: 235–248, 1977.

Miller SS and Steinberg RH. Passive ionic properties of frog retinal pigment epithelium. J Membr Biol 36: 337–372, 1977.

Minamizono A, Tomi M, Hosoya and KI. Inhibition of dehydroascorbic acid transport across the rat blood-retinal and -brain barriers in experimental diabetes. Biological and Pharmaceutical Bulletin, 29: 2148–2150, 2006.

Mitchell P, Foran S. Guidelines for the Management of Diabetic Retinopathy. The National Health and Medical Research Council (NHMRC). Australian Diabetes Society for the Department of Health and Ageing. 2008.

Moncada S and Bolanos JP. Nitric oxide, cell bioenergetics and neurodegeneration. Neurochem 97: 1676-1689, 2006.

Moncada S, Higgs A The L-arginine-nitric oxide pathway. N Engl J Med. 329: 2002-12, 1993.

Mora RC, Bonilha VL, Shin BC, Hu J, Cohen-Gould L, Bok D, Rodriguez-Boulan E. Bipolar assembly of caveolae in retinal pigment epithelium. Am J Physiol Cell Physiol 290: C832–C843, 2006.

Nagelhus EA, Horio Y, Inanobe A, Fujita A, Haug FM, Nielsen S, Kurachi Y, and Ottersen OP. Immunogold evidence suggests that coupling of K¬ siphoning and water transport in rat retinal Muller cells is mediated by a coenrichment of Kir4.1 and AQP4 in specific membrane domains. Glia 26: 47–54, 1999.

Naggar H, Ola MS, Moore P, Huang W, Bridges CC, Ganapathy V, Smith SB. Downregulation of reduced-folate transporter by glucose in cultured RPE cells and in RPE of diabetic mice. Invest Ophthalmol Vis Sci 43: 556-63, 2002.

Neufeld AH, Kawai Si, Das S, Vora S, Gachie E, Connor JR, Manning PT. Loss of retinal ganglion cells following retinal ischemia: the role of inducible nitric oxide synthase. Exp Eye Res 75:521-528, 2002.

Nusrat, A. Parkos CA, Verkade P, Foley CS, Liang TW, Innis-Whitehouse W, Eastburn KK, Madara JL. Tight junctions are membrane microdomains. J Cell Sci 113: 1771–1781, 2000.

Obrosova IG, Minchenko AG, Frank RN, Seigel GM, Zsengeller Z, Pacher P, et al. Poly(ADP-ribose) polymerase inhibitors counteract diabetes- and hypoxia-induced retinal vascular endothelial growth factor overexpression. Int J Mol Med 14: 55– 64, 2004.

Panneerselvam, M., Tsutsumi, Y. M., Bonds, J. A., Horikawa, Y. T. et al., Dark chocolate receptors: epicatechin-induced cardiac protection is dependent on delta-opioid receptor stimulation. Am J Physiol Heart Circ Physiol 299: 1604–1609, 2010.

Pradhan, A. A., Befort, K., Nozaki, C., Gaveriaux-Ruff, C. & Kieffer, B. L. The delta opioid receptor: an evolving target for the treatment of brain disorders. Trends Pharmacol Sci 32: 581–590, 2011.

Park CS, Pardhasaradhi K, Gianotti C, Villegas E, Krishna G. Human retina expresses both constitutive and inducible isoforms of nitric oxide synthase mRNA. Biochem Biophys Res Commun 205: 85-91, 1994.

Parton RG, Simons K. The multiple faces of caveolae. Nat Rev Mol Cell Biol 8: 185–194, 2007.

Patel RP, Levonen A, Crawford JH, Darley-Usmar VM. Mechanisms of the pro- and antioxidant actions of nitric oxide in atherosclerosis. Cardiovasc Res 47: 465-474, 2000.

Pautler EL, Ennis SR. The effect of induced diabetes on the electroretinogram components of the pigmented rat. Invest Ophthalmol Vis Sci 19(6): 702-5, 1980.

Pinto CC, Silva KC, Biswas SK, Martins N, de Faria JB, de Faria JM. Arterial hypertension exacerbates oxidative stress in early diabetic retinopathy. Free Radic Res 41: 1151-1158, 2007.

Provis JM. Development of the Primate Retinal Vasculature. Progress in Retinal and Eye Research 2001: 20: 799-821.

Rahner C, Fukuhara M, Peng S, Kojima S, Rizzolo LJ. The apical and basal environments of the retinal pigment epithelium regulate the maturation of tight junctions during development. J Cell Sci 1;117(Pt 15):3307-18, 2004.

Ramiro-Puig E, Castell M. Cocoa: antioxidant and immunomodulator. Br J Nutr 101: 931-40, 2009.

Rizzolo LJ, Heiges M. The polarity of the retinal pigment epithelium is developmentally regulated. Exp Eye Res 53: 549–553, 1991.

Rodeberg DA, Chaet MS, Bass RC, Arkovitz MS, Garcia VF. Nitric oxide: an overview. Am J Surg 170: 292-303, 1995.

Roesch K, Jadhav AP, Trimarchi JM., Stadler MB, Roska B, Sun BB, Cepko CL. The transcriptome of retinal Müller glial cells. J Comp Neurol 509: 225–238, 2008.

Rosales MA, Silva KC, Lopes de Faria JB, Lopes de Faria JM. Exogenous SOD mimetic tempol ameliorates the early retinal changes reestablishing the redox status in diabetic hypertensive rats. Invest Ophthalmol Vis Sci 51: 4327-4336, 2010.

Rosenfeld RJ, Bonaventura J, Szymczyna BR, MacCoss MJ, Arvai AS, Yates JR 3rd, Tainer JA, Getzoff ED.Nitric-oxide synthase forms N-NO-pterin and S-NO-cys: implications for activity, allostery, and regulation. Biol Chem 285: 31581-9, 2010.

Roy MS. Diabetic retinopathy in African Americans with type 1 diabetes: the New Jersey 725. II. Risk factors. Arch Ophthalmol 118: 105-115, 2000.

Saint-Geniez M, D'Amore PA. Development and pathology of the hyaloids, choroidal and retinal vasculature. The International Journal of Developmental Biology 48: 1045-1058, 2004.

Salceda R and Contreras-Cubas C. Ascorbate uptake in normal and diabetic rat retina and retinal pigment Journal of Biomedicine and Biotechnology 9 epithelium. Comparative Biochemistry and Physiology C 146: 175–179, 2007.

Salceda R, Hernández-Espinosa C, Sánchez-Chávez G. L-arginine uptake in normal and diabetic rat retina and retinal pigment epithelium. Neurochem Res 33: 1541-5, 2008.

Schmetterer L, Findl O, Fasching P, et al. Nitric oxide and ocular blood flow in patients with IDDM. Diabetes. 46: 653–658, 1997.

Schmidt HH, Walter U. NO at work. Cell 78: 919-925, 1994.

Schroder S, Brad M, Schimid-Schonbein GW, Reim M, Schimid-Schonbein H. Microvascular network topology of the human retinal vessels. Fortschr. Ophthalmol 87: 52-58, 1990.

Schubert W, Frank PG, Razani B, Park DS, Chow CW, Lisanti MP. Caveolae-deficient endothelial cells show defects in the uptake and transport of albumin in vivo. J Biol Chem 276: 48619–48622, 2001.

Schuhmacher S, Oelze M, Bollmann F, Kleinert H, Otto C, Heeren T, Steven S, Hausding M, Knorr M, Pautz A, Reifenberg K, Schulz E, Gori T, Wenzel P, Münzel T, Daiber A. Vascular dysfunction in experimental diabetes is improved by pentaerithrityl tetranitrate but not isosorbide-5-mononitrate therapy Diabetes 60: 2608-16, 2011.

Selmi C, Mao TK, Keen CL, Schmitz HH, Eric Gershwin M. The anti-inflammatory properties of cocoa flavanols. J Cardiovasc Pharmacol 47: S163–S171, S172–S166, 2006.

Senanayake PD, Calabro A, Hu JG, Bonilha VL, Darr A, Bok D, Hollyfield JG. Glucose utilization by the retinal pigment epithelium: evidence for rapid uptake and storage in glycogen, followed by glycogen utilization. Experimental Eye Research 83: 235–246, 2006.

Sennlaub F, Courtois Y, Goureau O. Inducible nitric oxide synthase mediatesthe change from retinal to vitreal neovascularization in ischemic retinopathy. J Clin Invest 107: 717-725, 2001.

Sharma S, Oliver-Fernandez A, Liu W, Buchholz P, Walt J. The impact of diabetic retinopathy on health-related quality of life. Curr Opin Ophthalmol 16: 155-159, 2005.

Silva KC, Pinto CC, Biswas SK, de Faria JB, de Faria JM.Hypertension increases retinal inflammation in experimental diabetes: a possible mechanism for aggravation of diabetic retinopathy by hypertension.Curr Eye Res. 32: 533-41. 2007.

Silva KC, Pinto CC, Biswas SK, Souza DS, de Faria JB, de Faria JM.Prevention of hypertension abrogates early inflammatory events in the retina of diabetic hypertensive rats.Exp Eye Res 85: 123-9, 2007.

Silva KC, Rosales MA, Hamassaki DE, Saito KC, Faria AM, Ribeiro PA, Faria JB, Faria JM. Green tea is neuroprotective in diabetic retinopathy.Invest Ophthalmol Vis Sci 54: 1325-36, 2013.

Simo R, Villarroel M, Corraliza L, Hernandez C, Garcia-Ramirez M: The retinal pigment epithelium: something more than a constituent of the blood-retinal barrier—implications for the pathogenesis of diabetic retinopathy. J Biomed Biotechnol: 2010:190724, 2010.

Singh SP, Wishnok JS, Keshive M, Deen WM, Tannenbaum SR. The chemistry of the S-nitrosoglutathione/glutathione system. ProcNatlAcadSci USA 93: 14428–14433, 1996.

Song MK, Roufogalis BD, Huang TH. Reversal of the Caspase-Dependent Apoptotic Cytotoxicity Pathway by Taurine from Lycium barbarum (Goji Berry) in Human Retinal Pigment Epithelial Cells: Potential Benefit in Diabetic Retinopathy. Evid Based Complement Alternat Med 2012: 323784, 2012.

Sonoda S, Spee C, Barron E, Ryan SJ, Kannan R, Hinton DR. A protocol for the culture and differentiation of highly polarized human retinal pigment epithelial cells. Nat Protoc 4: 662-673, 2009.

Stamer WD, Bok D, Hu J, Jaffe GJ, and McKay BS. Aquaporin-1 channels in human retinal pigment epithelium: role in transepithelial water movement. Invest Ophthalmol Vis Sci 44: 2803–2808, 2003.

Stamler JS, Lamas S, Fang FC. Nitrosylation, the prototypic redox-based signaling mechanism. Cell 106: 675–683, 2001.

Stamler JS, Simon DI, Osborne JA, Mullins ME, Jaraki O, Michel T,et al. S-nitrosylation of proteins with nitric oxide: synthesis and characterization of biologically active compounds. ProcNatlAcadSci USA 89: 444–448, 1992.

Steinberg RH, Linsenmeier RA, Griff ER. Three light-evoked responses of the retinal pigment epithelium. Vision Res 23:1315-23, 1983.

Streilein JW, Ma N, Wenkel H, Ng TF, and Zamiri P. Immunobiology and privilege of neuronal retina and pigment epithelium transplants. Vision Res 42: 487–495, 2002.

Sugawara R, Hikichi T, Kitaya N, Mori F, Nagaoka T, Yoshida A, Szabo C. Peroxynitrite decomposition catalyst, FP15, and poly (ADP-ribose) polymerase inhibitor, PJ34, inhibit leukocyte entrapment in the retinal microcirculation of diabetic rats. Curr Eye Res 29: 11–16, 2004.

Takeuchi K, Morizane Y, Kamami-Levy C, Suzuki J, Kayama M, Cai W, Miller JW, Vavvas DG. AMP-dependent kinase inhibits oxidative stress-induced caveolin-1 phosphorylation and endocytosis by suppressing the dissociation between c-Abl and Prdx1 proteins in endothelial cells. J Biol Chem. 288: 20581-91, 2013.

Taubert D, Roesen R, Lehmann C, Jung N, Schomig E. Effects of low habitual cocoa intake on blood pressure and bioactive nitric oxide: a randomized controlled trial. JAMA 298: 49–60, 2007.

Tentori L, Lacal PM, Muzi A, et al. Poly (ADP-ribose) polymerase (PARP) inhibition or PARP-1 gene deletion reduces angiogenesis. Eur J Cancer 43: 2124–2133, 2007.

Tilton RG, Chang K, Hasan KS, et al. Prevention of diabetic vascular dysfunction by guanidines: inhibition of nitric oxide synthase versus advanced glycation end-product formation. Diabetes 42: 221–232, 1993.

Trudeau K, Roy S, Guo W, Hernández C, Villarroel M, Simó R, Roy S. Fenofibric acid reduces fibronectin and collagen type IV overexpression in human retinal pigment epithelial cells grown in conditions mimicking the diabetic milieu: functional implications in retinal permeability. Invest Ophthalmol Vis Sci 52: 6348-54, 2011.

United Kingdom Prospective Diabetes Study Group. Intensive blood glucose control with sulphonylureas or insulin compared with conventional treatment and risk of complications in patients with type 2 diabetes (UKPDS 33). Lancet 352: 837-853,1998.

Valko M, Leibfritz D, Moncol J, Cronin MT, Mazur M, Telser J. Free radicals and antioxidants in normal physiological functions and human disease. Int J Biochem Cell Biol 39: 44-84, 2007.

Villarroel M, Garcia-Ramirez M, Corraliza L, Hernandez C, Simo R. Effects of high glucose concentration on the barrier function and the expression of tight junction proteins in human retinal pigment epithelial cells. Exp Eye Res 89: 913–920, 2009.

Vinores SA, Gadegbeku C, Campochiaro PA, Green WR. Immunohistochemical localization of blood-retinal barrier breakdown in human diabetics. Am J Pathol 134: 231–235, 1989.

Wild S, Roglic G, Green A, *et al.* Global prevalence of diabetes: estimates for the year 2000 and projections for 2030. Diabetes Care 27: 1047-1053, 2004.

Wong GKT, Marsden PA. Nitric oxide synthases: regulation in disease. Nefrol Dial Transplant 11: 215-220, 1996.

Xie P, Fujii I, Zhao J, Shinohara M, Matsukura M.A novel polysaccharide compound derived from algae extracts protects retinal pigment epithelial cells from high glucose-induced oxidative damage in vitro. Biol Pharm Bull 35: 1447-53, 2012.

Xu B, Chiu J, Feng B, Chen S, Chakrabarti S. PARP activation and the alteration of vasoactive factors and extracellular matrix protein in retina and kidney in diabetes. Diabetes Metab Res Rev 24: 404-412, 2008.

Xu HZ, Le YZ. Significance of outer blood-retina barrier breakdown in diabetes and ischemia. Invest Ophthalmol Vis Sci 52: 2160-4, 2011.

Ying J, Clavreul N, Sethuraman M, Adachi T, Cohen RA. Thiol oxidation in signaling and response to stress: detection and quantification of physiological and pathophysiological thiolmodifications.Free Radic Biol Med 43: 1099–1108, 2007.

Yokoyama T, Yamane K, Minamoto A, Tsukamoto H, Yamashita H, Izumi S, Hoppe G, Sears JE, Mishima HK.High glucose concentration induces elevated expression of anti-oxidant and proteolytic enzymes in cultured human retinal pigment epithelial cells. Exp Eye Res 83: 602-9, 2006.

Yoshikawa T, Ogata N, Izuta H, Shimazawa M, Hara H, Takahashi K. Increased expression of tight junctions in ARPE-19 cells under endoplasmic reticulum stress. Curr Eye Res 36: 1153-63, 2011.

Yu SW, Wang H, Poitras MF, Coombs C, Bowers WJ, Federoff HJ, Poirier GG, Dawson TM, Dawson VL. Mediation of poly (ADP-ribose) polymerase-1-dependent cell death by apoptosis inducing factor. Science 297: 259-263, 2002.

Yuan Z, Feng W, Hong J, Zheng Q, Shuai J, Ge Y. p38MAPK and ERK promote nitric oxide production in cultured human retinal pigmented epithelial cells induced by high concentration glucose. Nitric Oxide 20: 9-15, 2009.

Zeng H, Spencer NY, Hogg N. Metabolism of S-nitrosoglutathione by endothelial cells. Am J Physiol Heart CircPhysiol 281: 432–439, 2001.

Zhang X, Saaddine JB, Chou CF, et al. Prevalence of diabetic retinopathy in the United States, 2005–2008. JAMA 304: 649–656, 2010.

Zheng L, Du Y, Miller C, Gubitosi-Klug RA, Ball S, Berkowitz BA, Kern TS. Critical role of inducible nitric oxide synthase in degeneration of retinal capillaries in mice with streptozotocin-induced diabetes. Diabetologia 50: 1987-1996, 2007.

Zheng L, Gong B, Hatala DA, Kern TS. Retinal ischemia and reperfusion causes capillary degeneration: similarities to diabetes. Invest Ophthalmol Vis Sci 48: 361-367, 2007.

Zheng L, Kern TS. Role of nitric oxide, superoxide, peroxynitrite and PARP in diabetic retinopathy. Front Biosci 14: 3974-3987, 2009.

Zheng L, Szabo C, Kern TS. Poly(ADP-ribose) polymerase is involved in the development of diabetic retinopathy via regulation of nuclear factor-κB. Diabetes 53: 2960–2967, 2004.

6. ANEXOS

Exogenous SOD Mimetic Tempol Ameliorates the Early Retinal Changes Reestablishing the Redox Status in Diabetic Hypertensive Rats

Mariana A. B. Rosales, Kamila C. Silva, José B. Lopes de Faria, and Jacqueline M. Lopes de Faria

Purpose. The purpose of this study was to investigate the efficacy of tempol (4-hydroxy-2,2,6,6-tetramethylpiperidine-*N*-oxyl), a superoxide dismutase mimetic, in preventing early retinal molecular changes in a model that combines hypertension and diabetes.

Methods. Four-week-old spontaneously hypertensive rats (SHR) were rendered diabetic by streptozotocin. Diabetic SHR rats (DM-SHR) were randomized to receive or not receive tempol treatment. After 20 days of induction of diabetes, the rats were euthanatized, and their retinas were collected.

Results. The early molecular markers of diabetic retinopathy (DR), glial fibrillary acidic protein, and fibronectin were evaluated by Western blot assays and showed an increase in DM-SHR compared with the SHR group. The oxidative balance, evaluated by superoxide production and nitric oxide end product levels estimated by a nitric oxide analyzer, and the counterpart antioxidative defense revealed an accentuated imbalance in DM-SHR compared with the SHR group. As a result, the product peroxynitrite, which was detected by immunohistochemistry for nitrotyrosine, was higher in the DM-SHR group. The retinal poly-ADP-ribose (PAR)–modified proteins, which reflect the activation of PAR polymerase (PARP), and the inducible nitric oxide synthase (iNOS) expressions were found to have increased in this group. Treatment with tempol reestablished the oxidative parameters and decreased the PAR-modified proteins, thus preventing extracellular matrix accumulation and glial reaction.

Conclusions. The administration of tempol prevented oxidative damage, decreased iNOS levels, and ameliorated the activation of PARP in the retinas of diabetic hypertensive rats. Consequently, the early molecular markers of DR, such as glial reaction (glial fibrillary acidic protein [GFAP]) and extracellular matrix accumulation (fibronectin), were prevented in tempol-treated rats. (*Invest Ophthalmol Vis Sci.* 2010;51:4327–4336) DOI:10.1167/iovs.09-4690

From the Renal Pathophysiology Laboratory, Investigation on Complications of Diabetes, Department of Internal Medicine, Faculty of Medical Sciences, University of Campinas (Unicamp), São Paulo, Brazil.

Supported by the State of São Paulo Research Foundation Grants 05/58189-5 and 08/54068-7. MABR was the recipient of a scholarship from the Coordination for the Improvement of Higher Education Personnel.

Submitted for publication September 25, 2009; revised January 4 and February 17, 2010; accepted March 8, 2010.

Disclosure: **M.A.B. Rosales**, None; **K.C. Silva**, None; **J.B. Lopes de Faria**, None; **J.M. Lopes de Faria**, None

Corresponding author: Jacqueline M. Lopes de Faria, Renal Pathophysiology Laboratory, Faculty of Medical Sciences, University of Campinas, P.O. Box 6111, Campinas, SP, Brazil; jmlfaria@fcm.unicamp.br.

Diabetes mellitus (DM) has become one of the most challenging health problems of the 21st century. Diabetic retinopathy (DR) is a vascular complication in either type 1 or type 2 diabetes, and it is considered the leading cause of blindness in developed countries.[1] It is characterized by extensive neurodegeneration and glial degeneration[2] accompanied by damage to the integrity of the vasculature, as evidenced by early breakdown of the blood-retinal barrier.[3] Risk factors in the development and progression of DR include glycemic control and hypertension.[4] Epidemiologic studies clearly identify hypertension as the most important independent risk factor for DR.[5] In the United Kingdom Prospective Diabetes Study Group, the control of hypertension reduced the progression of DR in 35% of cases, surpassing even glycemic control.[5]

The renin-angiotensin system (RAS) has been implicated in the progression of DR.[6] Moreover, overactivity of retinal RAS, which has been shown to be independent of systemic RAS,[7] promotes endothelial cell proliferation in DR.[8] We have recently demonstrated that angiotensin II type 1 receptor blockage ameliorates diabetic retinal neurodegeneration by reestablishing oxidative balance and mitochondrial function.[9]

Superoxide dismutase (SOD) catalyzes the conversion of superoxide (O_2^-) to hydrogen peroxide (H_2O_2), which can then be turned into water by catalase or the glutathione (GSH) peroxidase system. Although SOD is the first line of physiological defense against oxidative stress, the reaction of O_2^- with nitric oxide (NO) is about three times faster than its reaction with SOD.[10] It has been demonstrated that nitroxides such as tempol exert a cytoprotective action against diverse oxidative insults[11] and catalyze the dismutation of superoxide to H_2O_2 plus O_2 (SOD-like activity). Previous studies demonstrated the beneficial effects of tempol in diabetic retinas for reducing leukostasis[12] and protecting the retina's neural cells.[13] Tempol was found to attenuate the aorta's response to angiotensin II (increasing O_2^- formation and inducing vasoconstriction); this effect was endothelium dependent and reversed by the inhibition of NO synthesis,[14] suggesting that tempol counteracts vasoconstriction by scavenging O_2^- and by increasing the bioavailability of NO.

The antioxidant defense enzymes responsible for scavenging free radicals and maintaining redox homeostasis, such as SOD, GSH reductase, peroxidase, and catalase, are diminished in the retinas of animals with diabetes.[15] In an animal model with genetic hypertension and streptozotocin-induced diabetes, the antioxidant system is reduced compared with that of the normotensive control.[16] Under DM conditions, the induction of the glycation reaction produces free radicals such as O_2^- and NO. NO interacts with O_2^- to form the highly reactive hydroxyl radical, peroxynitrite, which leads to reactive oxidative damage. Peroxynitrite interacts with lipids, DNA, and proteins, resulting in damaging cellular effects. The effects on DNA are the most damaging to cell function. Nitrosative stress

induces DNA single-strand breaks and leads to overactivation of the DNA repair enzyme poly-(ADP-ribose) polymerase (PARP). PARP is the enzyme that cleaves nicotinamide adenine dinucleotide (NAD+) to form nicotinamide and a PAR polymer. Generally, the activation of PARP contributes to energy failure,[17] transcriptional gene regulation, and the induction of apoptosis/necrosis.[17] In DM, PARP activation contributes to endothelial cell dysfunction and appears to be central in the mechanisms by which hyperglycemia induces diabetic vascular dysfunction.[18] In animal studies with PARP-1 knockout mice that were fed a 30% galactose diet for 2 months, Xu et al.[19] showed that the hyperhexosemia-induced oxidative stress and increased expression of fibronectin observed in wild-type control groups were not observed in PARP-1$^{-/-}$ hyperhexosemic mice, suggesting that the PARP blockade in this animal model might prevent hyperhexosemia-induced effects. In addition, a previous paper addressing endothelial dysfunction in diabetes complications showed that PARP-deficient endothelial cells incubated with high glucose did not exhibit the production of reactive nitrogen and oxygen species, consequent single-strand DNA breakage, or metabolic and functional impairments.[20] PARP activation may also cause NF-κB activation.[21] Zheng et al.[21] demonstrated that in streptozotocin-induced diabetes and in in vitro studies, the use of a specific PARP inhibitor (PJ-34) prevented the early apoptosis of retinal vascular cells and the development of acellular capillaries and pericyte ghosts in bovine retinal endothelial cells (BRECs). It also inhibited the NF-κB activation and inflammatory markers in BRECs.[21] By using PARP inhibitors or knocking out PARP genes, both NF-κB activation and transcription of NF-κB–dependent genes, such as inducible nitric oxide synthase (iNOS) or intracellular adhesion molecule (ICAM)-1, can be reduced.[22] This suggests that the inhibition of PARP activation might prevent the consequences of inflammation or oxidative stress by modifying the NF-κB–dependent pathways. In our previous studies, we revealed that after 20 days of diabetes, SHR showed increased expression of the early inflammatory markers NF-κB, ICAM-1, and microglial activation.[23] In a recent study by Drel et al.,[24] treatment with PARP inhibitors prevented apoptosis, glial reaction, and nitrosative imbalance in experimental diabetes retina.

In view of the evidence that the prevalence of hypertension is very high among patients with diabetes and that antioxidants can provide protective benefits for the treatment of DR, we sought to investigate in vivo whether treatment with tempol would prevent the early molecular events in the pathogenesis of retinopathy. We have already demonstrated that the early molecular changes observed in the diabetic retina are more evident and first detected in concomitance with arterial hypertension and experimental diabetes.[16,23,25] A number of papers investigating the mechanisms of tempol are in hypertensive animal models or in vitro studies.[26,27] For this purpose, we used a murine model of genetically hypertensive (spontaneously hypertensive rats [SHR]) and experimentally induced diabetes. Among diabetic SHR, tempol treatment prevented the early molecular changes of DR through the reestablishment of the redox status, thus decreasing the amounts of modified PAR proteins and iNOS expression in the retinal tissue.

Methods

Research Design and Methods

The protocol for this study complies with the guidelines of the Brazilian College for Animal Experimentation, and it was approved by the local Animal Research Ethics Committee (CEEA/IB/Unicamp, protocol number 1833–1). It is also in accordance with the ARVO Statement for the Use of Animals in Ophthalmic and Vision Research. Taconic (Germantown, NY) provided the SHR and the genetic control Wistar Kyoto (WKY) rats used in the present study, and we bred them in our animal facility. Experimental diabetes was induced in 4-week-old male SHR (DM-SHR) by injecting streptozotocin (STZ; 60 mg/kg; Sigma, St. Louis, MO) dissolved in a sodium citrate buffer (pH 4.5) through the tail vein after overnight fasting. The WKY control normotensive rats and the control SHR (CT-SHR) received only the citrate buffer. From the first day after diabetes induction, each DM-SHR was randomized to receive or not to receive a daily intraperitoneal injection of tempol (DM-SHR tempol; 250 mg/kg/d, 1.45 μmol/g). We used an enzymatic colorimetric GOD-PAP assay (Merck, Darmstadt, Germany) to measure plasma glucose levels 72 hours after the STZ or citrate buffer injection and on the day before euthanatizing the rats. Rats with plasma glucose values ≥15 mM were considered diabetic for the present study. We obtained systolic blood pressure by indirect tail-cuff plethysmography in unanesthetized rats with a physiograph (MK III; Narco Bio-System, Houston, TX). Twenty days after diabetes induction, the rats were euthanatized, and their retinas were detached from the retinal pigment epithelium cell layer and collected for colorimetric assays and Western blot analysis, or their eye globes were prepared for immunohistochemistry assays.

Western Blot Analysis for GFAP, FN, Cu-Zn SOD, PARP, and iNOS

The retinas were lysed in 300 μL of a buffer containing 2% SDS and 60 mmol Tris-HCl (pH 6.8), supplemented with a protease inhibitor cocktail (Complete; Boehringer-Mannheim, Indianapolis, IN). After centrifugation, we measured protein concentrations with the Bradford method.[28] SDS-PAGE and Western blot analysis were performed as described.[16] To assess the protein expression of GFAP, FN, iNOS, and Cu-Zn SOD and to detect PARP polymers, the membrane was incubated for an additional hour with antibodies against goat polyclonal anti-GFAP (1:100; Santa Cruz Biotechnology, Santa Cruz, CA), goat polyclonal anti-FN (1:1000; Calbiochem-Novabiochem, La Jolla, CA), rabbit polyclonal anti-iNOS (1:500; Cell Signaling Technology, Beverly, MA), rabbit polyclonal anti-Cu-Zn SOD (1:4000; AbFrontier, Seoul, Korea), or anti-PARP mouse monoclonal antibody (1:1000; Trevigen, Gaithersburg, MD), along with horseradish peroxidase–conjugated appropriate secondary antibodies and were developed by the chemiluminescence method (Super Signal CL-HRP Substrate System; Pierce, Rockford, IL). A densitometer (Bio-Rad, Hercules, CA) scanned exposed films, and image analysis software (Multi-Analyst Macintosh Software for Image Analysis Systems; Apple, Cupertino, CA) quantitatively analyzed them. Equal loading and transfer were ascertained by reprobing the membranes for β-actin.

Immunohistochemistry for GFAP, Nitrotyrosine, and PAR-Modified Proteins in Retinal Tissues

After quenching endogenous peroxidase, the sections were incubated with nonfat milk. Tissue sections were then incubated with goat polyclonal anti-GFAP (Santa Cruz Biotechnology), rabbit polyclonal anti-nitrotyrosine antibody (Upstate Cell Signaling Solutions, Lake Placid, NY), and mouse monoclonal anti-PAR (Trevigen). The antibody anti-PARP detects PAR polymers. Appropriate secondary antibodies were applied to the tissue sections. Labeled nuclei were detected with a tissue staining kit (ABC Vectastain; Vector Laboratories, Burlingame, CA) and diaminobenzidine tetrahydrochloride (DAB)/chloride/hydrogen peroxide and were counterstained with hematoxylin (only for nitrotyrosine). For the negative controls, staining was performed without the primary antibody. Quantitative analyses were performed as a percentage of positive cells per square millimeter of retina with ImageJ software (developed by Wayne Rasband, National Institutes of Health, Bethesda, MD; available at http://rsb.info.nih.gov/ij/index.html). An observer with no knowledge of the studied groups counted the positivity under high-power microscopic fields (1000×).

TABLE 1. Physiological Characteristics of the Studied Animals

Groups	Initial Body Weight (g)	Final Body Weight (g)	SBP (mm Hg)	Glycemia (mmol/L)
WKY (n = 28)	117.2 ± 21.1	288.5 ± 26.0	129.2 ± 18.3	9.6 ± 1.2
CT-SHR (n = 27)	70.4 ± 8.4*	196.0 ± 20.7†	152.8 ± 11.1‖	9.1 ± 2.0
DM-SHR (n = 31)	69.9 ± 10.5*	125.4 ± 34.6†‡	151.1 ± 21.4‖	29.5 ± 4.0¶
DM-SHR tempol (n = 30)	68.3 ± 8.0*	107.4 ± 18.5†‡§	152.6 ± 14.6‖	29.9 ± 6.0¶

SBP, systolic blood pressure.
* $P < 0.0001$ vs. WKY.
† $P < 0.0001$ vs. WKY.
‡ $P < 0.0001$ vs. CT-SHR.
§ $P = 0.03$ vs. nontreated SHR rats.
‖ $P = 0.003$ vs. WKY.
¶ $P < 0.0001$ vs. nondiabetic rats.

Detection of Superoxide Anion Production in Retinal Tissue

Lucigenin (bis-N-methylacridinium nitrate) (Invitrogen Inc., Eugene, OR) was used to measure superoxide anion production.[29] The retinas were isolated and placed in tubes containing RPMI-1640 medium (Gibco/BRL, Life Technologies, Inc., Gaithersburg, MD) at 37°C in a humidified atmosphere of 95% air/5% CO_2. Lucigenin (25 mM) was added, and photon emission was measured over 10 seconds; repeated measurements were made over a 3-minute period with a luminometer (TD 20-E Luminometer; Promega, Sunnyvale, CA). Superoxide production was expressed in relative luminescence units (RLU)/min/mg protein. Protein concentration was measured using the Bradford method[28] with BSA as the standard.

Measurements of Nitric Oxide End Products (NO_x^-; Nitrite and Nitrate) in Retina Tissue

Various cell types in the picomolar to nanomolar range produce NO, which has a very short half-life in biological fluids. Thus, the stable products of NO oxidation nitrite (NO_2^-) and nitrate (NO_3^-) are often analyzed instead to estimate the NO level in biological fluid. The NO_2^- and NO_3^- concentrations were detected using an NO chemiluminescence analyzer (NOA; Sievers Instruments Inc., Boulder, CO) in retina samples. With a syringe, 4-μL aliquots of supernatant were added to a purge chamber containing vanadium chloride (VCl_3; 97°C) (Sigma-Aldrich, St. Louis, MO) in 1 N HCl under a nitrogen atmosphere. The VCl_3 solution reduces nitrites and nitrates to NO gas, which the NOA detects. NO was liberated from the samples into the gaseous head space and was conducted to the NOA, where it reacted with the ozone to produce a chemiluminescent signal. The amount of light was proportional to the NO concentration, which was calculated from a standard curve of known NO_3^- concentrations. Each sample was analyzed in triplicate.

Measurement of Activity of Cu-Zn SOD

The enzyme activity of Cu-Zn SOD in retinal protein was measured using a kit from Cayman Chemical (Ann Arbor, MI), according to the

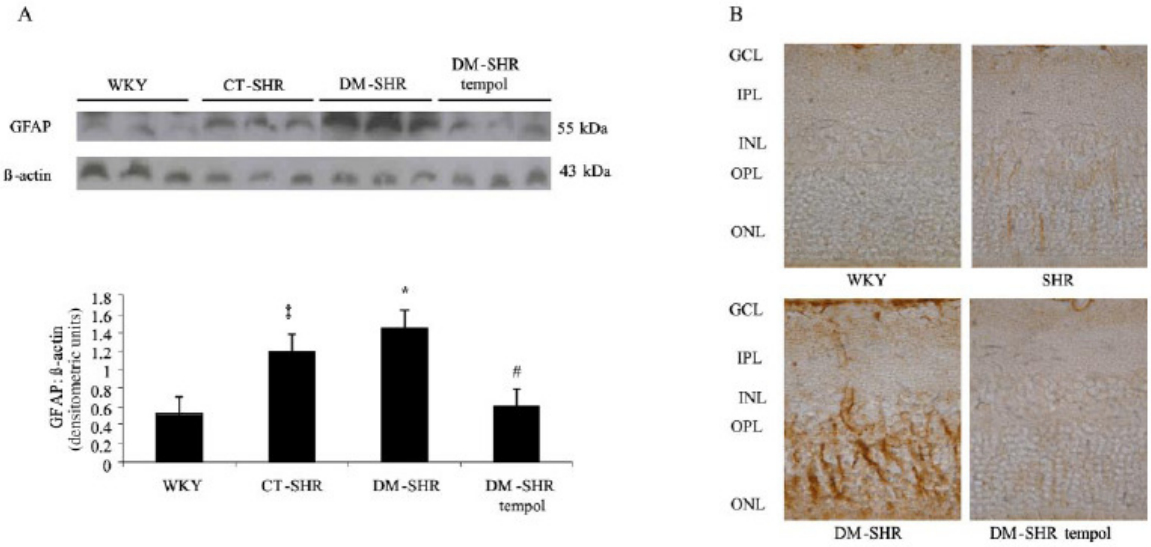

FIGURE 1. (**A**) Western blot of retinal lysates for GFAP from studied rats. The membranes were reprobed with anti-β-actin antibody as a control for protein loading. Bars represent mean ± SD of the band densities of the GFAP/β-actin ratio expressed in arbitrary densitometric units (1.18 ± 0.2 vs. 0.51 ± 0.2 arbitrary densitometric units for CT-SHR vs. WKY rats, respectively, ‡$P = 0.001$; 1.43 ± 0.2 vs. 0.51 ± 0.2 arbitrary densitometric units for DM-SHR vs. WKY rats, respectively, *$P = 0.0001$; and 0.51 ± 0.2 vs. 0.59 ± 0.2 arbitrary densitometric units for WKY vs. DM-SHR tempol groups, respectively, #$P = 0.7$). (**B**) Representative photomicrograph of the immunolocalization of GFAP in retinal sections. *Brown*: presence of immunoreactivity of GFAP. GCL, ganglion cell layer; IPL, inner plexiform layer; INL, inner nuclear layer; ONL, outer nuclear layer; OPL, outer plexiform layer.

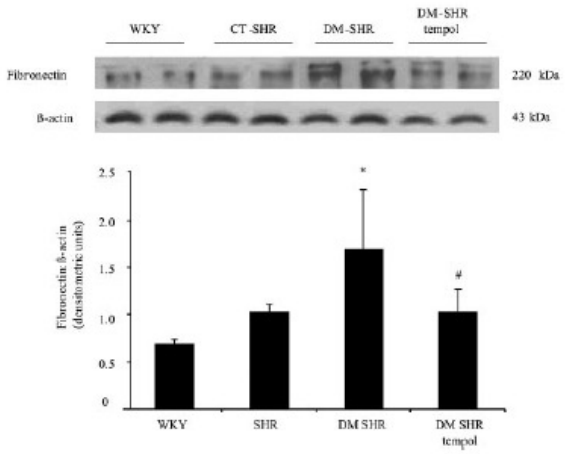

FIGURE 2. Western blot of retinal lysates for FN from studied rats. The membranes were reprobed with anti–β-actin antibody as a control for protein loading. Bars represent mean ± SD of the band densities of FN/β-actin ratio expressed in arbitrary densitometric units (1.7 ± 0.6 vs. 0.7 ± 0.04 arbitrary densitometric units for DM-SHR vs. WKY rats, respectively, $*P = 0.004$; 1.7 ± 0.6 vs. 1.02 ± 0.09 arbitrary densitometric units for DM-SHR vs. CT-SHR rats, respectively, $*P = 0.02$; and 1.02 ± 0.2 vs. 1.7 ± 0.6 arbitrary densitometric units for DM-SHR tempol vs. DM-SHR, respectively, $\#P = 0.02$).

manufacturer's instructions. The kit utilizes a tetrazolium salt for detection of superoxide radicals generated by xanthine oxidase and hypoxanthine. One unit of SOD is defined as the amount of enzyme needed for a 50% dismutation of the superoxide radical. The assay measures activity of Cu-Zn SOD in tissue. The standard curve was generated using a controlled SOD standard. The reaction was initiated by adding 20 μL diluted xanthine oxidase. A spectrophotometer (Elx800; BioTek, Winooski, VT) monitored the absorbance continuously at 450 nm. Protein concentrations were measured by the Bradford method.[28]

Determination of Reduced Glutathione Levels in the Retina

Retinal GSH levels were measured using the method described previously,[30] with a few modifications, also described previously.[16] Absorbance was read at 412 nm, and the GSH concentration was expressed as μM GSH/μg retinal protein. GSH was used as an external standard for the preparation of a standard curve.

Statistical Analysis

Results were expressed as mean ± SD, unless otherwise stated. We used one-way analysis of variance (ANOVA) followed by Fisher's protected least significant difference test to assess differences among the groups. All comparisons were carried out with statistical software (StatView; SAS Institute, Cary, NC). The significance level adopted was $P < 0.05$.

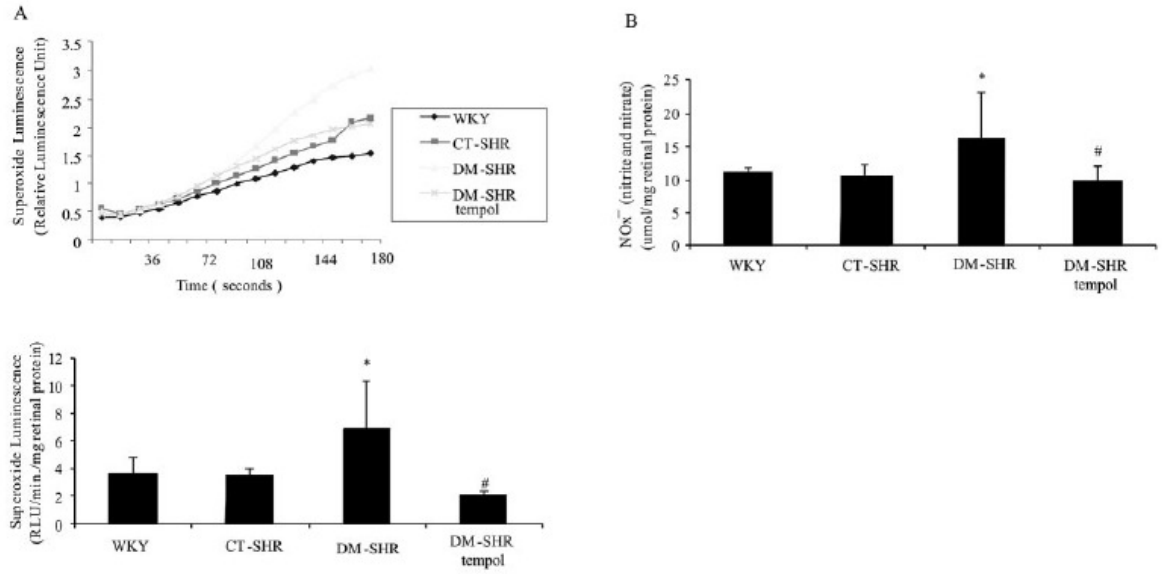

FIGURE 3. (A) Total superoxide generation in retinal tissue. Superoxide anion production from the retinas of control, diabetic SHR, and diabetic SHR treated with tempol was measured every 12 seconds for 3 minutes with the lucigenin-enhanced chemiluminescence method. The peak level of superoxide generation was observed around 3 minutes after lucigenin was added to the reaction buffer containing the retinas from different groups. Bars represent mean ± SD. All data shown are of $n \geq 6$ observations (6.8 ± 3.5 vs. 3.7 ± 1.2 RLU/min/mg protein for DM-SHR vs. WKY rats, respectively, $*P = 0.05$; and 2.1 ± 0.2 vs. 6.8 ± 3.4 RLU/min/mg protein for DM-SHR tempol vs. DM-SHR rats, respectively, $\#P = 0.01$). (B) Nitrite (NO_2^-) and nitrate (NO_3^-), the stable products of NO oxidation, are often analyzed to estimate the NO level in biological fluid by NO chemiluminescence analyzer. Results are corrected for protein concentration and are expressed as μmol NO_x^- per milligram of protein. Each sample was analyzed in triplicate (19.2 ± 4.4 vs. 11.2 ± 0.5 μmol NO/mg protein for DM-SHR vs. WKY rats, respectively, $*P = 0.004$; 19.2 ± 4.4 vs. 10.6 ± 1.7 μmol NO/mg protein for DM-SHR vs. CT-SHR rats, respectively, $*P = 0.003$; and 10.0 ± 2.0 vs. 19.2 ± 4.4 μmol NO/mg protein for DM-SHR tempol vs. DM-SHR rats, respectively, $\#P = 0.001$).

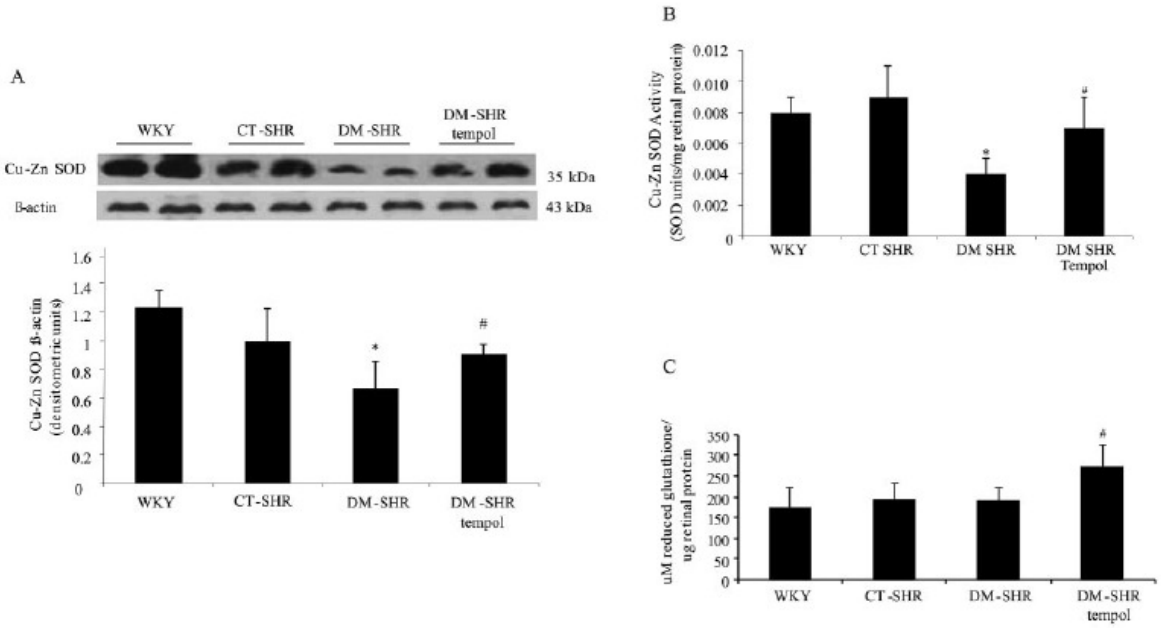

FIGURE 4. (A) Western blot of retinal lysates for Cu-Zn SOD from studied rats. The membranes were reprobed with anti-β-actin antibody as a control for protein loading. Bars represent mean ± SD of the band densities of the Cu-Zn SOD/β-actin ratio expressed in arbitrary densitometric units (0.65 ± 0.20 vs. 1.20 ± 0.10 arbitrary densitometric units for DM-SHR vs. WKY rats, respectively, $^*P = 0.0008$; 0.65 ± 0.20 vs. 1.00 ± 0.20 arbitrary densitometric units for DM-SHR vs. CT-SHR, respectively, $^*P = 0.02$; and 0.89 ± 0.08 vs. 0.65 ± 0.20 arbitrary densitometric units for DM-SHR tempol vs. DM-SHR, respectively, $\#P = 0.04$). (B) The enzyme activity of Cu-Zn SOD in retinal protein was measured. The standard curve was generated using a quality-controlled SOD standard. Each sample was analyzed in triplicate (0.004 ± 0.001 vs. 0.008 ± 0.001 U SOD/mg protein for DM-SHR vs. WKY rats, respectively, $^*P = 0.002$; 0.004 ± 0.001 vs. 0.009 ± 0.002 U SOD/mg protein for DM-SHR vs. CT-SHR rats, respectively, $^*P = 0.001$; and 0.007 ± 0.002 vs. 0.004 ± 0.001 U SOD/mg protein for DM-SHR tempol vs. DM-SHR, respectively, $\#P = 0.01$). (C) Concentration of reduced GSH from the retinas of studied rats (μM GSH/μg of retinal protein). GSH was not affected by the presence of hypertension or short-term diabetes, and treatment with tempol increased its levels ($\#P = 0.01$).

RESULTS

Physiological Characteristics of the Studied Groups

The body weights of the 4-week-old SHR were lower than those of the age-matched WKY rats ($P < 0.0001$). The weight gain was lower in DM-SHR than in CT-SHR ($P < 0.0001$), and tempol treatment significantly reduced the body weights of treated DM-SHR compared with nontreated SHR ($P = 0.03$). Systolic blood pressure was significantly higher in the SHR groups than in the WKY rat group ($P = 0.004$) and was not affected by the treatment. Plasma glucose levels were higher in diabetic rats than in the nondiabetic group ($P < 0.0001$) and were not affected by tempol treatment (Table 1).

Glial Reaction and Fibronectin Retinal Accumulation

To assess retinal lesions in this short-term study of diabetes and hypertension, we used the retinal expression of GFAP and fibronectin. These two abnormalities have been identified as early markers of retinal lesion in diabetes.[31,32] We did not use classic morphologic methods, such as retinal capillary morphology, in trypsin digest retinas because the abnormalities seen in this preparation, such as acellular capillaries and pericyte ghosts, required longer-term diabetes to be detected.[33,34] GFAP levels were evaluated by Western blot analysis and immunohistochemistry. In the Western blot assay, increased GFAP levels in CT-SHR were observed compared with WKY rats ($P = 0.001$), and this expression was exacerbated in the DM-SHR group ($P = 0.0001$). Treatment with tempol prevented the enhancement of GFAP expression, maintaining levels similar to those of the control WKY levels ($P = 0.7$; Fig. 1A). With immunohistochemistry, we observed an incrementally higher glial activity in the DM-SHR group compared with the CT-SHR and WKY groups. The treatment reestablished this expression to approximately the same levels as those of the CT-SHR group (Fig. 1B).

The retinal expression of FN increased in the DM-SHR group when compared with the WKY ($P = 0.004$) and CT-SHR ($P = 0.02$) groups. Treatment with tempol ($P = 0.02$) prevented the retinal expression of FN (Fig. 2).

Evaluation of Oxidative/Antioxidative Systems and Peroxynitrite Oxidative Damage in Retinal Tissue

The redox state is dependent on the balance between free radicals and antioxidant systems that influence tyrosine nitration and oxidative damage of lipids, proteins, and nucleic acids. For estimation of the oxidative status in retinal tissue, we evaluated the production of O_2^- and NO_x^- and the antioxidative system's GSH concentrations and the activity and expression of Cu-Zn SOD.

Superoxide production in the retina, evaluated by the lucigenin-enhanced chemiluminescence method, was increased in the DM-SHR group compared with the CT-SHR group ($P < 0.05$), and tempol treatment reestablished superoxide produc-

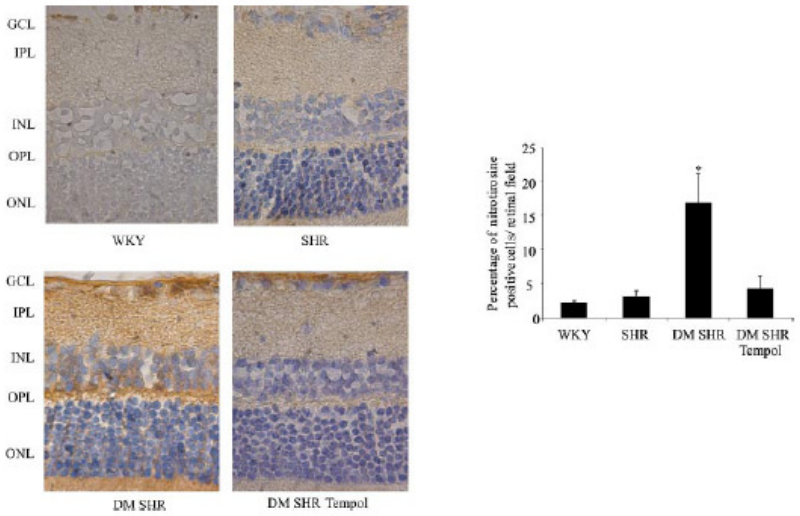

FIGURE 5. Representative photomicrograph of immunolocalization of nitrotyrosine. *Brown*: presence of nitrotyrosine. Bars represent mean ± SD of the percentage of positive cells per square millimeter of retina (2.03 ± 0.3 vs. 16.7 ± 4.5 percentage of positive cells per square millimeter of retina WKY vs. DM-SHR rats, respectively, $^*P < 0.0001$; 3.03 ± 0.8 vs. 16.7 ± 4.5 percentage of positive cells per square millimeter of retina CT-SHR vs. DM-SHR rats, respectively, $^*P = 0.0001$; and 3.03 ± 0.8 vs. 4.1±1.0 percentage of positive cells per square millimeter of retina CT-SHR vs. DM-SHR tempol-treated rats, respectively, $^*P = 0.6$). GCL, ganglion cell layer; IPL, inner plexiform layer; INL, inner nuclear layer; ONL, outer nuclear layer; OPL, outer plexiform layer.

tion to normal levels ($P = 0.01$; Fig. 3A). Additionally, retinal NO_x^- production was increased in the DM-SHR group compared with control groups ($P = 0.004$ vs. WKY and $P = 0.003$ vs. SHR), in which tempol treatment ($P = 0.01$) prevented retinal NO_x^- production (Fig. 3B).

Antioxidant defense was evaluated by retinal expression, Cu-Zn SOD activity, and GSH levels in retinal tissue. Two isoforms of SOD have Cu and Zn at their catalytic center and are localized to the intracellular cytoplasmic compartment and extracellularly.[35] Marked reduction was observed in Cu-Zn SOD retinal expression in the DM-SHR group compared with the WKY ($P = 0.0008$) and the CT-SHR ($P = 0.02$) groups. Similarly, Cu-Zn SOD activity was significantly decreased in DM-SHR compared with WKY and CT-SHR ($P = 0.002$ and $P = 0.001$, respectively). Tempol treatment protected both the expression and the activity of Cu-Zn SOD from the effect of short-term diabetes and hypertension. The expression of Cu-Zn SOD was restored in tempol-treated DM-SHR compared with DM-SHR ($P = 0.04$), and the activity of Cu-Zn SOD was similar in the CT-SHR and WKY ($P = 0.1$) groups (Figs. 4A, 4B).

Although the presence of hypertension or short-term diabetes did not affect the levels of GSH in the retina ($P = 0.4$), treatment with tempol increased its levels by approximately 47% compared with all other groups ($P = 0.01$). This effect may be explained by the metabolism of hydrogen peroxide by the catalase-like actions of tempol, which diminish the formation of hydroxyl radicals, thus increasing the levels of GSH available in the retinal tissue (Fig. 4C).

An immunoreaction for NT in retinal tissue detected the product peroxynitrite, generated by the reaction between NO and O_2^-. There was an evident increase of NT in the retinas of DM-SHR compared with WKY and SHR ($P < 0.0001$ and $P = 0.0001$, respectively). By the mechanism of a SOD mimetic, tempol competed with NO by O_2^- and dismuted it to peroxide hydrogen and oxygen, leading to marked reduction of NT levels in the treated DM-SHR group similar to those observed in the SHR group ($P = 0.6$; Fig. 5).

Expression of Ribosylated Proteins in the Retinal Tissue of Tempol-Treated Rats

Nitrosative stress induces DNA single-strand breaks, leading to the overactivation of PARP. In the present study, the activation of PARP represented by the catalysis of the transference of ADP-ribose groups from NAD to target proteins (poly(ADP-ribosyl)ation), was accessed through the amount of PAR-modified proteins by Western blot and immunohistochemistry analyses. In Western blot analyses, the presence of hypertension in the CT-SHR increased the content of PAR ribosylated polymers compared with the normotensive WKY rats ($P = 0.04$). The concomitance of both diabetes and hypertension in the DM-SHR significantly increased these levels compared with WKY and CT-SHR ($P < 0.001$ and $P = 0.02$, respectively). Treatment with tempol in the DM-SHR reestablished this parameter to SHR levels ($P = 0.3$; Fig. 6A). As detected by immunohistochemistry, the distribution of PAR polymer–positive cells was homogeneous among the ganglion cells in both the inner and outer nuclear layers. The presence of hypertension solely and in concomitance with diabetes revealed a significant increase in PAR polymer–positive retinal cells compared with the WKY group ($P = 0.01$ and $P = 0.006$, respectively), suggesting the activation of PARP evaluated through the amount of PAR-modified proteins. Treatment with a SOD mimetic for 20 days reestablished this element to WKY levels ($P = 0.7$; Fig. 6B).

iNOS Expression Associated with Poly(ADP-ribosyl)ation in Retinal Tissue

iNOS has been shown to cause DNA breaks and the subsequent activation of PARP, which was recently implicated in early diabetic retinal changes.[21,36] Other investigators have shown that with specific PARP inhibitors or knocking out of the PARP gene, NF-κB activation and transcription of NF-κB–dependent genes, such as inducible nitric oxide synthase, are reduced,[21,37] suggesting that the inhibition of poly(ADP-ribosyl)ation might prevent the consequences of inflammation or stress by modification of NF-κB–dependent pathways. In the present work, we addressed the retinal expression of iNOS, which may be accepted as an indicator of the NF-κB–dependent pathways and PARP activation. A significant increase in retinal iNOS expression was demonstrated in the DM-SHR group compared with the WKY group ($P = 0.04$), and the treatment with tempol restored it to normal levels ($P = 0.26$; Fig. 7).

DISCUSSION

The findings presented herein demonstrate that the systemic administration of tempol reestablished the cell's oxidative parameters and thus prevented the poly(ADP-ribosyl)ation of

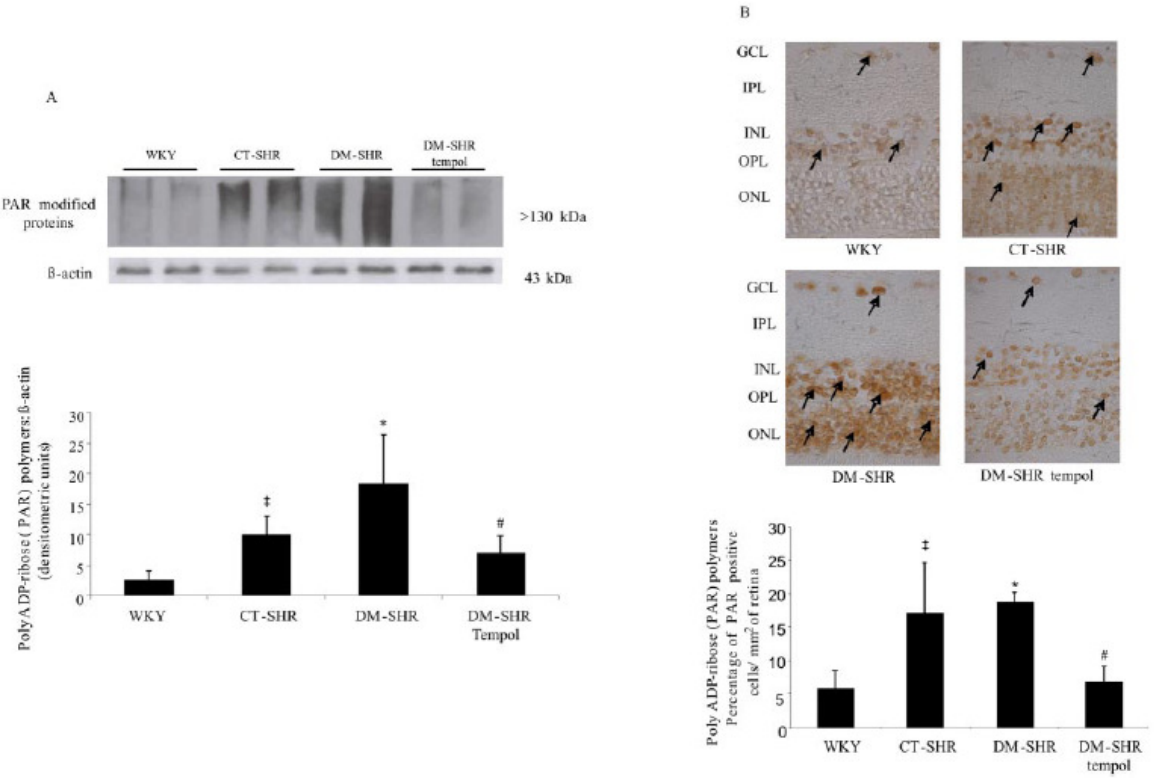

FIGURE 6. (**A**) Western blot of retinal lysates for PAR-modified proteins from studied rats. The membranes were reprobed with anti–β-actin antibody as a control for protein loading. Bars represent mean ± SD of the band densities of the PAR-modified proteins/β-actin ratio expressed in arbitrary densitometric units (2.4 ± 1.5 vs. 9.8 ± 3.2 arbitrary densitometric units for WKY vs. CT-SHR rats, respectively, ‡$P = 0.04$; 2.4 ± 1.5 vs. 18.3 ± 7.8 arbitrary densitometric units for WKY vs. DM-SHR rats, respectively, *$P < 0.0001$; 9.8 ± 3.2 vs. 18.3 ± 7.8 for CT-SHR vs. DM-SHR rats, respectively, *$P = 0.02$; and 9.8 ± 3.2 vs. 6.6 ± 3.1 for CT-SHR vs. DM-SHR tempol-treated rats, respectively, #$P = 0.3$). (**B**) Representative photomicrograph of immunolocalization of PAR polymer-positive cells in retinal sections. A *dark brown* nucleus indicates the presence of immunoreactivity of PAR. Bars represent mean ± SD of the percentage of positive cells per square millimeter of retina (5.8 ± 2.5 vs. 16.8 ± 7.6 percentage of positive cells per square millimeter of retina WKY vs. CT-SHR rats, respectively, ‡$P = 0.01$; 5.8 ± 2.5 vs. 18.6 ± 1.5 percentage of positive cells per square millimeter of retina WKY vs. DM-SHR rats, respectively, *$P = 0.006$; and 5.8 ± 2.5 vs. 6.7 ± 2.3 percentage of positive cells per square millimeter of retina WKY vs. DM-SHR tempol rats, respectively, #$P = 0.7$). GCL, ganglion cell layer; IPL, inner plexiform layer; INL, inner nuclear layer; ONL, outer nuclear layer; OPL, outer plexiform layer.

proteins and iNOS expression in the retinas of diabetic hypertensive rats. Consequently, the early molecular changes of DR, represented here by FN accumulation and increased GFAP expression, were prevented in tempol-treated rats.

Serious retinal injuries such as retinal detachment,[38] glaucoma,[39] and DR,[2,40,41] can trigger retinal reactive gliosis and neurodegeneration characterized by changes in astrocyte and Müller cell morphologies and increased production of intermediate filament proteins (GFAP).[42] Retinal Müller cells and blood vessels are in close apposition and are likely to interact with each other.[43] It has been suggested that the increase in vascular permeability in DR may be caused by the effects of diabetes that alter the neural components of the retina, demonstrated by increased production of vascular endothelial growth factor by Müller cells and neurons,[44–46] leading to a breakdown in the interactions among neurons, glia, and endothelial cells.[47] Thickening of the basal lamina that surrounds the endothelial cells and pericytes of the retinal capillaries because of extracellular matrix accumulation[48,49] is another finding early in DR pathogenesis, and this is believed to be pivotal in the progression of DR. This concept was based on the findings in DM animal models in which the downregulation of FN synthesis partially prevented retinal basal lamina thickening and prevented classic early vascular changes, such as the apoptosis of pericytes and the development of acellular capillaries.[50] In in vitro studies, Oshitari et al.[51] downregulated several components of the extracellular matrix, such as fibronectin, laminin, and collagen type IV, and thus reduced vascular leakage in streptozotocin-induced diabetes.[51] In light of this, fibronectin accumulation and GFAP expression might be used as molecular markers of diabetic changes in the retina in short-term experimental diabetes.

DM increases oxidative stress, which plays a key regulatory role in the development of its complications.[52] Because oxidative stress may be the promoter of many alterations implicated in the pathogenesis of DR, representing an imbalance between excess formation and the impaired removal of reactive oxygen species (ROS), the antioxidant defense system of the cell is a crucial part of the overall oxidative stress experienced by a cell. A number of works have demonstrated beneficial effects of antioxidant treatment in the diabetic retina. Antioxidants may act at different levels, may inhibit the formation of ROS or scavengers of free radicals, or may increase the antioxidant defense enzyme capabilities.[53] For instance, long-term lipoic

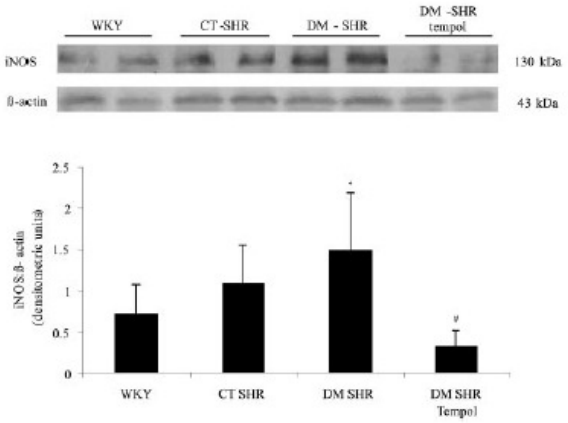

FIGURE 7. Western blot of retinal lysates for iNOS from studied rats. The membranes were reprobed with anti–β-actin antibody as a control for protein loading. Bars represent mean ± SD of the band densities of the iNOS/β-actin ratio expressed in arbitrary densitometric units (1.1 ± 0.4 vs. 0.7 ± 0.3 arbitrary densitometric units for CT-SHR vs. WKY rats, respectively, $P = 0.26$; 1.5 ± 0.7 vs. 1.1 ± 0.4 arbitrary densitometric units for DM-SHR vs. CT-SHR rats, respectively, $P = 0.17$; 1.5 ± 0.7 vs. 0.7 ± 0.3 arbitrary densitometric units for DM-SHR vs. WKY rats, respectively, $^*P = 0.04$; 1.5 ± 0.7 vs. 0.3 ± 0.2 arbitrary densitometric units for DM-SHR vs. DM-SHR tempol, respectively, $^*P = 0.001$; and 0.7 ± 0.3 vs. 0.3 ± 0.2 arbitrary densitometric units for WKY vs. DM-SHR tempol, respectively, $\#P = 0.25$).

acid treatment attenuated the apoptosis of rat retinal capillary cells and decreased the levels of 8-hydroxy-2′-deoxyguanosine and NT in diabetic rats,[54] and short-term treatment prevented the significant decrease of GSH content, normalized the malondialdehyde concentration, and restored the electroretinogram *b*-wave amplitude.[55] In addition, dietary supplementation with multi-antioxidants, including vitamins C and E, in diabetic rats prevented the inhibition of retinal GSH reductase, GSH peroxidase, SOD activities,[56] and superoxide production.[57] It also reduced the development of retinal acellular capillaries and pericyte ghosts.[15] In addition, the overexpression of mitochondrial SOD in hemizygous transgenic mice (MnSOD-Tg) prevented diabetic retinal oxidative stress, protecting the mitochondria from dysfunction.[58]

Previous studies demonstrated that PARP activation increased vasoactive factors, such as endothelin-1 and ECM protein production, in diabetes and that PAR-modified proteins are associated with increased oxidative stress upregulation in the retina.[19] Among the PARPs, nuclear PARP-1 is a DNA damage-activated enzyme and is the most abundant and commonly studied member of the family. Its enzymatic activity leads to PAR formation, and it was first described more than 40 years ago.[59] More recently, PARP increased in importance when it was discovered to mediate nitric oxide-induced neuronal death.[60] ROS-dependent DNA damage is thought to play a major role in triggering PARP-1 hyperactivity during ischemia. In the pathogenesis of DR, ischemia causes structural changes and a breakdown of the blood retinal barrier.[61] PARP-1 hyperactivation causes cell death because of cellular accumulation of the PARP-1 product, PAR, which causes the translocation of the apoptosis-inducing factor from mitochondria to the nucleus and the activation of a caspase-independent programmed cell death pathway.[62] In experimental models of brain ischemia, the use of a PARP-1 inhibitor, PJ34, preserved the endothelial tight junctions and decreased the expression of ICAM-1, thus limiting leukocyte infiltration to the ischemic brain.[63]

Tempol is a cell membrane-permeable nitroxide and is among the most potent of the nitroxides for protecting cells and tissues from the damaging effects of ROS.[64] Tempol has multiple antioxidant actions because of the ability of nitroxides to inhibit three or more sequential sites in an oxidative chain (for example, O_2^-, H_2O_2, and OH^-). This may underlie its efficacy in diverse models of oxidative stress. Tempol is free of serious toxic effects in animal models. Despite these apparently beneficial effects in a wide range of animal models, tempol has yet to be developed as a drug for human use.[65] Matsumoto et al.[66] tested the toxic effects of five nitroxides, and tempol was the least toxic. These toxic or lethal doses of tempol are approximately 30-fold higher than the therapeutic dose for the reduction of blood pressure. In addition, tempol had no adverse effects on gene mutation in Chinese hamster.[67] The reaction rate constant for tempol with O_2^- has been determined to be 3.4×10^5 mol · L · s. This makes it a much more efficient antioxidant than vitamins because the rate constant for the interaction of SOD with O_2^- is approximately 1.6 to 2.4×10^9 mol · L · s. For vitamin E with O_2^-, the rate constant is 0.59 mol · L · s.[68] Tempol has two reaction sites with OH^- that can be derived from ROS-like peroxynitrite. In cell cultures, tempol catalyzes the SOD reaction and protects against oxidative stress.[69] In addition, exposure to conditions of oxidative stress in cultured coronary endothelial cells leads to an increase in NO end products, namely nitrite and nitrate. In the presence of tempol, these effects are reversed.[27]

In experimental models[70] and in postmortem retinas from diabetic patients,[71] as well as in the vitreous fluid from diabetic patients with proliferative diabetic retinopathy,[72] increased levels of NO end products and the upregulation of iNOS have been reported. In line with this evidence, the treatment with tempol in this study reduced the NO end products and the superoxide production observed in retinas of diabetic SHR rats. In the treatment, tempol acted as an O_2^- scavenger, reducing nitric oxide end products and increasing GSH biosynthesis, thereby reestablishing the oxidative-nitrosative status of the diabetic retina. Similarly, we observed the prevention of Cu-Zn SOD retinal expression/activity reduction in treated diabetic rats. Further studies are required to address whether the variation in Cu-Zn SOD expression and activity plays a role in the effect of tempol in retinal tissue.

In conclusion, our data reveal the potential therapeutic role of tempol in the early phases of DR. In hypertensive diabetic rats, treatment with tempol reestablished the redox status by acting as an O_2^- scavenger, which enhances the GSH biosynthesis and Cu-Zn SOD activity, thus preventing oxidative damage. These effects were associated with a reduction in retinal extracellular matrix accumulation and glial reaction. It may be that mechanism conferred by tempol to protect against early molecular changes in the retinas of diabetic hypertensive rats acts through the counteraction of oxidative-nitrosative stress, thus diminishing the amount of ADP-ribosylated proteins.

Acknowledgments

The authors thank Gabriela F. P. de Souza and Marcelo G. de Oliveira for their assistance in the measurements of nitric oxide end products.

References

1. Patz A, Smith RE. The ETDRS and Diabetes 2000. *Ophthalmology.* 1991;98:739–740.
2. Barber AJ. A new view of diabetic retinopathy: a neurodegenerative disease of the eye. *Prog Neuropsychopharmacol Biol Psychiatry.* 2003;27:283–290.
3. Cunha-Vaz JG, Fonseca JR, Abreu JF, Ruas MA. Detection of early retinal changes in diabetes by vitreous fluorophotometry. *Diabetes.* 1979;28:16–19.

4. Dodson PM. Diabetic retinopathy: treatment and prevention. *Diab Vasc Dis Res.* 2007;4:S9–S11.
5. The UKPDS Study Group. Tight blood pressure control and risk of macrovascular and microvascular complications in type 2 diabetes: UKPDS 38. UK Prospective Diabetes Study Group. *BMJ.* 1998;317:703–713.
6. Danser AH, van den Dorpel MA, Deinum J, et al. Renin, prorenin, and immunoreactive renin in vitreous fluid from eyes with and without diabetic retinopathy. *J Clin Endocrinol Metab.* 1989;68:160–167.
7. Kawamura H, Kobayashi M, Li Q, et al. Effects of angiotensin II on the pericyte-containing microvasculature of the rat retina. *J Physiol.* 2004;561:671–683.
8. Moravski CJ, Kelly DJ, Cooper ME, et al. Retinal neovascularization is prevented by blockade of the renin-angiotensin system. *Hypertension.* 2000;36:1099–1104.
9. Silva KC, Rosales MA, Biswas SK, Lopes de Faria JB, Lopes de Faria JM. Diabetic retinal neurodegeneration is associated with mitochondrial oxidative stress and is improved by angiotensin receptor blocker in a model that combines hypertension and diabetes. *Diabetes.* 2009;58:1382–1390.
10. Beckman JS, Koppenol WH. Nitric oxide, superoxide, and peroxynitrite: the good, the bad, and the ugly. *Am J Physiol Cell Physiol.* 1996;40:C1424–C1437.
11. Krishna MC, Russo A, Mitchell JB, Goldstein S, Dafni H, Samuni A. Do nitroxide antioxidants act as scavengers of O_2^- or as SOD mimics? *J Biol Chem.* 1996;271:26026–26031.
12. Chen P, Guo AM, Edwards PA, Trick G, Scicli AG. Role of NADPH oxidase and ANG II in diabetes-induced retinal leukostasis. *Am J Physiol Regul Integr Comp Physiol.* 2007;293:R1619–R1629.
13. El-Remessy AB, Khalil IE, Matragoon S, et al. Neuroprotective effect of (−) Delta9-tetrahydrocannabinol and cannabidiol in N-methyl-D-aspartate-induced retinal neurotoxicity: involvement of peroxynitrite. *Am J Pathol.* 2003;163:1997–2008.
14. Shastri S, Gopalakrishnan V, Poduri R, Di Wang H. Tempol selectively attenuates angiotensin II evoked vasoconstrictor responses in spontaneously hypertensive rats. *J Hypertens.* 2002;20:1381–1391.
15. Kowluru RA, Tang J, Kern TS. Abnormalities of retinal metabolism in diabetes and experimental galactosemia, VII: effect of long-term administration of antioxidants on the development of retinopathy. *Diabetes.* 2001;50:1938–1942.
16. Pinto CC, Silva KC, Biswas SK, Martins N, de Faria JB, de Faria JM. Arterial hypertension exacerbates oxidative stress in early diabetic retinopathy. *Free Radic Res.* 2007;41:1151–1158.
17. Schreiber V, Dantzer F, Ame JC, de Murcia G. Poly(ADP-ribose): novel functions for an old molecule. *Nat Rev Mol Cell Biol.* 2006;7:517–528.
18. Chiu J, Xu BY, Chen S, Feng B, Chakrabarti S. Oxidative stress-induced, poly (ADP-ribose) polymerase-dependent upregulation of ET-1 expression in chronic diabetic complications. *Can J Physiol Pharmacol.* 2008;86:365–372.
19. Xu B, Chiu J, Feng B, Chen S, Chakrabarti S. PARP activation and the alteration of vasoactive factors and extracellular matrix protein in retina and kidney in diabetes. *Diabetes Metab Res Rev.* 2008;24:404–412.
20. Garcia Soriano F, Virág L, Jagtap P, et al. Diabetic endothelial dysfunction: the role of poly(ADPribose) polymerase activation. *Nat Med.* 2001;7:108–113.
21. Zheng L, Szabó C, Kern TS. Poly(ADP-ribose) polymerase is involved in the development of diabetic retinopathy via regulation of nuclear factor-κB. *Diabetes.* 2004;53:2960–2967.
22. Chiarugi A, Moskowitz MA. Poly(ADP-ribose) polymerase-1 activity promotes NF-κB-driven transcription and microglial activation: implication for neurodegenerative disorders. *J Neurochem.* 2003;85:306–317.
23. Silva KC, Pinto CC, Biswas SK, Souza DS, de Faria JB, de Faria JM. Prevention of hypertension abrogates early inflammatory events in the retina of diabetic hypertensive rats. *Exp Eye Res.* 2007;85:123–129.
24. Drel VR, Xu W, Zhang J, et al. Poly (ADP-ribose) polymerase inhibition counteracts cataract formation and early retinal changes in streptozotocin-diabetic rats. *Invest Ophthalmol Vis Sci.* 2008;50:1778–1790.
25. Silva KC, Pinto CC, Biswas SK, de Faria JB, de Faria JM. Hypertension increases retinal inflammation in experimental diabetes: a possible mechanism for aggravation of diabetic retinopathy by hypertension. *Curr Eye Res.* 2007;32:533–541.
26. Schnackenberg CG, Wilcox CS. Two-week administration of tempol attenuates both hypertension and renal excretion of 8-isoprostaglandin $F_{2\alpha}$. *Hypertension.* 1999;33:424–428.
27. Vaziri ND, Ding Y. Effect of lead on nitric oxide synthase expression in coronary endothelial cells: role of superoxide. *Hypertension.* 2001;37:223–226.
28. Bradford MM. A rapid and sensive method for the quantification of microgram quantities of protein utilizing the principle of protein dye binding. *Anal Biochem.* 1976;72:248–254.
29. Li Y, Zhu H, Kuppusamy P, Roubaud V, Zweier JL, Trush MA. Validation of lucigenin (bis-N-methylacridinium) as a chemiluminigenic probe for detecting superoxide anion radical production by enzymatic and cellular systems. *J Biol Chem.* 1998;273:2015–2023.
30. Beutler E, Duron O, Kelly BM. Improved method for the determination of blood glutathione. *J Lab Clin Med.* 1963;61:882–888.
31. Yoshida Y, Yamagishi S, Matsui T, et al. Protective role of pigment epithelium-derived factor (PEDF) in early phase of experimental diabetic retinopathy. *Diabetes Metab Res Rev.* 2009;25:678–686.
32. Roy S, Lorenzi M. Early biosynthetic changes in the diabetic-like retinopathy of galactose-fed rats. *Diabetologia.* 1996;39:735–738.
33. Joussen AM, Doehmen S, Le ML, et al. TNF-alpha mediated apoptosis plays an important role in the development of early diabetic retinopathy and long-term histopathological alterations. *Mol Vis.* 2009;15:1418–1428.
34. Gardiner TA, Anderson HR, Stitt AW. Inhibition of advanced glycation end-products protects against retinal capillary basement membrane expansion during long-term diabetes. *J Pathol.* 2003;201:328–333.
35. Zelko IN, Mariani TJ, Folz RJ. Superoxide dismutase multigene family: a comparison of the CuZn-SOD (SOD1), Mn-SOD (SOD2), and EC-SOD (SOD3) gene structures, evolution, and expression. *Free Radic Biol Med.* 2002;33:337–349.
36. Zheng L, Gong B, Hatala DA, Kern TS. Retinal ischemia and reperfusion causes capillary degeneration: similarities to diabetes. *Invest Ophthalmol Vis Sci.* 2007;48:361–367.
37. Le Page C, Sanceau J, Drapier JC, Wietzerbin J. Inhibitors of ADP-ribosylation impair inducible nitric oxide synthase gene transcription through inhibition of NF κB activation. *Biochem Biophys Res Commun.* 1998;243:451–457.
38. Lewis GP, Matsumoto B, Fisher SK. Changes in the organization and expression of cytoskeletal proteins during retinal degeneration induced by retinal detachment. *Invest Ophthalmol Vis Sci.* 1995;36:2404–2416.
39. Wang L, Cioffi GA, Cull G, Dong J, Fortune B. Immunohistologic evidence for retinal glial cell changes in human glaucoma. *Invest Ophthalmol Vis Sci.* 2002;43:1088–1094.
40. Mizutani M, Gerhardinger C, Lorenzi M. Muller cell changes in human diabetic retinopathy. *Diabetes.* 1998;47:445–449.
41. Barber AJ, Antonetti DA, Gardner TW. Altered expression of retinal occludin and glial fibrillary acidic protein in experimental diabetes: the Penn State Retina Research Group. *Invest Ophthalmol Vis Sci.* 2000;41:3561–3568.
42. Lewis GP, Fisher SK. Up-regulation of glial fibrillary acidic protein in response to retinal injury: its potential role in glial remodeling and a comparison to vimentin expression. *Int Rev Cytol.* 2003;230:263–290.
43. Stone J, Dreher Z. Relationship between astrocytes, ganglion cells and vasculature of the retina. *J Comp Neurol.* 1987;255:35–49.
44. Stone J, Itin A, Alon T, et al. Development of retinal vasculature is mediated by hypoxia-induced vascular endothelial growth factor (VEGF) expression by neuroglia. *J Neurosci.* 1995;15:4738–4747.
45. Amin RH, Frank RN, Kennedy A, Eliott D, Puklin JE, Abrams GW. Vascular endothelial growth factor is present in glial cells of the retina and optic nerve of human subjects with nonproliferative diabetic retinopathy. *Invest Ophthalmol Vis Sci.* 1997;38:36–47.

46. Tretiach M, Madigan MC, Wen L, Gillies MC. Effect of Muller cell co-culture on in vitro permeability of bovine retinal vascular endothelium in normoxic and hypoxic conditions.*Neurosci Lett.* 2005;378:160–165.
47. Antonetti DA, Lieth E, Barber AJ, Gardner TW. Molecular mechanisms of vascular permeability in diabetic retinopathy. *Semin Ophthalmol.* 1999;14:240–248.
48. Lorenzi M, Gerhardinger C. Early cellular and molecular changes induced by diabetes in the retina. *Diabetologia.* 2001;44:791–804.
49. Cai J, Boulton M. The pathogenesis of diabetic retinopathy: old concepts and new questions. *Eye.* 2002;16:242–260.
50. Roy S, Sato T, Paryani G, Kao R. Downregulation of fibronectin overexpression reduces basement membrane thickening and vascular lesions in retinas of galactose-fed rats. *Diabetes.* 2003;52:1229–1234.
51. Oshitari T, Polewski P, Chadda M, Li AF, Sato T, Roy S. Effect of combined antisense oligonucleotides against high-glucose- and diabetes-induced overexpression of extracellular matrix components and increased vascular permeability. *Diabetes.* 2006;55:86–92.
52. Brownlee M. Biochemistry and molecular cell biology of diabetic complications. *Nature.* 2001;414:813–820.
53. Kowluru RA, Chan PS. Oxidative stress and diabetic retinopathy. *Exp Diabetes Res.* 2007;2007:43603.
54. Kowluru RA, Odenbach S. Effect of long-term administration of α-lipoic acid on retinal capillary cell death and the development of retinopathy in diabetic rats. *Diabetes.* 2004;53:3233–3238.
55. Johnsen-Soriano S, Garcia-Pous M, Arnal E, et al. Early lipoic acid intake protects retina of diabetic mice. *Free Radic Res.* 2008;42:613–617.
56. Kowluru RA, Kern TS, Engerman RL. Abnormalities of retinal metabolism in diabetes or experimental galactosemia, IV: antioxidant defense system. *Free Radic Biol Med.* 1997;22:587–592.
57. Mustata GT, Rosca M, Biemel KM, et al. Paradoxical effects of green tea (*Camellia sinensis*) and antioxidant vitamins in diabetic rats: improved retinopathy and renal mitochondrial defects but deterioration of collagen matrix glycoxidation and cross-linking. *Diabetes.* 2005;54:517–526.
58. Kowluru RA, Kowluru V, Xiong Y, Ho YS. Overexpression of mitochondrial superoxide dismutase in mice protects the retina from diabetes-induced oxidative stress. *Free Radic Biol Med.* 2006;41:1187–1190.
59. Chambon P, Weill JD, Mandel P. Nicotinamide mononucleotide activation of new DNA-dependent polyadenylic acid synthesizing nuclear enzyme. *Biochem Biophys Res Commun.* 1963;11:39–43.
60. Zhang J, Dawson VL, Dawson T, Snyder SH. Nitric oxide activation of poly(ADP-ribose) synthetase in neurotoxicity. *Science.* 1994;263:687–689.
61. Kaur C, Foulds WS, Ling EA. Blood-retinal barrier in hypoxic ischaemic conditions: basic concepts, clinical features and management. *Prog Retin Eye Res.* 2008;27:622–647.
62. Yu SW, Andrabi SA, Wang H, et al. Apoptosis-inducing factor mediates poly(ADP-ribose) (PAR) polymer-induced cell death. *Proc Natl Acad Sci USA.* 2006;103:18314–18319.
63. Zhang Y, Park TS, Gidday JM. Hypoxic preconditioning protects human brain endothelium from ischemic apoptosis by Akt-dependent survivin activation. *Am J Physiol Heart Circ Physiol.* 2007;292:H2573–H2581.
64. Li WG, Zhang XY, Wu YJ, Gao MT, Zheng RL. The relationship between structure and antioxidative activity of piperidine nitroxides. *J Pharm Pharmacol.* 2006;58:941–949.
65. Wilcox CS, Pearlman A. Chemistry and antihypertensive effects of tempol and other nitroxides. *Pharmacol Rev.* 2008;60:418–469.
66. Matsumoto K, Krishna MC, Mitchell JB. Novel pharmacokinetic measurement using electron paramagnetic resonance spectroscopy and simulation of in vivo decay of various nitroxyl spin probes in mouse blood. *J Pharmacol Exp Ther.* 2004;310:1076–1083.
67. An J, Hsie AW. Effects of an inhibitor and a mimic of superoxide dismutase on bleomycin mutagenesis in Chinese hamster ovary cells. *Mutat Res.* 1992;270:167–175.
68. Mitchell JB, Samuni A, Krishna MC, et al. Biologically active metal-independent superoxide dismutase mimics. *Biochemistry.* 1990;29:2802–2807.
69. Samuni A, Winkelsberg D, Pinson A, Hahn SM, Mitchell JB, Russo A. Nitroxide stable radicals protect beating cardiomyocytes against oxidative damage. *J Clin Invest.* 1991;87:1526–1530.
70. Du Y, Smith MA, Miller CM, Kern TS. Diabetes induced nitrative stress in the retina, and correction by aminoguanidine. *J Neurochem.* 2002;80:771–779.
71. Abu El-Asrar AM, Desmet S, Meersschaert A, Dralands L, Missotten L, Geboes K. Expression of the inducible isoform of nitric oxide synthase in the retinas of human subjects with diabetes mellitus. *Am J Ophthalmol.* 2001;4:551–556.
72. Hernández C, Lecube A, Segura RM, Sararols L, Simó R. Nitric oxide and vascular endothelial growth factor concentrations are increased but not related in vitreous fluid of patients with proliferative diabetic retinopathy. *Diabet Med.* 2002;19:655–660.

LISTA DE ARTIGOS PUBLICADOS COMO COLABORADORA DURANTE O DOUTORADO

Silva KC, **Rosales MA**, Hamassaki DE, Saito KC, Faria AM, Ribeiro PA, Faria JB, Faria JM. Green tea is neuroprotective in diabetic retinopathy. Invest Ophthalmol Vis Sci. 54: 1325-1336, 2013. doi: 10.1167/iovs.12-10647.

Duarte DA, Silva KC, **Rosales MA**, Lopes de Faria JB, Lopes de Faria JM. The concomitance of hypertension and diabetes exacerbating retinopathy: the role of inflammation and oxidative stress. Curr Clin Pharmacol. 8: 266-77, 2013.

Silva KC, **Rosales MA**, de Faria JB, de Faria JM. Reduction of inducible nitric oxide synthase via angiotensin receptor blocker prevents the oxidative retinal damage in diabetic hypertensive rats. Curr Eye Res 35: 519-28, 2010. doi:10.3109/02713681003664923.